P-12-19

# Groundwater flow modelling to support the repository sealing project

Steven Joyce, Serco

Niko Marsic, Kemakta Konsult AB

April 2018

**Svensk Kärnbränslehantering AB**
Swedish Nuclear Fuel
and Waste Management Co

Box 3091, SE-169 03 Solna
Phone +46 8 459 84 00

ISSN 1651-4416
**SKB P-12-19**
ID 1348852
April 2018

# Groundwater flow modelling to support the repository sealing project

Steven Joyce, Serco

Niko Marsic, Kemakta Konsult AB

# Contents

# 1 Introduction

A reference design has been specified for the proposed spent nuclear fuel repository at Forsmark. However, there has been little investigation of alternative designs for the repository to date. Therefore, a project has been started to study concepts related to the sealing of the repository. The goals of the Repository Sealing Project are to:

- Develop and detail a reference design for the sealing and its components.
- Adapt the reference design to the conditions at Forsmark.
- Obtain a base situation on a conceptual level, which should be good enough to:
  - Be able to reach decisions on changing the design for the repository sealing.
  - In the next step, be able to carry out system design for a revised reference design.
  - Be able to update the documentation on the repository sealing at the end of 2013.

The purpose of the modelling reported here is to investigate alternative designs of the repository sealing and their influence on groundwater flow and transport in the repository area, particularly in proximity to the ramp and central area shafts. The influence of the ramp and shaft properties on the performance measures for the recharge and discharge pathways to the repository are considered. The recharge pathways are important for considering the flow of potentially dilute or oxygenated water to the repository. The discharge pathways are important for the transport of radionuclides to the surface.

Another task reported here is the study of the influence of sealed investigation boreholes on groundwater flow and performance measures relevant for penetration of oxygen and radionuclide transport. A sensitivity analysis is performed where the hydraulic properties of the sealed boreholes are varied.

Two climate situations are considered, one during the temperate period soon after complete closure and re-saturation of the repository, and one during the glacial period when the ice front is located roughly above the middle of the repository (ice front location II).

# 2 Model description

All of the models considered in this report are derived from block 1 of the SR-Site Hydrogeological base case repository-scale model, as described in Joyce et al. (2010). This block consists of the north-western part of the repository and includes two main tunnels with their associated deposition tunnels, the central area, with associated shafts, and the ramp. It is roughly 1.3 km by 2.1 km horizontally and extends vertically from an elevation of −800 m up to the bottom of the soil layer, i.e. up to about 4 m below ground surface. All elevations are in metres above sea level (datum RHB 70).

The main tunnels, deposition tunnels and deposition holes are represented as a continuous porous medium (CPM) in order to better represent the backfill and to model the detailed flow within these features. The other repository structures (transport tunnels, central area, ramps and shafts) are represented as deterministic fractures with appropriate hydraulic and transport properties. Figure 2-1 shows the repository structures in block 1. The CPM structures are coloured green and the fracture structures are coloured blue. If parts of main tunnels or deposition tunnels from a neighbouring block are included within the domain of block 1, then they are represented as fractures with appropriate properties. This ensures the connectivity of repository structures with the boundaries of the block, where appropriate.

An excavation damaged zone (EDZ) is also represented in the model as a set of fractures with appropriate hydraulic and transport properties. In the case of the main and deposition tunnels, the EDZ is represented as a set of horizontal fractures below each tunnel, with a vertical cross fracture present to provide an intersection with the tunnel floor. For the transport tunnels and ramp, the EDZ fractures are horizontal relative to the structure and intersect the bottom of the tunnel fractures. In the case of the ramp, the EDZ matches the slope of the ramp. For the shafts, the EDZ fractures intersect the centre of the shaft fractures. There is no EDZ included for the central area tunnels as it would have little effect given the relatively high conductivity of the backfill in those tunnels. Figure 2-2 shows the EDZ, coloured red, below a main tunnel and some deposition tunnels.

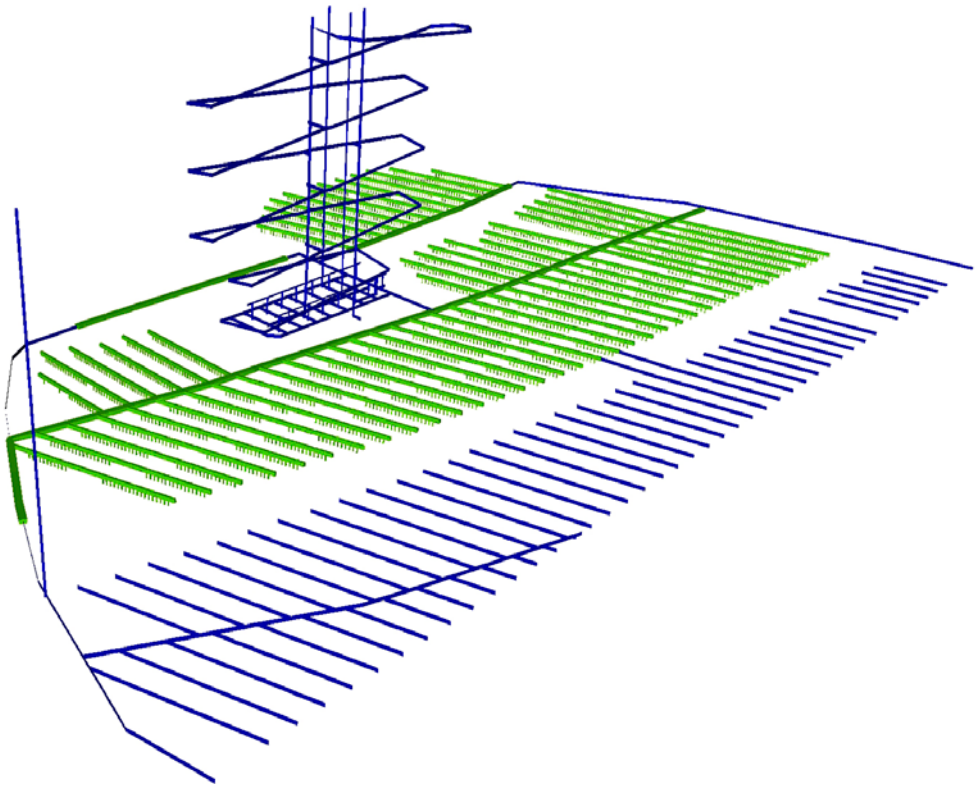

***Figure 2-1.*** *SR-Site Forsmark block 1 repository-scale structures. The CPM structures are coloured green and the fracture structures are coloured blue.*

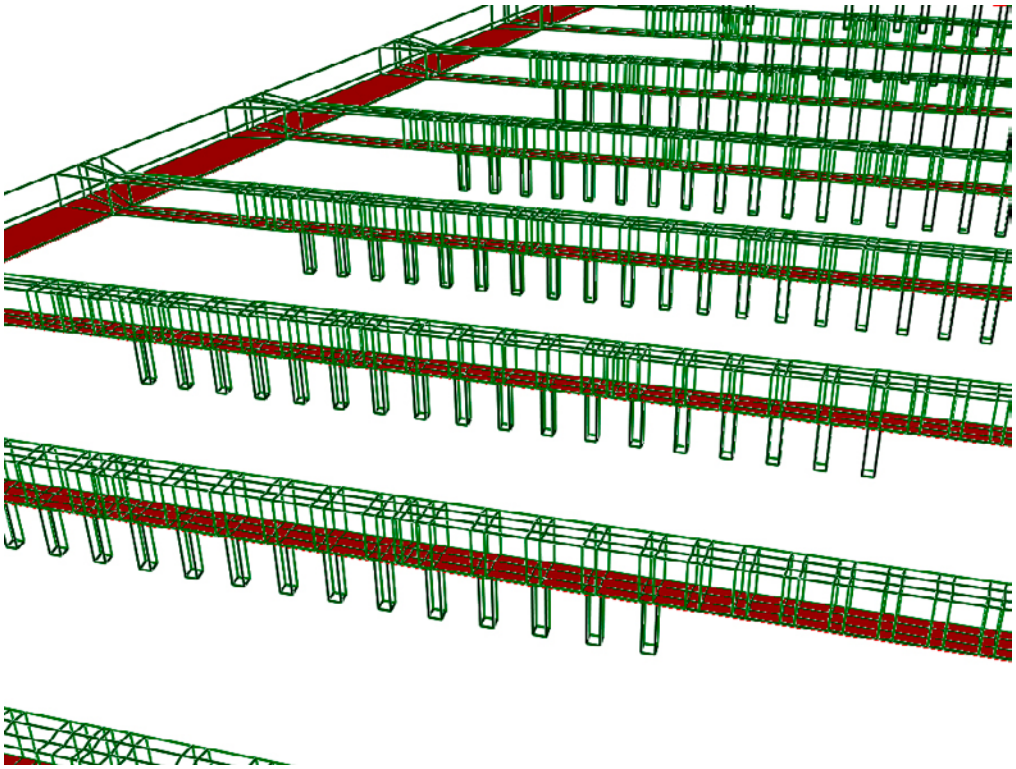

***Figure 2-2.*** *Close-up view of some block 1 deposition tunnels and part of a main tunnel. Tunnels are shown in green wireframe and the EDZ is coloured red.*

The model also includes the deformation zones and sheet joints, representing the hydraulic conductor domain (HCD), as fracture surfaces with appropriate hydraulic properties. It also includes a discrete fracture network (DFN) representation of the hydraulic rock mass domain (HRD) fractures.

Block 1 contains 1,994 deposition hole locations. As for SR-Site, three particles are released per deposition hole, corresponding to the Q1 (into a fracture intersecting a deposition hole), Q2 (into the EDZ) and Q3 (into the deposition tunnel, 1 m above the floor) release types. The particles are then tracked until they reach the boundaries of the model. Backward particle tracking is also carried out for the Q1 release locations to find the recharge pathways for the deposition holes, i.e. it tracks where the flow is coming from to each deposition hole. In SR-Site, the particles were continued in the site-scale model from the points where they exited the repository-scale blocks. However, for this study the particles will not be continued and so the performance measures will be truncated at the block boundaries. This should be sufficient, as the purpose of the study is to compare different variants where the variations are expected to have a fairly local effect, rather than to look at the absolute values of the performance measures.

The properties of the repository structures used in the SR-Site Hydrogeological base case repository-scale model are given in Table 2-1. The properties used by the variants, where applicable, are given in Table 2-2. The SR-Site properties are used for each case, except when variant properties apply that are applicable to that case.

For each case, a steady-state groundwater flow calculation is carried out using pressure boundary conditions and densities interpolated from a regional-scale model, as described in Joyce et al. (2010). Pressures and densities corresponding to 2000 AD for the temperate period and to glacial ice front location II for the glacial period are used in two separate simulations for each case. Following the flow calculations for each climate situation, particle tracking calculations are carried out. All calculations are carried out using ConnectFlow version 10.1.1 (Serco 2011a, b, c).

**Table 2-1. Properties used for repository structures in the SR-Site Hydrogeological base case (Joyce et al. 2010, Table 4-2).**

| Structure | Height (m) | Width (m) | Hydraulic conductivity (m/s) | Porosity (−) |
|---|---|---|---|---|
| Main tunnel | 6 | 10 | $1.0 \times 10^{-10}$ | 0.45 |
| Transport tunnel | 6 | 7 | $1.0 \times 10^{-10}$ | 0.45 |
| Deposition tunnel | 6 | 4 | $1.0 \times 10^{-10}$ | 0.45 |
| Deposition hole | 8 | 1.5 | $1.0 \times 10^{-12}$ | 0.41 |
| Central area tunnel | 6 | 7 | $1.0 \times 10^{-5}$ | 0.45 |
| Ramp | 6 | 5.2 | $1.0 \times 10^{-10}$ | 0.45 |
| Elevator shaft | 4.34 | 4.34 | $1.0 \times 10^{-10}$ | 0.45 |
| Skip shaft | 3.96 | 3.96 | $1.0 \times 10^{-10}$ | 0.45 |
| Air intake shaft | 3.32 | 3.32 | $1.0 \times 10^{-10}$ | 0.45 |
| Air exhaust shaft | 2.81 | 2.81 | $1.0 \times 10^{-10}$ | 0.45 |
| Deposition area air exhaust shaft | 3.07 | 3.07 | $1.0 \times 10^{-10}$ | 0.45 |
| Top sealing | N/A | N/A | $1.0 \times 10^{-1}$ | N/A |
| EDZ | 0.3 | N/A | $3.3 \times 10^{-8}$ | $1.0 \times 10^{-4}$ |

**Table 2-2. Variant repository structure properties.**

| Structure | Height (m) | Width (m) | Hydraulic conductivity (m/s) | Porosity (−) |
|---|---|---|---|---|
| Ramp | 6 | 5.2 | To be varied | 0.45 |
| Elevator shaft | 4.34 | 4.34 | To be varied | 0.45 |
| Skip shaft | 3.96 | 3.96 | To be varied | 0.45 |
| EDZ (where present) | 0.3 | N/A | To be varied | $1.0 \times 10^{-4}$ |
| Section with coarsely crushed rock | Depends on location | Depends on location | $1.0 \times 10^{-5}$ | 0.45 |
| Section with crushed compacted rock | Depends on location | Depends on location | $1.0 \times 10^{-8}$ | 0.2 |
| Investigation borehole, Case 1 Filled with bentonite | Depends on hole | 0.08 | As good as the rock or better, i.e. $< 10^{-10}$ m/s | 0.41 |
| Investigation borehole, Case 2 Filled with fine well graded rock | Depends on hole | 0.08 | $1.0 \times 10^{-8}$ | 0.2 |

## 2.1 Ramp and shaft variants

This study considers a number of variants where alternative properties are considered for the ramp and shafts, as specified in Table 2-2. In some cases, the properties of the EDZ in the ramp and shafts are also varied. A summary of the cases is given in Table 2-3. These cases are described in more detail in the following sections.

**Table 2-3. Case summary.**

| Case | Summary |
|---|---|
| SR-Site hydrogeological base case | Ramp and shafts filled with bentonite from the central area to −200 m and with rock blocks (top sealing) above −200 m. |
| Alternative 1A | Ramp and shafts filled with bentonite from the central area to −200 m, with coarsely crushed rock from −200 m to −50 m and with rock blocks (top sealing) above −50 m. |
| Alternative 1B | As for alternative 1A, but the shafts are filled with crushed compacted rock. |
| Alternative 2 | Ramp and shafts filled with bentonite from the central area to −370 m, with coarsely crushed rock from −370 m to −50 m and with rock blocks (top sealing) above −50 m. |
| Alternative 1A, more transmissive ramp/shaft EDZ | Alternative 1A, but with a hydraulic conductivity of $3.3 \times 10^{-6}$ m/s for the ramp and shaft EDZ. |
| Alternative 2, more transmissive ramp/shaft EDZ | Alternative 2, but with a hydraulic conductivity of $3.3 \times 10^{-6}$ m/s for the ramp and shaft EDZ. |
| Alternative 2, no ramp/shaft EDZ | Alternative 2, but with no ramp or shaft EDZ. |

### 2.1.1 Alternative 1A

In Alternative 1A, the ramp is filled with bentonite from the central area up to where highly transmissive deformation zones, e.g. the sheet joints, are intersected. This is estimated to be at an elevation of around −200 m. Visualisation of the locations of the most transmissive fractures showed that no fractures with transmissivities greater than $1 \times 10^{-5}$ m$^2$/s intersected the ramp below −190 m and no fractures with transmissivities greater than $1 \times 10^{-6}$ m$^2$/s intersected the ramp below −213 m for the SR-Site Hydrogeological base case model, as shown in Figure 2-3 to Figure 2-5. Therefore, −200 m was chosen as an appropriate upper elevation for the bentonite backfill in the ramp and shafts in the context of this modelling. The visualisation was done for one realisation of the model, but the other realisations are based on the same depth dependent statistical fracture properties and so the chosen depth is likely to be suitable for all realisations.

Between −200 m and −50 m, the ramp and shafts are filled with coarsely crushed rock and above −50 m with rock blocks and concrete. The hydraulic conductivity, K, for the rock block section is taken to be $1 \times 10^{-1}$ m/s. Figure 2-6 shows the repository structures in the Alternative 1A model.

A variant of the Alternative 1A case is considered to examine the influence of the EDZ in the ramp and shafts. In this variant, the hydraulic conductivity of the EDZ in the ramp and shafts is increased to $3.3 \times 10^{-6}$ m/s.

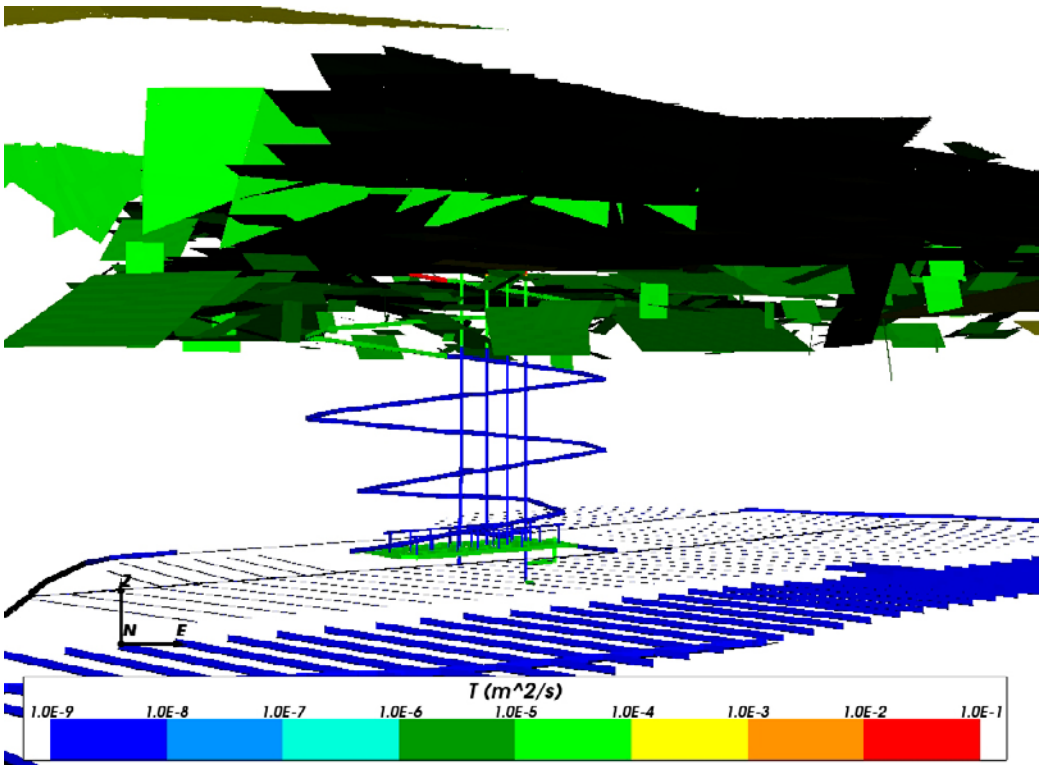


***Figure 2-3.*** *Fractures with transmissivities greater than $1 \times 10^{-5}$ m$^2$/s in relation to the ramp in the SR-Site Hydrogeological base case model.*

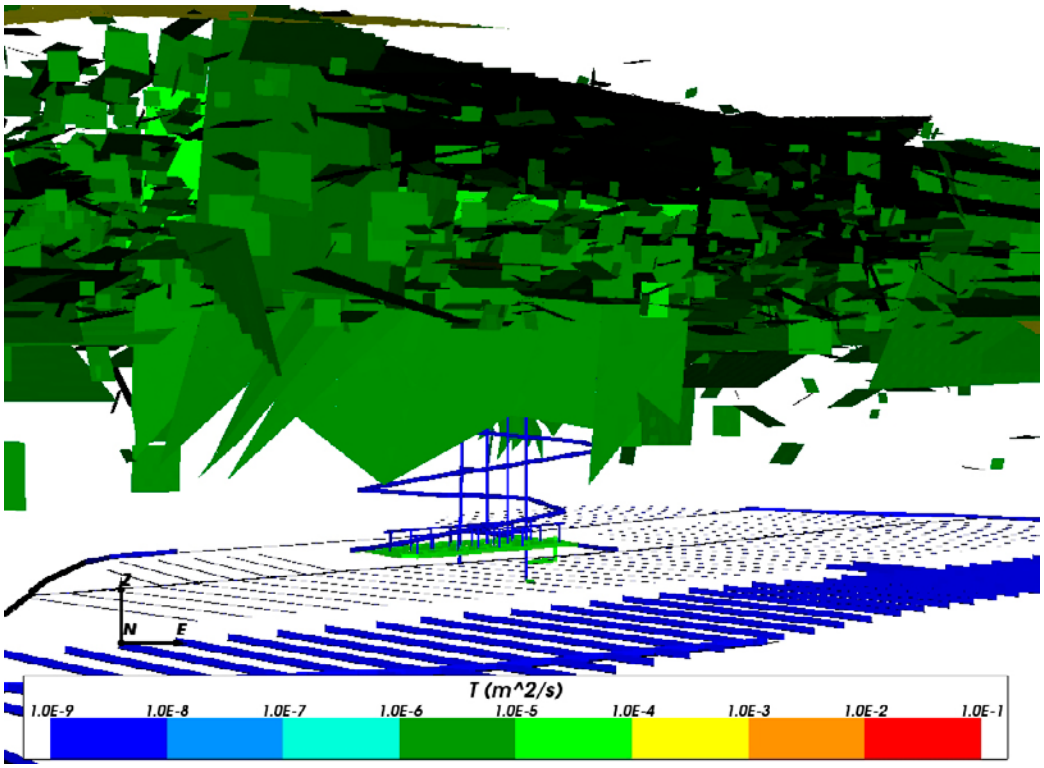


***Figure 2-4.*** *Fractures with transmissivities greater than $1 \times 10^{-6}$ $m^2/s$ in relation to the ramp in the SR-Site Hydrogeological base case model.*

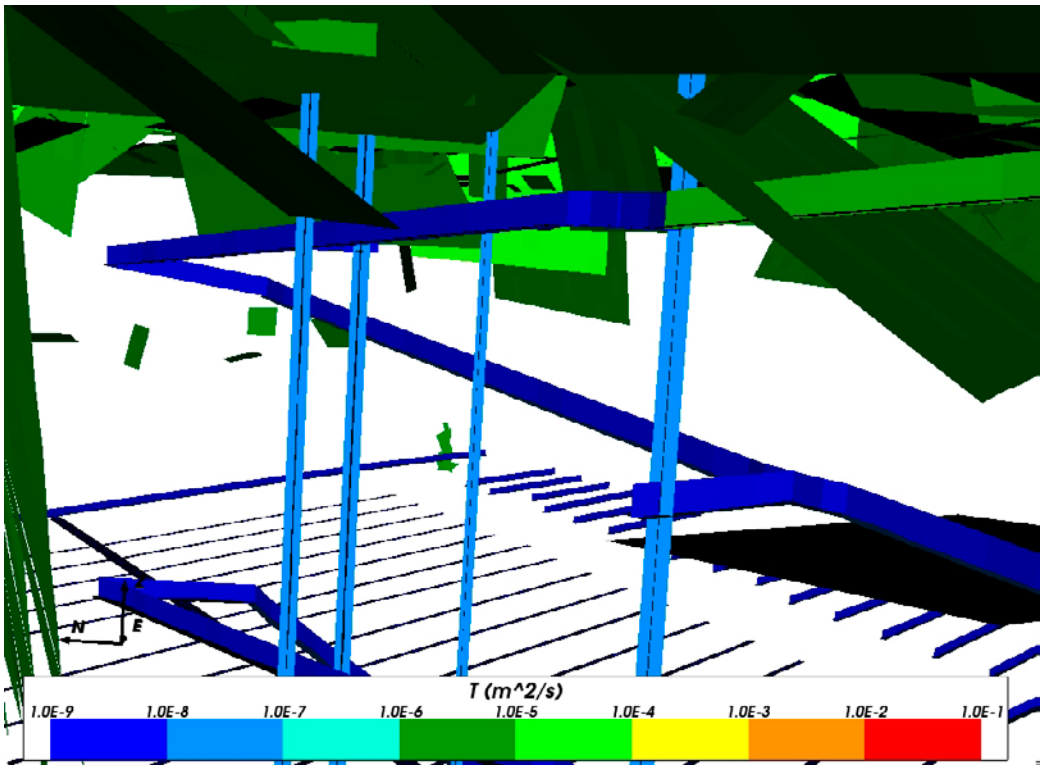


***Figure 2-5.*** *Close up view of fractures with transmissivities greater than $1 \times 10^{-6}$ $m^2/s$ in relation to the ramp in the SR-Site Hydrogeological base case model.*

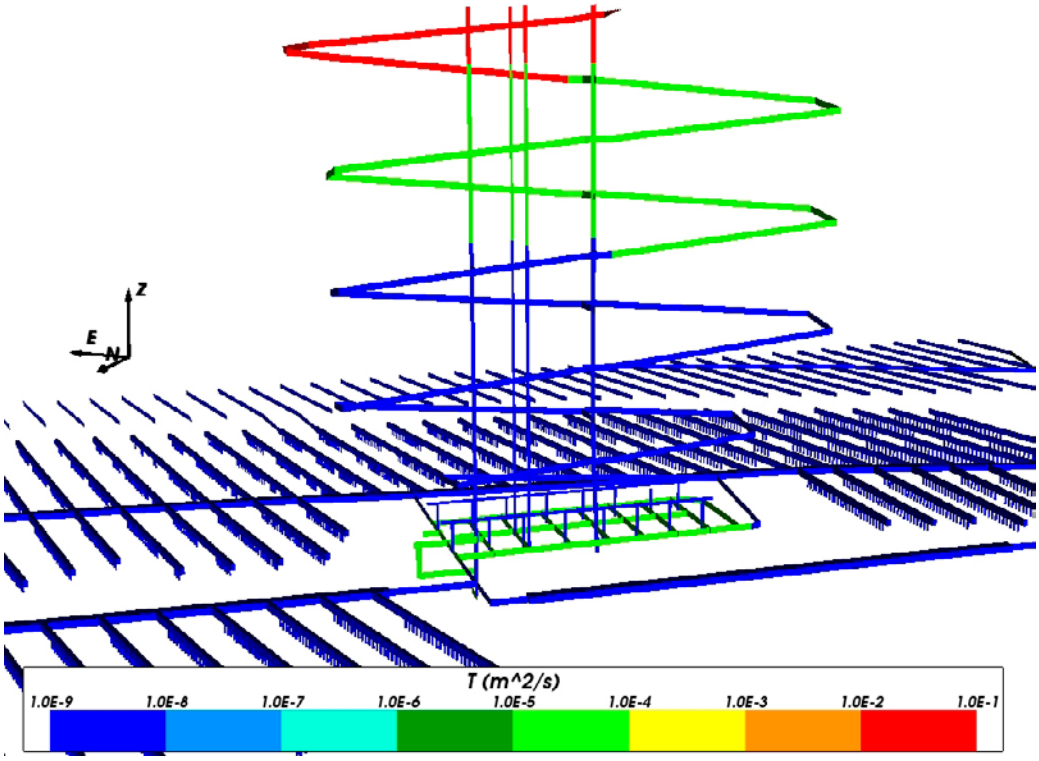


***Figure 2-6.*** *Repository structures for Alternative 1A coloured by transmissivity (fracture representation) or hydraulic conductivity (CPM representation).*

### 2.1.2 Alternative 1B

Alternative 1B is the same as Alternative 1A, except that the shafts are filled with crushed and compacted rock (hydraulic conductivity $1.0 \times 10^{-8}$ m/s) for their entire lengths. Figure 2-7 shows the repository structures in the Alternative 1B model. There are no EDZ variants of this model.

### 2.1.3 Alternative 2

In Alternative 2, the ramp is filled with bentonite from the central area up to 100 m above the repository area. In the model, this is taken to be at an elevation of −370 m.

Between −370 m and −50 m the ramp and shafts are filled with coarsely crushed rock and above −50 m with rock blocks and concrete. The hydraulic conductivity, K, for the rock block section is taken to be $1 \times 10^{-1}$ m/s. Figure 2-8 shows the repository structures in the Alternative 2 model.

Two variants of the Alternative 2 case are considered to examine the influence of the EDZ in the ramp and shafts. In the first variant, the hydraulic conductivity of the EDZ in the ramp and shafts is increased to $3.3 \times 10^{-6}$ m/s. In the second variant, the EDZ for the ramp and shafts is removed.

The standard case consists of an HCD with deterministic depth dependent properties and one realisation of a stochastic HRD. Two additional realisations (denoted r2 and r3) are also considered for this case. Each additional realisation consists of a different realisation of an HCD with stochastic properties, representing lateral heterogeneity, and a different realisation of an HRD. These correspond to realisations r2 and r3 in the SR-Site temperate period modelling.

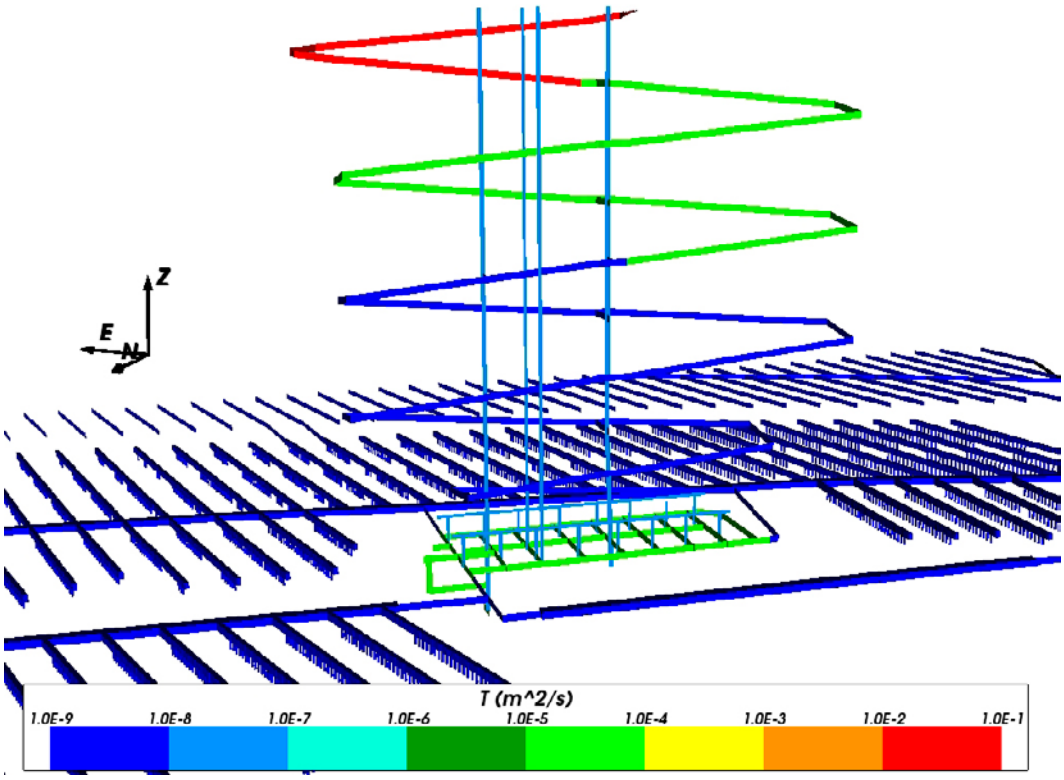


***Figure 2-7.*** *Repository structures for Alternative 1B coloured by transmissivity (fracture representation) or hydraulic conductivity (CPM representation).*

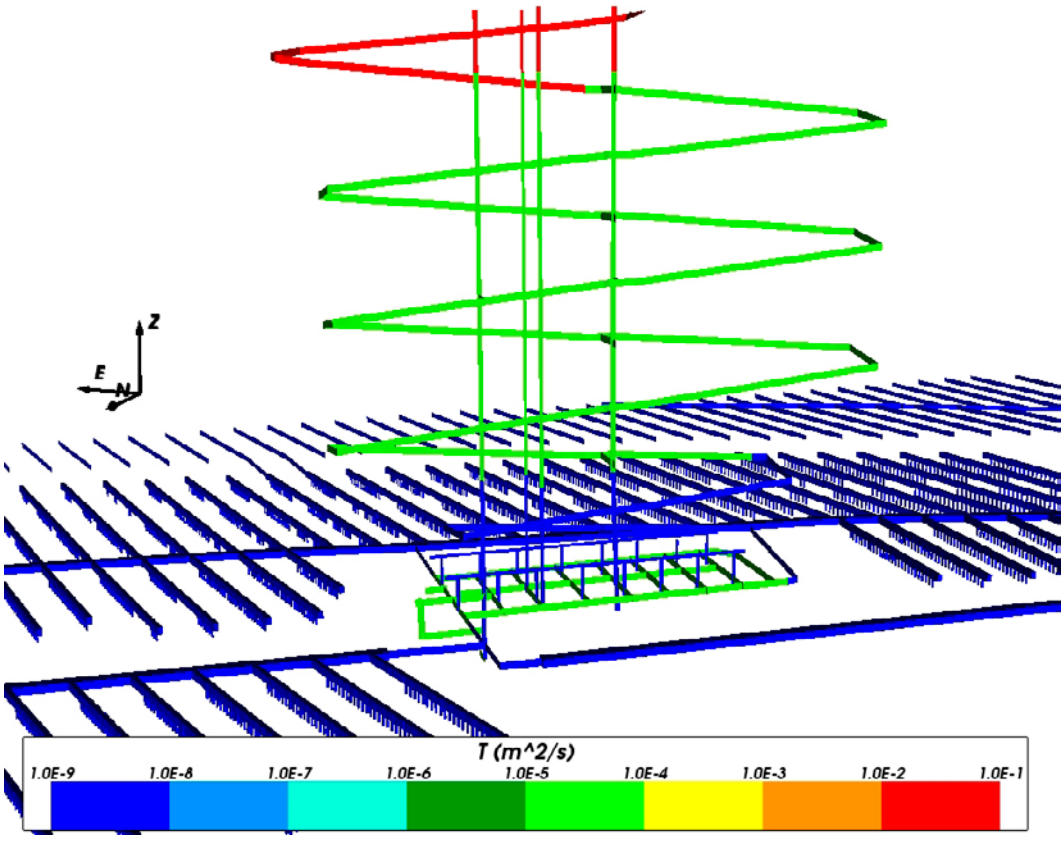


***Figure 2-8.*** *Repository structures for Alternative 2 coloured by transmissivity (fracture representation) or hydraulic conductivity (CPM representation).*

## 2.2 Sealing of investigation boreholes

In this task, an analysis is performed of what hydraulic conductivity would be acceptable in the sealed investigation boreholes without influencing the performance measures relevant for penetration of oxygen and radionuclide transport too much. The task is to try to find the appropriate hydraulic conductivity (K) of the filling material. Properties for two cases were suggested to start with. One with the reference design (Case 1) which means hydraulic properties similar to the rock or better (the boreholes will mainly be filled with bentonite, i.e. $K <= 10^{-10}$ m/s) and one with $K = 10^{-8}$ m/s (Case 2), which is achieved by filling the boreholes with fine, well graded rock. Apart from these two cases, a sensitivity series was set up, applying conductivities from $10^{-7}$ m/s up to $10^{-2}$ m/s in steps of an order of magnitude. The borehole properties used are given in Table 3-25.

In the reference design, borehole sections intersected by transmissive fracture zones are filled with silica concrete, which is permeable and erosion-resistant. In this study, no such features were included due to time constraints.

The hydrogeological model developed for Alternative 1A, as described in Section 2.1.1, was used as a base for the borehole model. That case consists of an HCD with deterministic depth dependent properties and one realisation of a stochastic HRD. Two additional realisations (denoted r2 and r3) are also considered for this case. Each additional realisation consists of a different realisation of an HCD with stochastic properties, representing lateral heterogeneity, and a different realisation of an HRD. These correspond to realisations r2 and r3 in the SR-Site temperate period modelling.

The existing investigation boreholes at Forsmark, within the model area of block 1, were then added to the repository-scale model as narrow deterministic fractures with a width and thickness of 0.08 m (equivalent to the diameter of a standard core-drilled Forsmark borehole). The block 1 model of the repository covers six percussion-drilled boreholes (HFM20-HFM23, HFM28 and HFM38) and eight core-drilled boreholes (KFM07A-C, KFM08A-C and KFM09A-B) at the Forsmark investigation site. The geometry of the boreholes was honoured in the model by using the coordinate data along the boreholes. However, for practical reasons, the cross-section of the boreholes had to be squared. Also, all the boreholes in the model have the same uniform thickness at all depths, which is not necessarily the case in reality, see Figure 2-9. However, it was outside the scope of this study to make an individually adjusted representation of every single borehole. Also, because there was no interest in studying the influence of individual boreholes, all boreholes were included in a single model.

The modelled HFM and KFM boreholes are shown, together with repository block 1, in Figure 2-10.

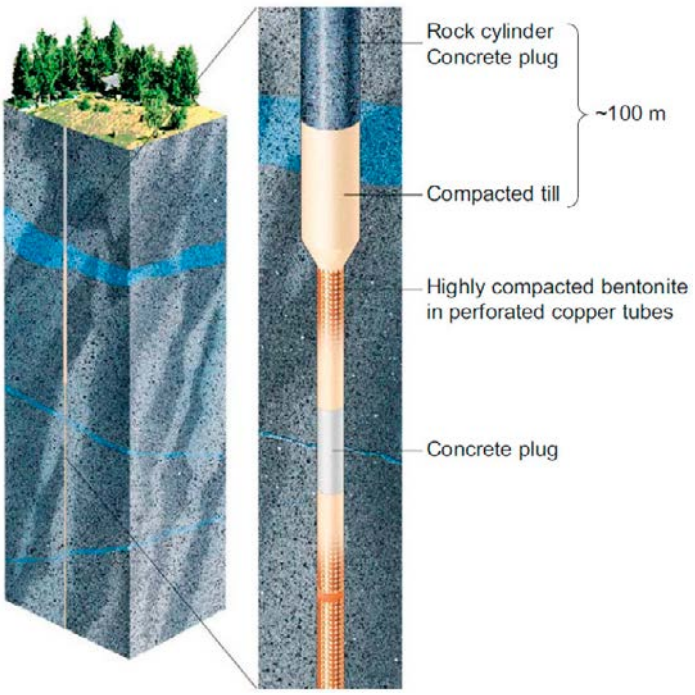


***Figure 2-9.*** *Sealing of investigation boreholes.*

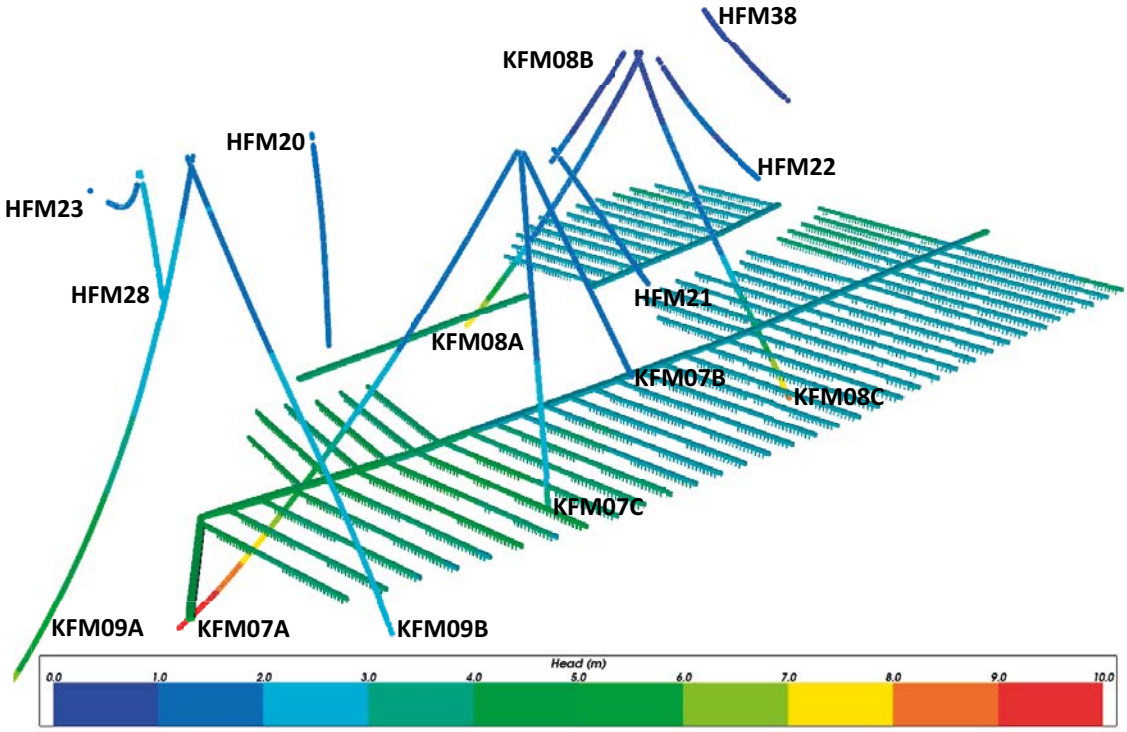


***Figure 2-10.*** *Modelled HFM and KFM boreholes shown together with the CPM repository structures in block 1. All structures are coloured by modelled head (blue is low, red is high). The surrounding DFN model has been removed for visibility.*

# 3 Results

The results give statistical summaries for the performance measures considered. The performance measures considered are travel time in the rock, $t_r$, equivalent Darcy Flux in the rock at the particle starting locations, $U_r$, and flow-related transport resistance in the rock, $F_r$. These are fully described in Joyce et al. (2010). The statistics reported are the median, standard deviation, 10$^{th}$ percentile and 90$^{th}$ percentile for those particles that successfully reach the model boundary ($U_r$ for Q3, $t_r$, and $F_r$) or for those particles that successfully start ($U_r$ for Q1 and Q2). A particle may not reach the model boundary if it becomes stuck due to numerical reasons. A particle successfully starts if there is a fracture available (Q1) and if the flow rate per unit fracture width exceeds $1.0 \times 10^{-6}$ m$^2$/y (Q1 and Q2) or the Darcy flux exceeds $1.0 \times 10^{-6}$ m/y (Q3). The same starting criteria are applied for both backward and forward particle tracking. Note that the $t_r$ and $F_r$ values only represent the portion of the path within block 1 and do not represent the full path to the ground surface, hence they will be partially truncated, especially for more horizontal paths or downward paths.

Cumulative distribution function (CDF) plots show the cumulative fraction of particles as a function of performance measure value. They allow the distribution of performance measure values to be readily seen, including the tails of those distributions. Normalised plots filter out particles that do not start and particles that do not reach the boundaries of the model and then re-normalise the proportions to the range zero to one.

Bar and whisker plots show side by side comparisons of statistical measures for each variant, including the median (red circle and line), 25$^{th}$ and 75$^{th}$ percentile (blue bar) and the 5$^{th}$ and 95$^{th}$ percentile (black "whiskers").

## 3.1 Ramp and shaft variants

Table 3-1 to Table 3-24 give statistical summaries for the performance measures for each of the cases for the temperate climate situation (2000 AD) and the glacial climate situation (glacial ice front location II). In general, the median $U_r$ and $F_r$ values are similar to those reported in Bockgård (2010), but the median $t_r$ values are about a factor of ten lower than those in Bockgård (2010). The differences in travel times could be due to differences in the transmissivity-transport aperture relationship, as discussed in Joyce et al. (2010).

Figure 3-1 to Figure 3-24 give the corresponding normalised cumulative distribution function (CDF) plots for the performance measures.

The results show that changing the properties of the ramp and shafts or the EDZ for the ramp and shafts has little effect on the performance measure statistics or the distribution of performance measures. The differences in median or 10$^{th}$ percentile values between the cases are at most around 25 % and usually much less.

Although there are differences in performance measures (particularly for $t_r$ and $U_r$) between the different realisations considered for alternative 2, there is little difference in performance measures between variants for a given realisation. This indicates that the effect of the ramp and shaft properties on performance measures is not sensitive to the realisation considered.

Figure 3-25 to Figure 3-28 for the Alternative 1A case show that the recharge pathways (purple) are mostly vertical and from below in the portion of the site covered by block 1. Even those few recharge pathways that originate on the top surface of the block 1 model are not close to the ramp. Therefore the properties of the ramp and shafts have little effect on the performance measures of the recharge pathways in the model.

Figure 3-25 and Figure 3-26 for the Alternative 1A case at 2000 AD show that the discharge pathways (orange) are mostly vertical and exit on the top surface of the block 1 model, i.e. the tops of the ramp and shaft are in a discharge area at 2000 AD. The exit points are dominated by the location of outcropping deformation zones, but a few particles exit near to the ramp. This suggests that the

properties of the ramp and shafts could have an effect on the performance measures for a few of the discharge pathways. This is reflected in minor changes to the $t_r$ and $F_r$ performance measures. The $U_r$ performance measure is largely unaffected by the changes to the ramp and shaft properties since it is calculated at, or close to, the starting location. These locations are generally distant from the ramp and shafts and so the flow at these locations, and hence $U_r$, is unlikely to be significantly affected by the ramp and shaft properties.

The Q2 and Q3 pathways seem to be less affected by changes in the ramp and shaft properties than the Q1 pathways. This suggests that the changes are not having a significant effect on the flows in the tunnels and EDZ. In the case of the EDZ, even though there is extensive connectivity between EDZ sections, the EDZ flow is largely between fractures intersecting tunnels and so is quite localised. Hence, changing the EDZ transmissivity in the ramp and shafts does not significantly affect the flow in the EDZ for the deposition tunnels.

Figure 3-27 and Figure 3-28 show the recharge (purple) and discharge (orange) pathways and exit locations for the Alternative 1A case for glacial ice front location II. Figure 3-27 shows all paths that reach a model boundary, whereas Figure 3-28 only shows the exit locations of particles successfully reaching the top surface. The discharge pathways are less vertical than at 2000 AD and they tend to exit more to the southeast. Thus the discharge pathways are even further from the ramp and so the effect on performance measures of the ramp and shaft properties is generally reduced under glacial conditions compared to temperate conditions. Most of the recharge is from the northwest, outside the repository area. The ice sheet pressure at the top of the ramp is largely dissipated by the sheet joints and extensive sub-horizontal fracturing in the upper 200 m of bedrock, and doesn't penetrate to repository depth, so there is no recharge to the repository from the top of the ramp. The general patterns of recharge and discharge at 2000 AD and for glacial ice front location II are consistent with those reported in Bockgård (2010).

Figure 3-29 for the Alternative 2 case at 2000 AD shows that the recharge and discharge exit locations are generally in the same locations as for the Alternative 1A case, but there are some changes for individual particles. Since the paths in the DFN are stochastic, they are sensitive to any change in the flow and this can lead to very different paths for individual particles.

Figure 3-30 to Figure 3-33 show Q1 paths for different cases at 2000 AD that use parts of the ramp or shafts, or both. However, there are only a few paths for each case that use the ramp or shafts. Also, only the upper parts of the ramp and shafts are used rather than the lower, bentonite filled sections. For the glacial climate situation the predominant flow towards the southeast carries particles away from the ramp and shafts and so they do not enter these structures.

### *Discharge temperate conditions*

**Table 3-1. Travel time in the rock, $t_r$, statistics for Q1 discharge particles released at 2000 AD and successfully reaching the model boundary (~25 %).**

| Case | $\log_{10}(t_r)$ [y] | | | |
|---|---|---|---|---|
| | Median | Std. dev. | 10 % | 90 % |
| SR-Site Hydrogeological base case | 2.285 | 0.397 | 1.772 | 2.719 |
| SR-Site Hydrogeological base case, realisation 2 | 2.221 | 0.461 | 1.760 | 2.641 |
| SR-Site Hydrogeological base case, realisation 3 | 2.128 | 0.413 | 1.595 | 2.662 |
| Alternative 1A | 2.277 | 0.385 | 1.768 | 2.707 |
| Alternative 1B | 2.286 | 0.373 | 1.753 | 2.700 |
| Alternative 2 | 2.292 | 0.396 | 1.779 | 2.752 |
| Alternative 2, realisation 2 | 2.186 | 0.481 | 1.766 | 2.585 |
| Alternative 2, realisation 3 | 2.151 | 0.408 | 1.597 | 2.597 |
| Alternative 1A, more transmissive ramp/shaft EDZ | 2.260 | 0.418 | 1.799 | 2.739 |
| Alternative 2, more transmissive ramp/shaft EDZ | 2.251 | 0.401 | 1.810 | 2.748 |
| Alternative 2, more transmissive ramp/shaft EDZ, realisation 2 | 2.203 | 0.471 | 1.680 | 2.611 |
| Alternative 2, more transmissive ramp/shaft EDZ, realisation 3 | 2.118 | 0.399 | 1.598 | 2.580 |
| Alternative 2, no ramp/shaft EDZ | 2.246 | 0.389 | 1.768 | 2.708 |

**Table 3-2. Initial equivalent Darcy flux in the rock, $U_r$, statistics for Q1 discharge particles released at 2000 AD and successfully starting (26 % to 31 %).**

| Case | $\log_{10}(U_r)$ [m/y] | | | |
|---|---|---|---|---|
| | Median | Std. dev. | 10 % | 90 % |
| SR-Site Hydrogeological base case | −5.321 | 1.039 | −6.719 | −4.135 |
| SR-Site Hydrogeological base case, realisation 2 | −5.419 | 1.147 | −6.753 | −3.924 |
| SR-Site Hydrogeological base case, realisation 3 | −5.164 | 1.196 | −6.655 | −3.443 |
| Alternative 1A | −5.322 | 1.037 | −6.712 | −4.132 |
| Alternative 1B | −5.322 | 1.037 | −6.712 | −4.132 |
| Alternative 2 | −5.323 | 1.039 | −6.723 | −4.134 |
| Alternative 2, realisation 2 | −5.424 | 1.146 | −6.752 | −3.924 |
| Alternative 2, realisation 3 | −5.157 | 1.196 | −6.656 | −3.443 |
| Alternative 1A, more transmissive ramp/shaft EDZ | −5.322 | 1.039 | −6.723 | −4.134 |
| Alternative 2, more transmissive ramp/shaft EDZ | −5.323 | 1.040 | −6.723 | −4.134 |
| Alternative 2, more transmissive ramp/shaft EDZ, realisation 2 | −5.424 | 1.145 | −6.752 | −3.926 |
| Alternative 2, more transmissive ramp/shaft EDZ, realisation 3 | −5.155 | 1.196 | −6.656 | −3.443 |
| Alternative 2, no ramp/shaft EDZ | −5.323 | 1.039 | −6.723 | −4.134 |

**Table 3-3. Flow-related transport resistance in the rock, $F_r$, statistics for Q1 discharge particles released at 2000 AD and successfully reaching the model boundary (~25 %).**

| Case | $\log_{10}(F_r)$ [y/m] | | | |
|---|---|---|---|---|
| | Median | Std. dev. | 10 % | 90 % |
| SR-Site Hydrogeological base case | 6.497 | 0.695 | 5.728 | 7.278 |
| SR-Site Hydrogeological base case, realisation 2 | 6.626 | 0.792 | 5.648 | 7.473 |
| SR-Site Hydrogeological base case, realisation 3 | 6.465 | 0.737 | 5.559 | 7.410 |
| Alternative 1A | 6.537 | 0.692 | 5.708 | 7.343 |
| Alternative 1B | 6.513 | 0.660 | 5.721 | 7.401 |
| Alternative 2 | 6.536 | 0.699 | 5.755 | 7.428 |
| Alternative 2, realisation 2 | 6.608 | 0.812 | 5.633 | 7.460 |
| Alternative 2, realisation 3 | 6.451 | 0.699 | 5.576 | 7.273 |
| Alternative 1A, more transmissive ramp/shaft EDZ | 6.504 | 0.745 | 5.652 | 7.477 |
| Alternative 2, more transmissive ramp/shaft EDZ | 6.497 | 0.708 | 5.674 | 7.460 |
| Alternative 2, more transmissive ramp/shaft EDZ, realisation 2 | 6.611 | 0.789 | 5.676 | 7.437 |
| Alternative 2, more transmissive ramp/shaft EDZ, realisation 3 | 6.443 | 0.712 | 5.552 | 7.316 |
| Alternative 2, no ramp/shaft EDZ | 6.531 | 0.697 | 5.683 | 7.363 |

**Table 3-4. Travel time in the rock, $t_r$, statistics for Q2 discharge particles released at 2000 AD and successfully reaching the model boundary (81 % to 93 %).**

| Case | $\log_{10}(t_r)$ [y] | | | |
|---|---|---|---|---|
| | Median | Std. dev. | 10 % | 90 % |
| SR-Site Hydrogeological base case | 2.242 | 0.377 | 1.747 | 2.671 |
| SR-Site Hydrogeological base case, realisation 2 | 2.177 | 0.421 | 1.748 | 2.546 |
| SR-Site Hydrogeological base case, realisation 3 | 2.056 | 0.409 | 1.572 | 2.584 |
| Alternative 1A | 2.234 | 0.362 | 1.764 | 2.650 |
| Alternative 1B | 2.243 | 0.377 | 1.761 | 2.695 |
| Alternative 2 | 2.223 | 0.372 | 1.757 | 2.651 |
| Alternative 2, realisation 2 | 2.170 | 0.419 | 1.743 | 2.541 |
| Alternative 2, realisation 3 | 2.063 | 0.422 | 1.562 | 2.604 |
| Alternative 1A, more transmissive ramp/shaft EDZ | 2.240 | 0.372 | 1.759 | 2.678 |
| Alternative 2, more transmissive ramp/shaft EDZ | 2.233 | 0.369 | 1.759 | 2.663 |
| Alternative 2, more transmissive ramp/shaft EDZ, realisation 2 | 2.158 | 0.429 | 1.738 | 2.538 |
| Alternative 2, more transmissive ramp/shaft EDZ, realisation 3 | 2.068 | 0.413 | 1.594 | 2.603 |
| Alternative 2, no ramp/shaft EDZ | 2.233 | 0.368 | 1.751 | 2.655 |

**Table 3-5. Initial equivalent Darcy flux in the rock, $U_r$, statistics for Q2 discharge particles released at 2000 AD and successfully starting (~100 %).**

| Case | $\log_{10}(U_r)$ [m/y] | | | |
|---|---|---|---|---|
| | Median | Std. dev. | 10 % | 90 % |
| SR-Site Hydrogeological base case | −2.100 | 0.373 | −2.483 | −1.559 |
| SR-Site Hydrogeological base case, realisation 2 | −2.127 | 0.312 | −2.492 | −1.770 |
| SR-Site Hydrogeological base case, realisation 3 | −2.082 | 0.363 | −2.551 | −1.634 |
| Alternative 1A | −2.100 | 0.373 | −2.483 | −1.558 |
| Alternative 1B | −2.100 | 0.373 | −2.484 | −1.557 |
| Alternative 2 | −2.100 | 0.373 | −2.483 | −1.558 |
| Alternative 2, realisation 2 | −2.127 | 0.313 | −2.492 | −1.771 |
| Alternative 2, realisation 3 | −2.083 | 0.364 | −2.551 | −1.629 |
| Alternative 1A, more transmissive ramp/shaft EDZ | −2.100 | 0.373 | −2.482 | −1.556 |
| Alternative 2, more transmissive ramp/shaft EDZ | −2.099 | 0.373 | −2.481 | −1.556 |
| Alternative 2, more transmissive ramp/shaft EDZ, realisation 2 | −2.127 | 0.314 | −2.492 | −1.771 |
| Alternative 2, more transmissive ramp/shaft EDZ, realisation 3 | −2.083 | 0.363 | −2.551 | −1.636 |
| Alternative 2, no ramp/shaft EDZ | −2.101 | 0.374 | −2.484 | −1.558 |

**Table 3-6. Flow-related transport resistance in the rock, $F_r$, statistics for Q2 discharge particles released at 2000 AD and successfully reaching the model boundary (81 % to 93 %).**

| Case | $\log_{10}(F_r)$ [y/m] | | | |
|---|---|---|---|---|
| | Median | Std. dev. | 10 % | 90 % |
| SR-Site Hydrogeological base case | 6.157 | 0.773 | 5.172 | 7.112 |
| SR-Site Hydrogeological base case, realisation 2 | 6.309 | 0.807 | 5.298 | 7.189 |
| SR-Site Hydrogeological base case, realisation 3 | 6.134 | 0.794 | 5.104 | 7.157 |
| Alternative 1A | 6.207 | 0.766 | 5.217 | 7.116 |
| Alternative 1B | 6.225 | 0.788 | 5.142 | 7.160 |
| Alternative 2 | 6.181 | 0.777 | 5.164 | 7.141 |
| Alternative 2, realisation 2 | 6.264 | 0.804 | 5.255 | 7.157 |
| Alternative 2, realisation 3 | 6.130 | 0.824 | 5.095 | 7.159 |
| Alternative 1A, more transmissive ramp/shaft EDZ | 6.211 | 0.770 | 5.197 | 7.126 |
| Alternative 2, more transmissive ramp/shaft EDZ | 6.201 | 0.783 | 5.227 | 7.183 |
| Alternative 2, more transmissive ramp/shaft EDZ, realisation 2 | 6.284 | 0.799 | 5.256 | 7.141 |
| Alternative 2, more transmissive ramp/shaft EDZ, realisation 3 | 6.145 | 0.812 | 5.087 | 7.120 |
| Alternative 2, no ramp/shaft EDZ | 6.205 | 0.762 | 5.137 | 7.108 |

**Table 3-7. Travel time in the rock, $t_r$, statistics for Q3 discharge particles released at 2000 AD and successfully reaching the model boundary (68 % to 79 %).**

| Case | $\log_{10}(t_r)$ [y] | | | |
|---|---|---|---|---|
| | Median | Std. dev. | 10 % | 90 % |
| SR-Site Hydrogeological base case | 2.229 | 0.366 | 1.739 | 2.635 |
| SR-Site Hydrogeological base case, realisation 2 | 2.171 | 0.426 | 1.739 | 2.541 |
| SR-Site Hydrogeological base case, realisation 3 | 2.042 | 0.396 | 1.549 | 2.534 |
| Alternative 1A | 2.218 | 0.369 | 1.733 | 2.645 |
| Alternative 1B | 2.222 | 0.354 | 1.757 | 2.616 |
| Alternative 2 | 2.219 | 0.356 | 1.749 | 2.615 |
| Alternative 2, realisation 2 | 2.162 | 0.428 | 1.741 | 2.538 |
| Alternative 2, realisation 3 | 2.029 | 0.401 | 1.565 | 2.550 |
| Alternative 1A, more transmissive ramp/shaft EDZ | 2.205 | 0.367 | 1.725 | 2.627 |
| Alternative 2, more transmissive ramp/shaft EDZ | 2.208 | 0.366 | 1.745 | 2.627 |
| Alternative 2, more transmissive ramp/shaft EDZ, realisation 2 | 2.156 | 0.434 | 1.730 | 2.542 |
| Alternative 2, more transmissive ramp/shaft EDZ, realisation 3 | 2.033 | 0.385 | 1.572 | 2.550 |
| Alternative 2, no ramp/shaft EDZ | 2.212 | 0.365 | 1.743 | 2.627 |

**Table 3-8. Initial equivalent Darcy flux in the rock, $U_r$, statistics for Q3 discharge particles released at 2000 AD and successfully starting (81 % to 83 %).**

| Case | $\log_{10}(U_r)$ [m/y] | | | |
|---|---|---|---|---|
| | Median | Std. dev. | 10 % | 90 % |
| SR-Site Hydrogeological base case | −3.384 | 0.701 | −4.278 | −2.725 |
| SR-Site Hydrogeological base case, realisation 2 | −3.414 | 0.719 | −4.376 | −2.785 |
| SR-Site Hydrogeological base case, realisation 3 | −3.371 | 0.719 | −4.379 | −2.771 |
| Alternative 1A | −3.380 | 0.721 | −4.450 | −2.742 |
| Alternative 1B | −3.376 | 0.675 | −4.259 | −2.731 |
| Alternative 2 | −3.394 | 0.699 | −4.322 | −2.717 |
| Alternative 2, realisation 2 | −3.407 | 0.743 | −4.355 | −2.776 |
| Alternative 2, realisation 3 | −3.367 | 0.710 | −4.365 | −2.781 |
| Alternative 1A, more transmissive ramp/shaft EDZ | −3.391 | 0.730 | −4.343 | −2.689 |
| Alternative 2, more transmissive ramp/shaft EDZ | −3.397 | 0.709 | −4.269 | −2.704 |
| Alternative 2, more transmissive ramp/shaft EDZ, realisation 2 | −3.402 | 0.711 | −4.246 | −2.755 |
| Alternative 2, more transmissive ramp/shaft EDZ, realisation 3 | −3.372 | 0.705 | −4.384 | −2.763 |
| Alternative 2, no ramp/shaft EDZ | −3.402 | 0.710 | −4.304 | −2.718 |

**Table 3-9. Flow-related transport resistance in the rock, $F_r$, statistics for Q3 discharge particles released at 2000 AD and successfully reaching the model boundary (68 % to 79 %).**

| Case | $\log_{10}(F_r)$ [y/m] | | | |
|---|---|---|---|---|
| | Median | Std. dev. | 10 % | 90 % |
| SR-Site Hydrogeological base case | 6.188 | 0.727 | 5.162 | 6.989 |
| SR-Site Hydrogeological base case, realisation 2 | 6.239 | 0.796 | 5.216 | 7.113 |
| SR-Site Hydrogeological base case, realisation 3 | 6.064 | 0.777 | 5.001 | 6.973 |
| Alternative 1A | 6.198 | 0.747 | 5.153 | 6.998 |
| Alternative 1B | 6.197 | 0.719 | 5.167 | 6.974 |
| Alternative 2 | 6.158 | 0.698 | 5.213 | 6.951 |
| Alternative 2, realisation 2 | 6.238 | 0.778 | 5.244 | 7.069 |
| Alternative 2, realisation 3 | 6.090 | 0.763 | 5.049 | 6.982 |
| Alternative 1A, more transmissive ramp/shaft EDZ | 6.154 | 0.727 | 5.166 | 6.958 |
| Alternative 2, more transmissive ramp/shaft EDZ | 6.152 | 0.736 | 5.164 | 6.971 |
| Alternative 2, more transmissive ramp/shaft EDZ, realisation 2 | 6.194 | 0.772 | 5.215 | 7.079 |
| Alternative 2, more transmissive ramp/shaft EDZ, realisation 3 | 6.082 | 0.743 | 5.084 | 6.968 |
| Alternative 2, no ramp/shaft EDZ | 6.179 | 0.734 | 5.154 | 6.997 |

### *Recharge temperate conditions*

**Table 3-10. Travel time in the rock, $t_r$, statistics for Q1 recharge particles released at 2000 AD and successfully tracked back to the model boundary (16 % to 23 %).**

| Case | $\log_{10}(t_r)$ [y] | | | |
|---|---|---|---|---|
| | Median | Std. dev. | 10 % | 90 % |
| SR-Site Hydrogeological base case | 1.852 | 0.674 | 0.831 | 2.480 |
| SR-Site Hydrogeological base case, realisation 2 | 1.840 | 0.682 | 1.008 | 2.478 |
| SR-Site Hydrogeological base case, realisation 3 | 1.589 | 0.656 | 0.764 | 2.300 |
| Alternative 1A | 1.830 | 0.684 | 0.864 | 2.484 |
| Alternative 1B | 1.830 | 0.664 | 0.915 | 2.498 |
| Alternative 2 | 1.844 | 0.674 | 0.844 | 2.437 |
| Alternative 2, realisation 2 | 1.843 | 0.699 | 0.921 | 2.514 |
| Alternative 2, realisation 3 | 1.609 | 0.678 | 0.657 | 2.321 |
| Alternative 1A, more transmissive ramp/shaft EDZ | 1.838 | 0.664 | 0.854 | 2.466 |
| Alternative 2, more transmissive ramp/shaft EDZ | 1.855 | 0.665 | 0.847 | 2.451 |
| Alternative 2, more transmissive ramp/shaft EDZ, realisation 2 | 1.852 | 0.667 | 0.826 | 2.390 |
| Alternative 2, more transmissive ramp/shaft EDZ, realisation 3 | 1.606 | 0.665 | 0.731 | 2.334 |
| Alternative 2, no ramp/shaft EDZ | 1.827 | 0.677 | 0.832 | 2.479 |

**Table 3-11. Initial equivalent Darcy flux in the rock, $U_r$, statistics for Q1 recharge particles released at 2000 AD and successfully starting (21 % to 27 %).**

| Case | $\log_{10}(U_r)$ [m/y] | | | |
|---|---|---|---|---|
| | Median | Std. dev. | 10 % | 90 % |
| SR-Site Hydrogeological base case | −5.298 | 1.070 | −6.702 | −4.087 |
| SR-Site Hydrogeological base case, realisation 2 | −5.482 | 1.229 | −6.800 | −3.755 |
| SR-Site Hydrogeological base case, realisation 3 | −5.136 | 1.241 | −6.615 | −3.345 |
| Alternative 1A | −5.304 | 1.069 | −6.703 | −4.087 |
| Alternative 1B | −5.304 | 1.069 | −6.703 | −4.087 |
| Alternative 2 | −5.304 | 1.070 | −6.703 | −4.087 |
| Alternative 2, realisation 2 | −5.483 | 1.229 | −6.796 | −3.755 |
| Alternative 2, realisation 3 | −5.139 | 1.240 | −6.612 | −3.348 |
| Alternative 1A, more transmissive ramp/shaft EDZ | −5.301 | 1.072 | −6.709 | −4.086 |
| Alternative 2, more transmissive ramp/shaft EDZ | −5.301 | 1.073 | −6.709 | −4.075 |
| Alternative 2, more transmissive ramp/shaft EDZ, realisation 2 | −5.485 | 1.228 | −6.797 | −3.756 |
| Alternative 2, more transmissive ramp/shaft EDZ, realisation 3 | −5.140 | 1.240 | −6.613 | −3.348 |
| Alternative 2, no ramp/shaft EDZ | −5.301 | 1.072 | −6.709 | −4.086 |

**Table 3-12. Flow-related transport resistance in the rock, $F_r$, statistics for Q1 recharge particles released at 2000 AD and successfully tracked back to the model boundary (16 % to 23 %).**

| Case | $\log_{10}(F_r)$ [y/m] | | | |
|---|---|---|---|---|
| | Median | Std. dev. | 10 % | 90 % |
| SR-Site Hydrogeological base case | 6.428 | 0.819 | 5.430 | 7.568 |
| SR-Site Hydrogeological base case, realisation 2 | 6.566 | 0.901 | 5.552 | 7.491 |
| SR-Site Hydrogeological base case, realisation 3 | 6.426 | 0.771 | 5.608 | 7.316 |
| Alternative 1A | 6.486 | 0.818 | 5.449 | 7.453 |
| Alternative 1B | 6.523 | 0.810 | 5.453 | 7.447 |
| Alternative 2 | 6.484 | 0.801 | 5.467 | 7.457 |
| Alternative 2, realisation 2 | 6.603 | 0.898 | 5.550 | 7.542 |
| Alternative 2, realisation 3 | 6.448 | 0.793 | 5.574 | 7.290 |
| Alternative 1A, more transmissive ramp/shaft EDZ | 6.445 | 0.770 | 5.485 | 7.394 |
| Alternative 2, more transmissive ramp/shaft EDZ | 6.506 | 0.806 | 5.505 | 7.434 |
| Alternative 2, more transmissive ramp/shaft EDZ, realisation 2 | 6.590 | 0.888 | 5.584 | 7.455 |
| Alternative 2, more transmissive ramp/shaft EDZ, realisation 3 | 6.405 | 0.748 | 5.631 | 7.305 |
| Alternative 2, no ramp/shaft EDZ | 6.493 | 0.807 | 5.427 | 7.450 |

### *Discharge glacial conditions*

**Table 3-13. Travel time in the rock, $t_r$, statistics for Q1 discharge particles released for glacial ice front location II and successfully reaching the model boundary (~29 %).**

| Case | $\log_{10}(t_r)$ [y] | | | |
|---|---|---|---|---|
| | Median | Std. dev. | 10 % | 90 % |
| SR-Site Hydrogeological base case | 0.470 | 0.512 | 0.118 | 0.960 |
| Alternative 1A | 0.481 | 0.499 | 0.089 | 0.934 |
| Alternative 1B | 0.488 | 0.428 | 0.122 | 0.938 |
| Alternative 2 | 0.507 | 0.454 | 0.150 | 0.977 |
| Alternative 1A, more transmissive ramp/shaft EDZ | 0.503 | 0.437 | 0.169 | 0.938 |
| Alternative 2, more transmissive ramp/shaft EDZ | 0.513 | 0.484 | 0.169 | 0.942 |
| Alternative 2, no ramp/shaft EDZ | 0.495 | 0.487 | 0.068 | 0.967 |

**Table 3-14. Initial equivalent Darcy flux in the rock, $U_r$, statistics for Q1 discharge particles released for glacial ice front location II and successfully starting (~35 %).**

| Case | $\log_{10}(U_r)$ [m/y] | | | |
|---|---|---|---|---|
| | Median | Std. dev. | 10 % | 90 % |
| SR-Site Hydrogeological base case | −3.578 | 1.342 | −5.716 | −2.254 |
| Alternative 1A | −3.575 | 1.340 | −5.693 | −2.258 |
| Alternative 1B | −3.576 | 1.341 | −5.692 | −2.257 |
| Alternative 2 | −3.572 | 1.341 | −5.692 | −2.259 |
| Alternative 1A, more transmissive ramp/shaft EDZ | −3.576 | 1.341 | −5.693 | −2.256 |
| Alternative 2, more transmissive ramp/shaft EDZ | −3.572 | 1.341 | −5.693 | −2.261 |
| Alternative 2, no ramp/shaft EDZ | −3.572 | 1.341 | −5.691 | −2.259 |

**Table 3-15. Flow-related transport resistance in the rock, $F_r$, statistics for Q1 discharge particles released for glacial ice front location II and successfully reaching the model boundary (~29 %).**

| Case | $\log_{10}(F_r)$ [y/m] | | | |
|---|---|---|---|---|
| | Median | Std. dev. | 10 % | 90 % |
| SR-Site Hydrogeological base case | 4.861 | 0.890 | 3.913 | 6.021 |
| Alternative 1A | 4.898 | 0.893 | 3.924 | 5.968 |
| Alternative 1B | 4.958 | 0.829 | 3.904 | 5.960 |
| Alternative 2 | 4.916 | 0.842 | 3.965 | 5.954 |
| Alternative 1A, more transmissive ramp/shaft EDZ | 4.917 | 0.845 | 3.976 | 6.071 |
| Alternative 2, more transmissive ramp/shaft EDZ | 4.895 | 0.851 | 3.952 | 5.892 |
| Alternative 2, no ramp/shaft EDZ | 4.897 | 0.874 | 3.914 | 6.008 |

**Table 3-16. Travel time in the rock, $t_r$, statistics for Q2 discharge particles released for glacial ice front location II and successfully reaching the model boundary (~90 %).**

| Case | $\log_{10}(t_r)$ [y] | | | |
|---|---|---|---|---|
| | Median | Std. dev. | 10 % | 90 % |
| SR-Site Hydrogeological base case | 0.462 | 0.486 | 0.078 | 0.915 |
| Alternative 1A | 0.454 | 0.507 | 0.068 | 0.917 |
| Alternative 1B | 0.461 | 0.506 | 0.056 | 0.910 |
| Alternative 2 | 0.451 | 0.478 | 0.035 | 0.881 |
| Alternative 1A, more transmissive ramp/shaft EDZ | 0.457 | 0.501 | −0.027 | 0.926 |
| Alternative 2, more transmissive ramp/shaft EDZ | 0.450 | 0.504 | 0.057 | 0.908 |
| Alternative 2, no ramp/shaft EDZ | 0.453 | 0.482 | 0.028 | 0.912 |

**Table 3-17. Initial equivalent Darcy flux in the rock, $U_r$, statistics for Q2 discharge particles released for glacial ice front location II and successfully starting (~100 %).**

| Case | $\log_{10}(U_r)$ [m/y] | | | |
|---|---|---|---|---|
| | Median | Std. dev. | 10 % | 90 % |
| SR-Site Hydrogeological base case | −0.021 | 1.003 | −2.489 | 0.356 |
| Alternative 1A | −0.022 | 1.003 | −2.489 | 0.357 |
| Alternative 1B | −0.023 | 1.003 | −2.489 | 0.358 |
| Alternative 2 | −0.011 | 1.005 | −2.489 | 0.361 |
| Alternative 1A, more transmissive ramp/shaft EDZ | −0.018 | 1.003 | −2.489 | 0.358 |
| Alternative 2, more transmissive ramp/shaft EDZ | −0.011 | 1.005 | −2.489 | 0.361 |
| Alternative 2, no ramp/shaft EDZ | −0.012 | 1.005 | −2.489 | 0.361 |

**Table 3-18. Flow-related transport resistance in the rock, $F_r$, statistics for Q2 discharge particles released for glacial ice front location II and successfully reaching the model boundary (~90 %).**

| Case | $\log_{10}(F_r)$ [y/m] | | | |
|---|---|---|---|---|
| | Median | Std. dev. | 10 % | 90 % |
| SR-Site Hydrogeological base case | 4.316 | 0.899 | 3.430 | 5.452 |
| Alternative 1A | 4.309 | 0.928 | 3.382 | 5.443 |
| Alternative 1B | 4.333 | 0.926 | 3.380 | 5.423 |
| Alternative 2 | 4.324 | 0.868 | 3.390 | 5.340 |
| Alternative 1A, more transmissive ramp/shaft EDZ | 4.309 | 0.918 | 3.342 | 5.422 |
| Alternative 2, more transmissive ramp/shaft EDZ | 4.320 | 0.900 | 3.394 | 5.420 |
| Alternative 2, no ramp/shaft EDZ | 4.346 | 0.876 | 3.419 | 5.405 |

**Table 3-19. Travel time in the rock, $t_r$, statistics for Q3 discharge particles released for glacial ice front location II and successfully reaching the model boundary (~84 %).**

| Case | $\log_{10}(t_r)$ [y] | | | |
|---|---|---|---|---|
| | Median | Std. dev. | 10 % | 90 % |
| SR-Site Hydrogeological base case | 0.459 | 0.427 | 0.057 | 0.855 |
| Alternative 1A | 0.449 | 0.409 | 0.010 | 0.835 |
| Alternative 1B | 0.444 | 0.425 | 0.028 | 0.834 |
| Alternative 2 | 0.427 | 0.426 | 0.005 | 0.843 |
| Alternative 1A, more transmissive ramp/shaft EDZ | 0.449 | 0.412 | 0.036 | 0.837 |
| Alternative 2, more transmissive ramp/shaft EDZ | 0.447 | 0.401 | 0.058 | 0.835 |
| Alternative 2, no ramp/shaft EDZ | 0.444 | 0.432 | −0.042 | 0.821 |

**Table 3-20. Initial equivalent Darcy flux in the rock, $U_r$, statistics for Q3 discharge particles released for glacial ice front location II and successfully starting (~90 %).**

| Case | $\log_{10}(U_r)$ [m/y] | | | |
|---|---|---|---|---|
| | Median | Std. dev. | 10 % | 90 % |
| SR-Site Hydrogeological base case | −1.565 | 0.869 | −2.899 | −0.951 |
| Alternative 1A | −1.551 | 0.841 | −2.822 | −0.969 |
| Alternative 1B | −1.530 | 0.862 | −2.855 | −0.939 |
| Alternative 2 | −1.547 | 0.868 | −2.945 | −0.902 |
| Alternative 1A, more transmissive ramp/shaft EDZ | −1.545 | 0.863 | −2.952 | −0.939 |
| Alternative 2, more transmissive ramp/shaft EDZ | −1.550 | 0.896 | −2.991 | −0.911 |
| Alternative 2, no ramp/shaft EDZ | −1.541 | 0.858 | −2.867 | −0.954 |

**Table 3-21. Flow-related transport resistance in the rock, $F_r$, statistics for Q3 discharge particles released for glacial ice front location II and successfully reaching the model boundary (~84 %).**

| Case | $\log_{10}(F_r)$ [y/m] | | | |
|---|---|---|---|---|
| | Median | Std. dev. | 10 % | 90 % |
| SR-Site Hydrogeological base case | 4.340 | 0.774 | 3.403 | 5.342 |
| Alternative 1A | 4.277 | 0.763 | 3.359 | 5.303 |
| Alternative 1B | 4.297 | 0.787 | 3.293 | 5.334 |
| Alternative 2 | 4.320 | 0.737 | 3.359 | 5.241 |
| Alternative 1A, more transmissive ramp/shaft EDZ | 4.336 | 0.768 | 3.340 | 5.268 |
| Alternative 2, more transmissive ramp/shaft EDZ | 4.305 | 0.735 | 3.348 | 5.250 |
| Alternative 2, no ramp/shaft EDZ | 4.300 | 0.741 | 3.303 | 5.251 |

### *Recharge glacial conditions*

**Table 3-22. Travel time in the rock, $t_r$, statistics for Q1 recharge particles released for glacial ice front location II and successfully tracked back to the model boundary (~29 %).**

| Case | $\log_{10}(t_r)$ [y] | | | |
|---|---|---|---|---|
| | Median | Std. dev. | 10 % | 90 % |
| SR-Site Hydrogeological base case | 0.345 | 0.636 | −0.614 | 0.988 |
| Alternative 1A | 0.357 | 0.669 | −0.527 | 0.996 |
| Alternative 1B | 0.337 | 0.640 | −0.454 | 0.977 |
| Alternative 2 | 0.343 | 0.651 | −0.548 | 0.973 |
| Alternative 1A, more transmissive ramp/shaft EDZ | 0.278 | 0.672 | −0.563 | 1.009 |
| Alternative 2, more transmissive ramp/shaft EDZ | 0.351 | 0.658 | −0.619 | 0.992 |
| Alternative 2, no ramp/shaft EDZ | 0.317 | 0.647 | −0.519 | 0.996 |

**Table 3-23. Initial equivalent Darcy flux in the rock, $U_r$, statistics for Q1 recharge particles released for glacial ice front location II and successfully starting (~35 %).**

| Case | $\log_{10}(U_r)$ [m/y] | | | |
|---|---|---|---|---|
| | Median | Std. dev. | 10 % | 90 % |
| SR-Site Hydrogeological base case | −3.562 | 1.282 | −5.548 | −2.278 |
| Alternative 1A | −3.562 | 1.280 | −5.548 | −2.285 |
| Alternative 1B | −3.561 | 1.279 | −5.548 | −2.285 |
| Alternative 2 | −3.560 | 1.280 | −5.555 | −2.294 |
| Alternative 1A, more transmissive ramp/shaft EDZ | −3.562 | 1.280 | −5.548 | −2.284 |
| Alternative 2, more transmissive ramp/shaft EDZ | −3.560 | 1.280 | −5.555 | −2.296 |
| Alternative 2, no ramp/shaft EDZ | −3.559 | 1.280 | −5.555 | −2.295 |

**Table 3-24. Flow-related transport resistance in the rock, $F_r$, statistics for Q1 recharge particles released for glacial ice front location II and successfully tracked back to the model boundary (~29 %).**

| Case | $\log_{10}(F_r)$ [y/m] | | | |
|---|---|---|---|---|
| | Median | Std. dev. | 10 % | 90 % |
| SR-Site Hydrogeological base case | 4.916 | 0.835 | 3.892 | 5.938 |
| Alternative 1A | 4.967 | 0.862 | 3.907 | 5.910 |
| Alternative 1B | 4.915 | 0.834 | 3.917 | 5.943 |
| Alternative 2 | 4.882 | 0.834 | 3.897 | 5.884 |
| Alternative 1A, more transmissive ramp/shaft EDZ | 4.870 | 0.868 | 3.858 | 5.954 |
| Alternative 2, more transmissive ramp/shaft EDZ | 4.911 | 0.827 | 3.935 | 5.897 |
| Alternative 2, no ramp/shaft EDZ | 4.871 | 0.833 | 3.906 | 5.853 |

### *Discharge temperate conditions*

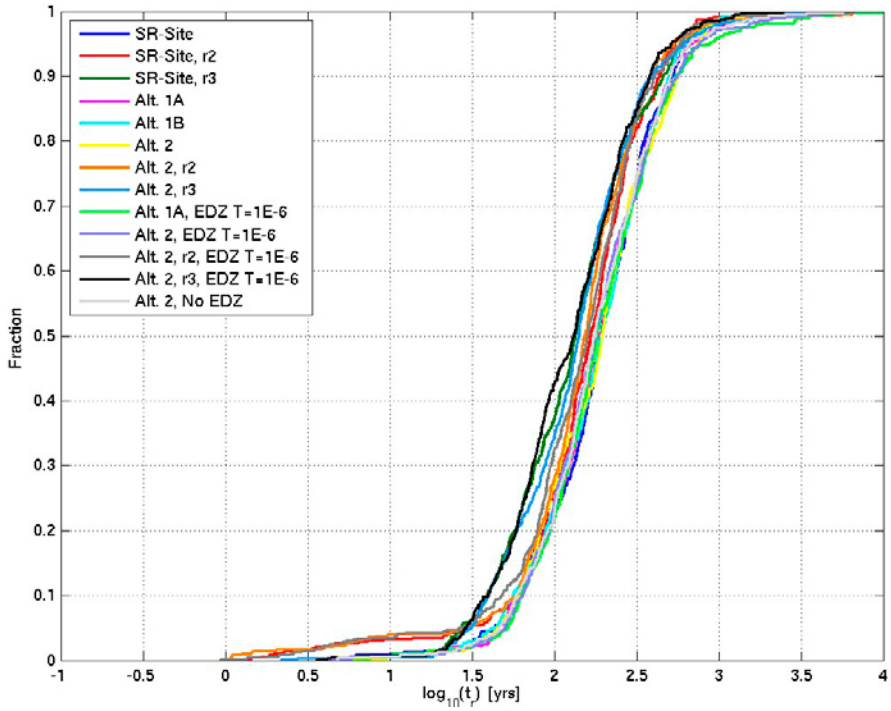


***Figure 3-1.*** *Travel time in the rock, $t_r$, normalised CDF plots for Q1 discharge particles released at 2000 AD and successfully reaching the model boundary (~25 %).*

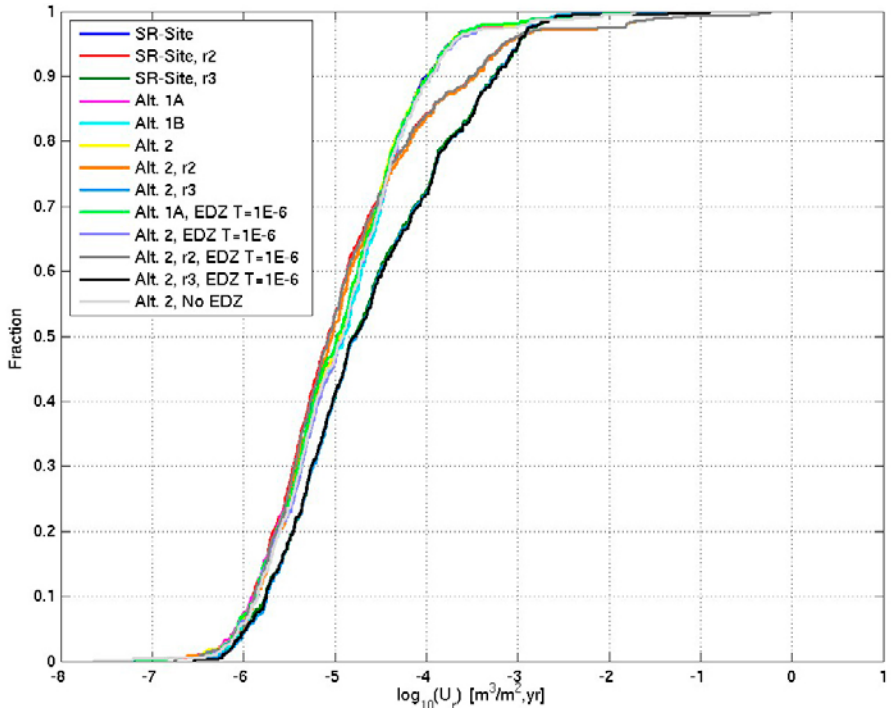


***Figure 3-2.*** *Initial equivalent Darcy flux in the rock, $U_r$, normalised CDF plots for Q1 discharge particles released at 2000 AD and successfully reaching the model boundary (~25 %).*

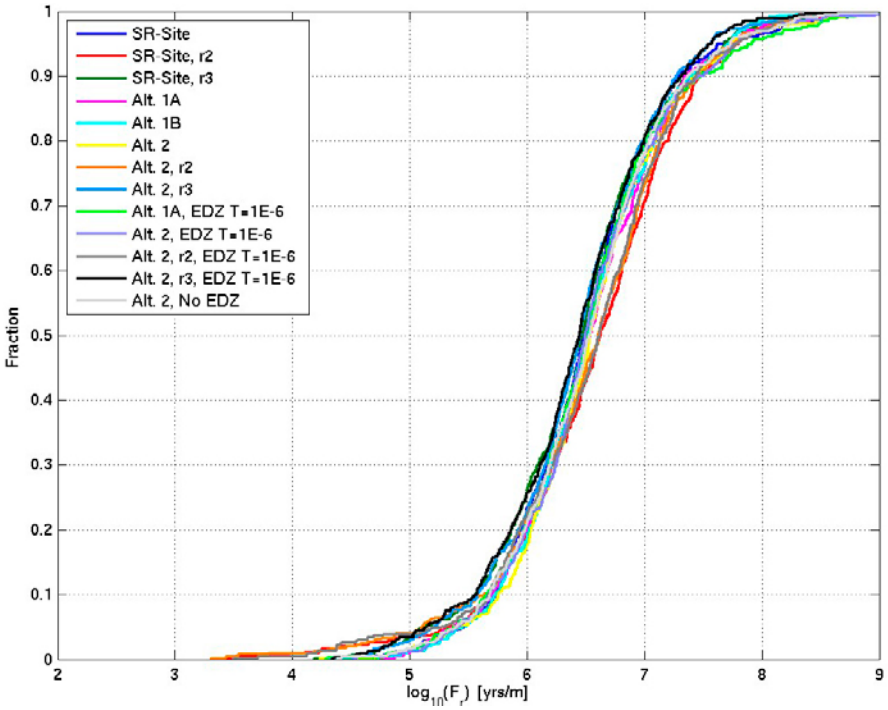


***Figure 3-3.*** *Flow-related transport resistance in the rock, $F_r$, normalised CDF plots for Q1 discharge particles released at 2000 AD and successfully reaching the model boundary (~25 %).*

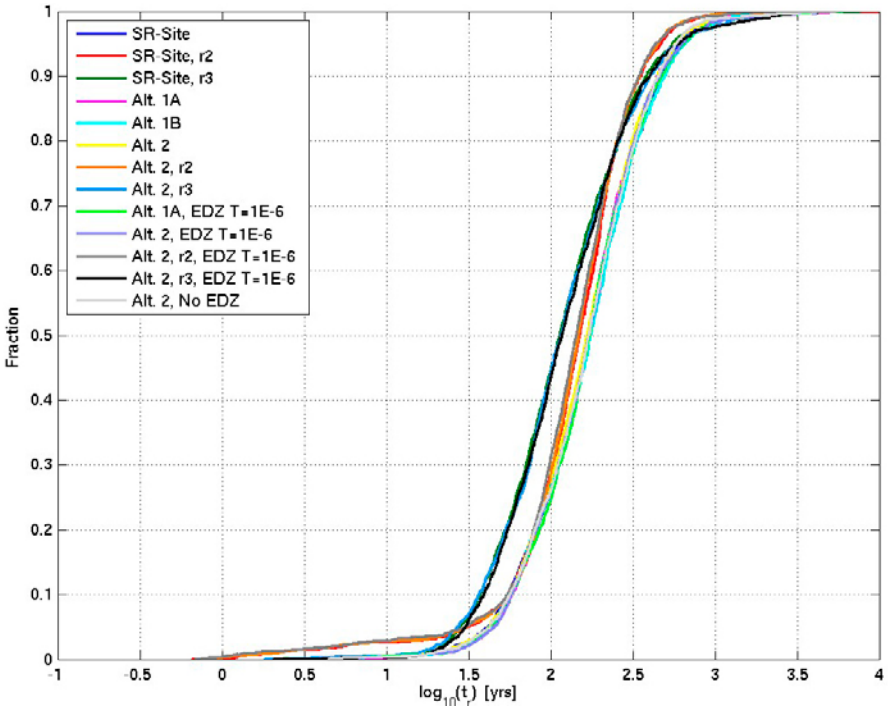


***Figure 3-4.*** *Travel time in the rock, $t_r$, normalised CDF plots for Q2 discharge particles released at 2000 AD and successfully reaching the model boundary (81 % to 93 %).*

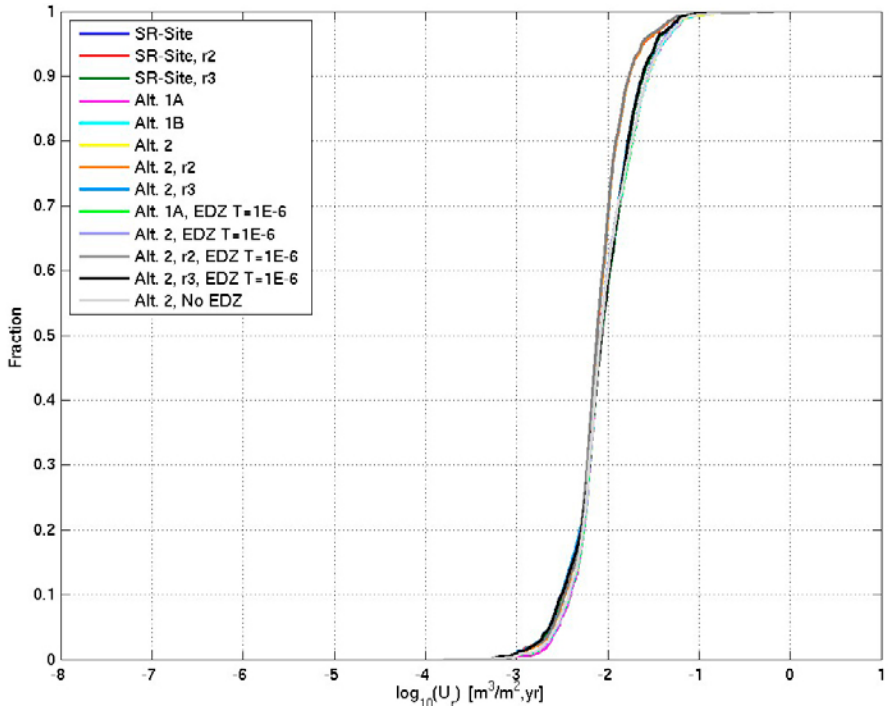


***Figure 3-5.*** *Initial equivalent Darcy flux in the rock, $U_r$, normalised CDF plots for Q2 discharge particles released at 2000 AD and successfully reaching the model boundary (81 % to 93 %).*

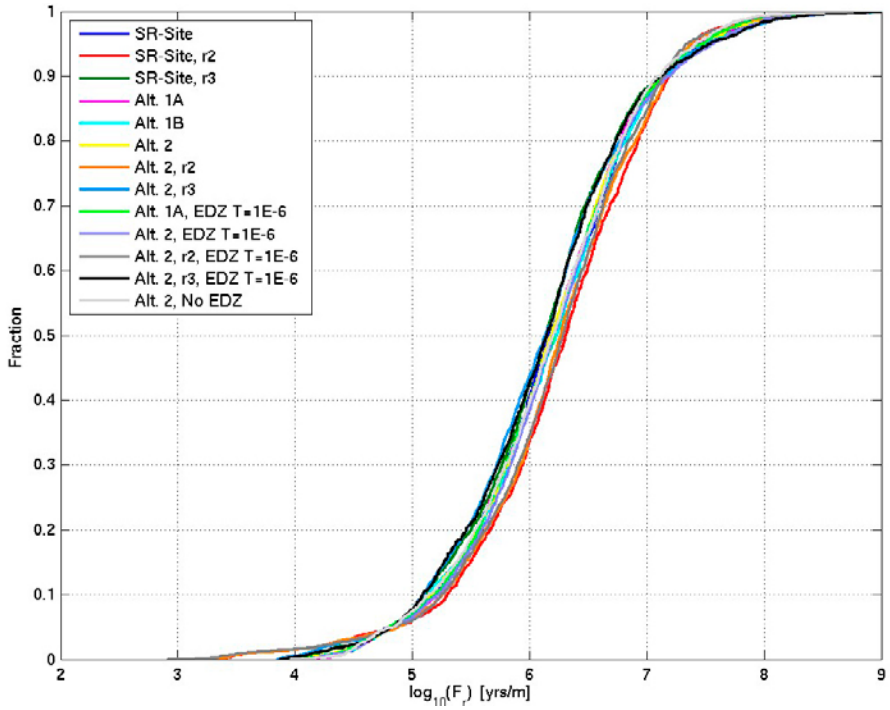


***Figure 3-6.*** *Flow-related transport resistance in the rock, $F_r$, normalised CDF plots for Q2 discharge particles released at 2000 AD and successfully reaching the model boundary (81 % to 93 %).*

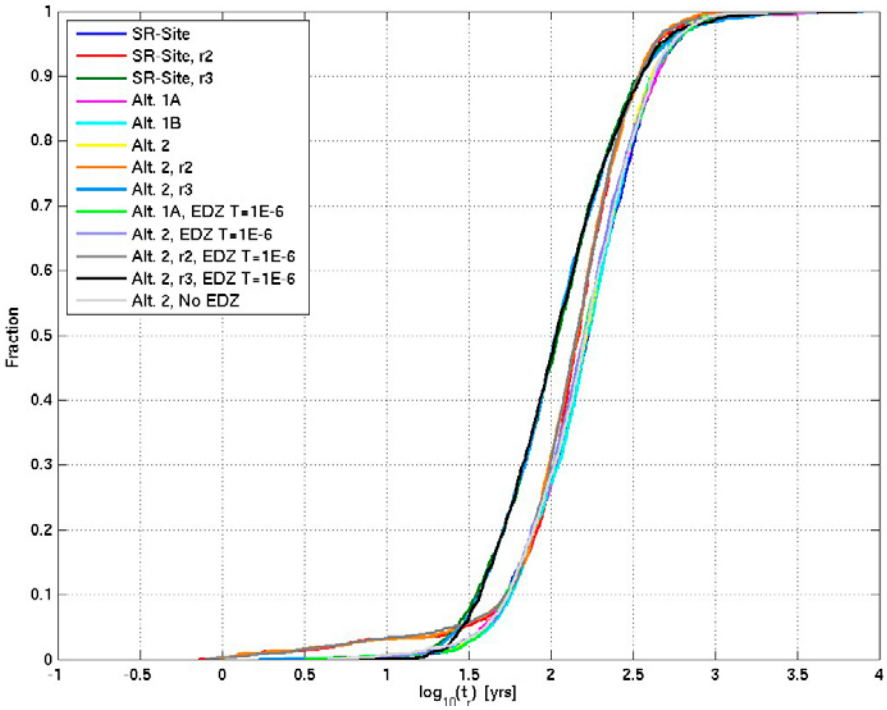


***Figure 3-7.*** *Travel time in the rock, $t_r$, normalised CDF plots for Q3 discharge particles released at 2000 AD and successfully reaching the model boundary (68 % to 79 %).*

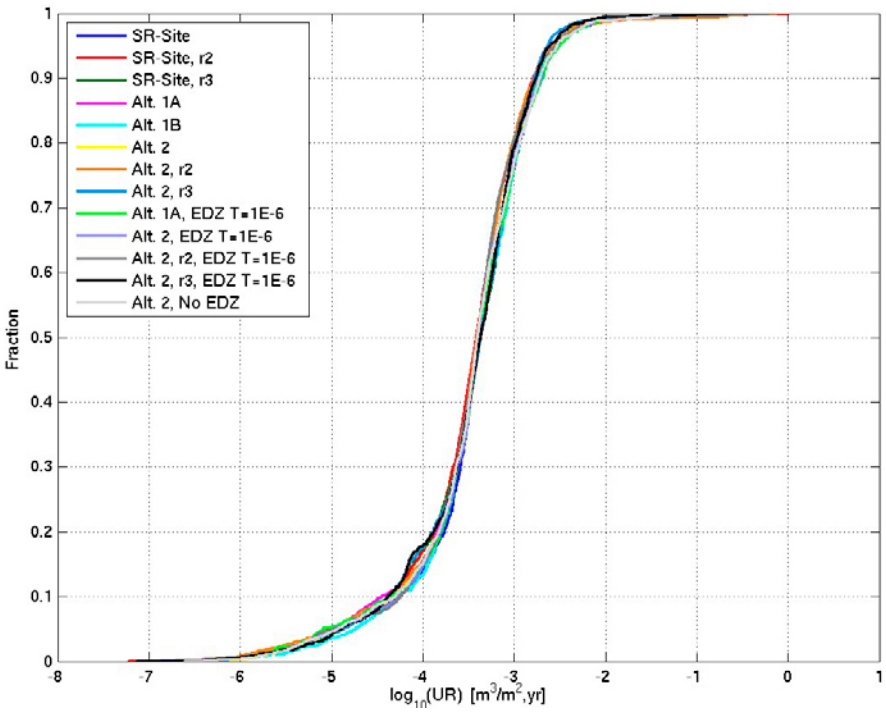


***Figure 3-8.*** *Initial equivalent Darcy flux in the rock, $U_r$, normalised CDF plots for Q3 discharge particles released at 2000 AD and successfully reaching the model boundary (68 % to 79 %).*

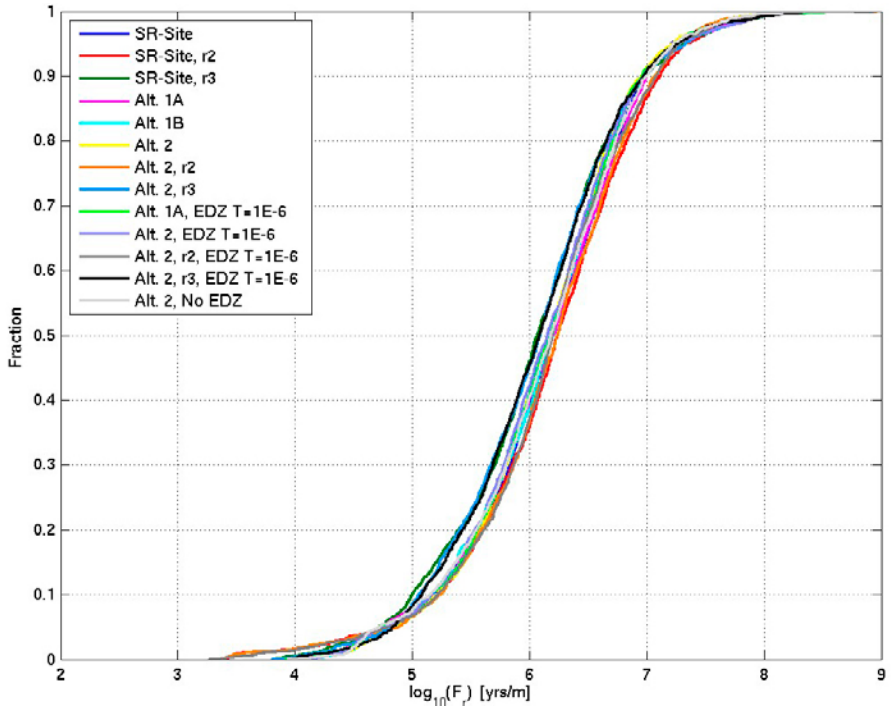


***Figure 3-9.*** *Flow-related transport resistance in the rock, $F_r$, normalised CDF plots for Q3 discharge particles released at 2000 AD and successfully reaching the model boundary (68 % to 79 %).*

### *Recharge temperate conditions*

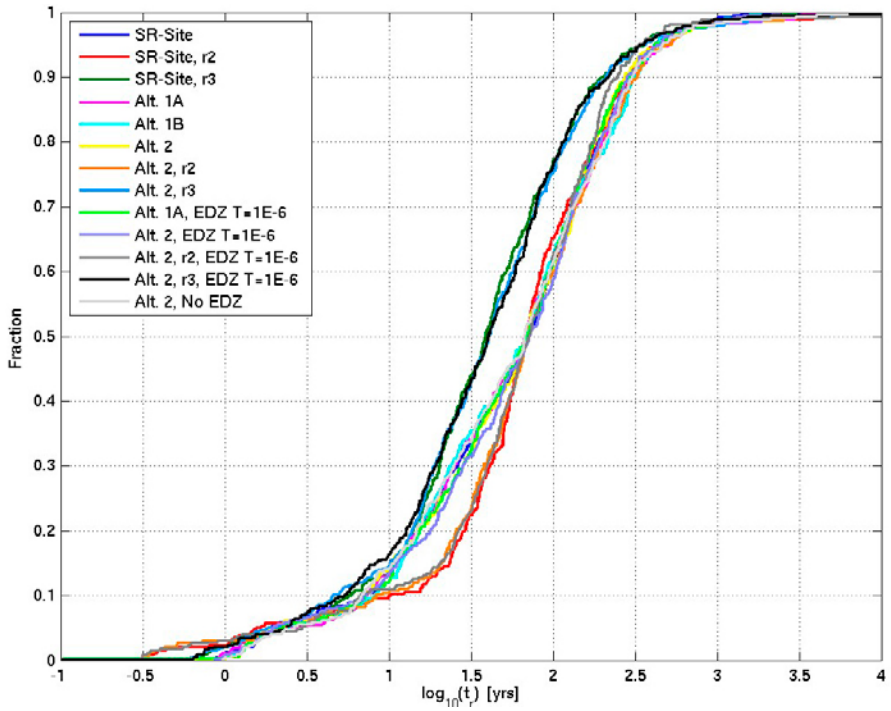


***Figure 3-10.*** *Travel time in the rock, $t_r$, normalised CDF plots for Q1 recharge particles released at 2000 AD and successfully tracked back to the model boundary (16 % to 23 %).*

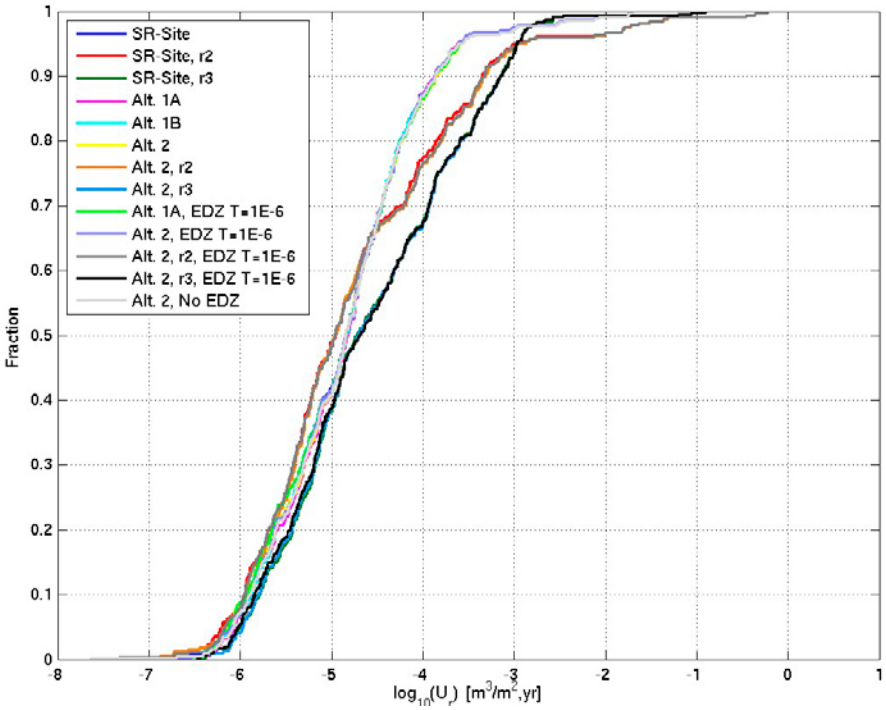


***Figure 3-11.*** *Initial equivalent Darcy flux in the rock, $U_r$, normalised CDF plots for Q1 recharge particles released at 2000 AD and successfully tracked back to the model boundary (16 % to 23 %).*

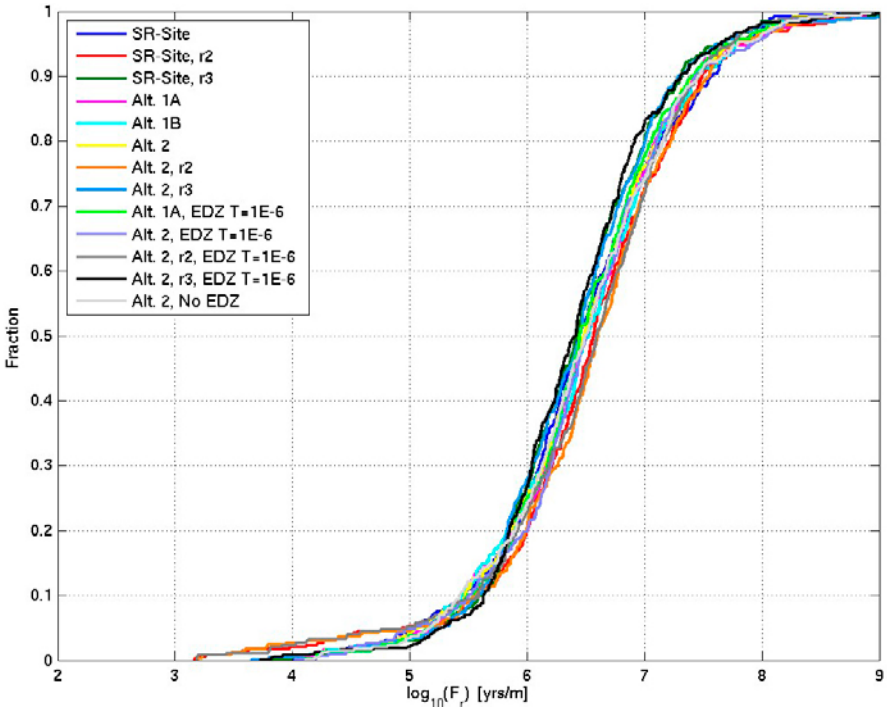


***Figure 3-12.*** *Flow-related transport resistance in the rock, $F_r$, normalised CDF plots for Q1 recharge particles released at 2000 AD and successfully tracked back to the model boundary (16 % to 23 %).*

### *Discharge glacial conditions*

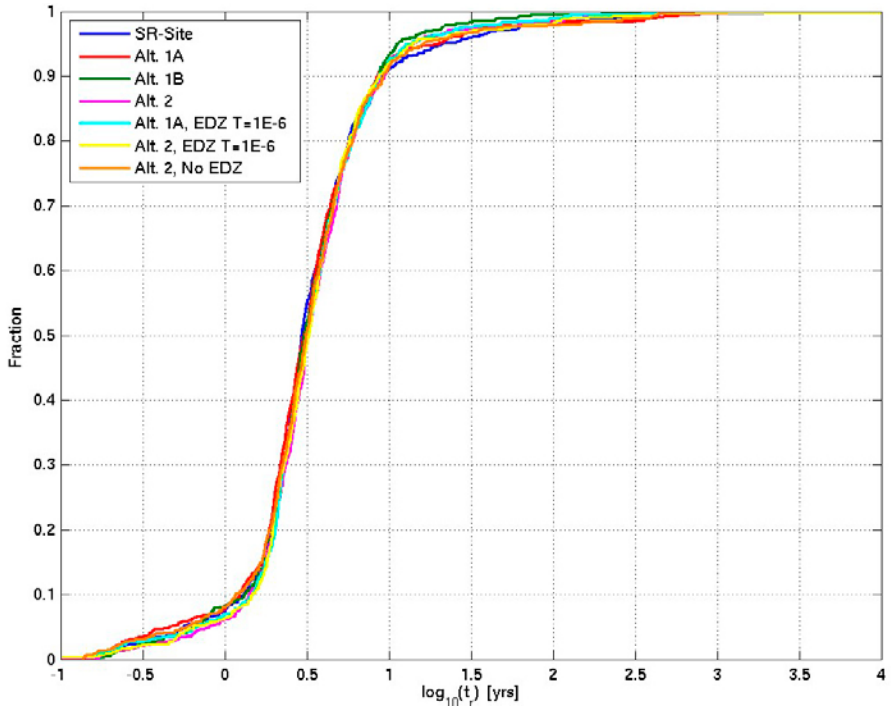


***Figure 3-13.*** *Travel time in the rock, $t_r$, normalised CDF plots for Q1 discharge particles released for glacial ice front location II and successfully reaching the model boundary (~29 %).*

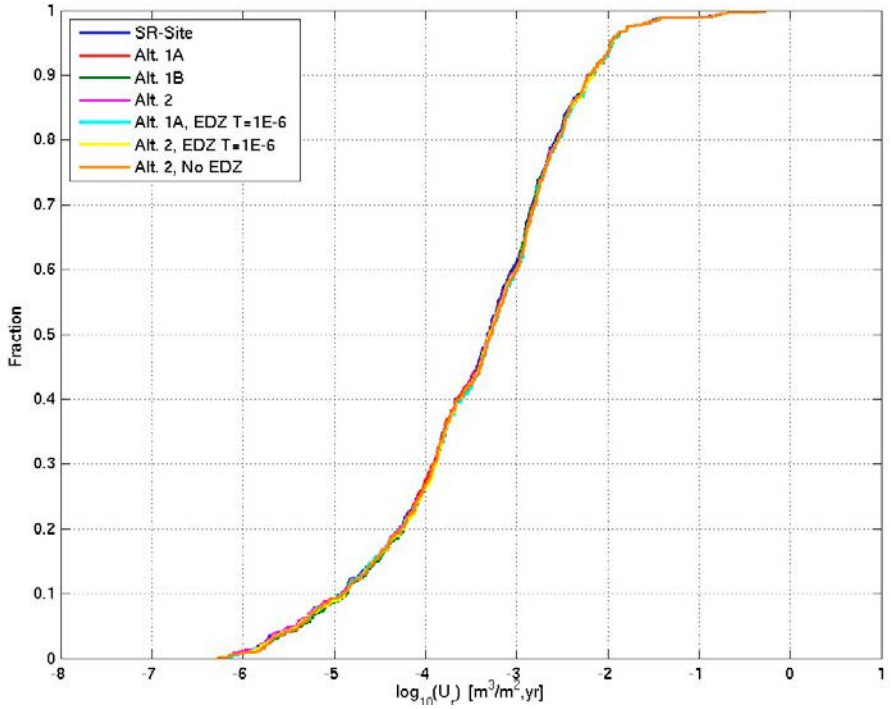


***Figure 3-14.*** *Initial equivalent Darcy flux in the rock, $U_r$, normalised CDF plots for Q1 discharge particles released for glacial ice front location II and successfully reaching the model boundary (~29 %).*

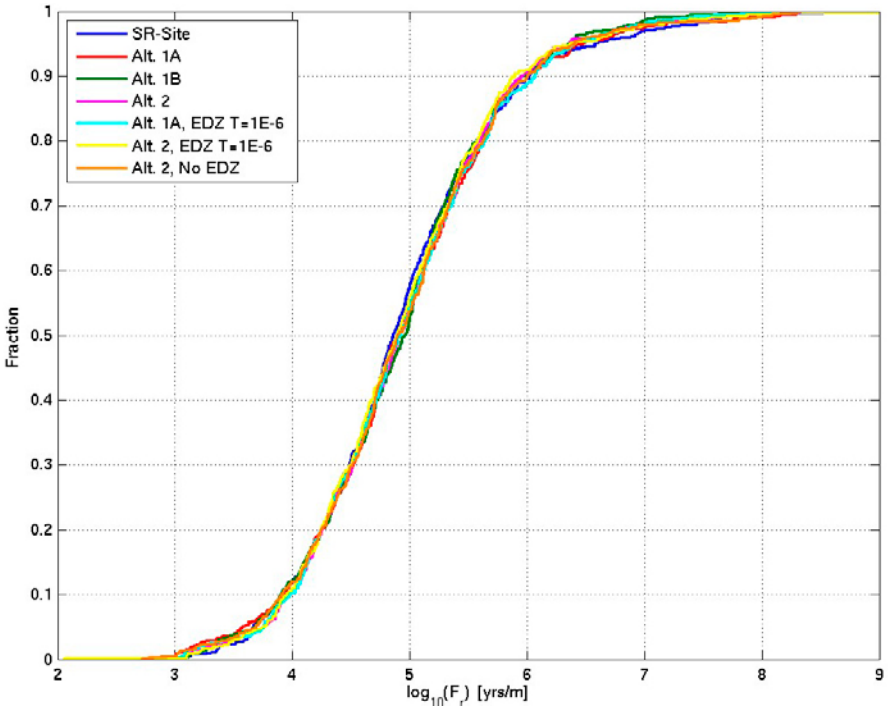


***Figure 3-15.*** *Flow-related transport resistance in the rock, $F_r$, normalised CDF plots for Q1 discharge particles released for glacial ice front location II and successfully reaching the model boundary (~29 %).*

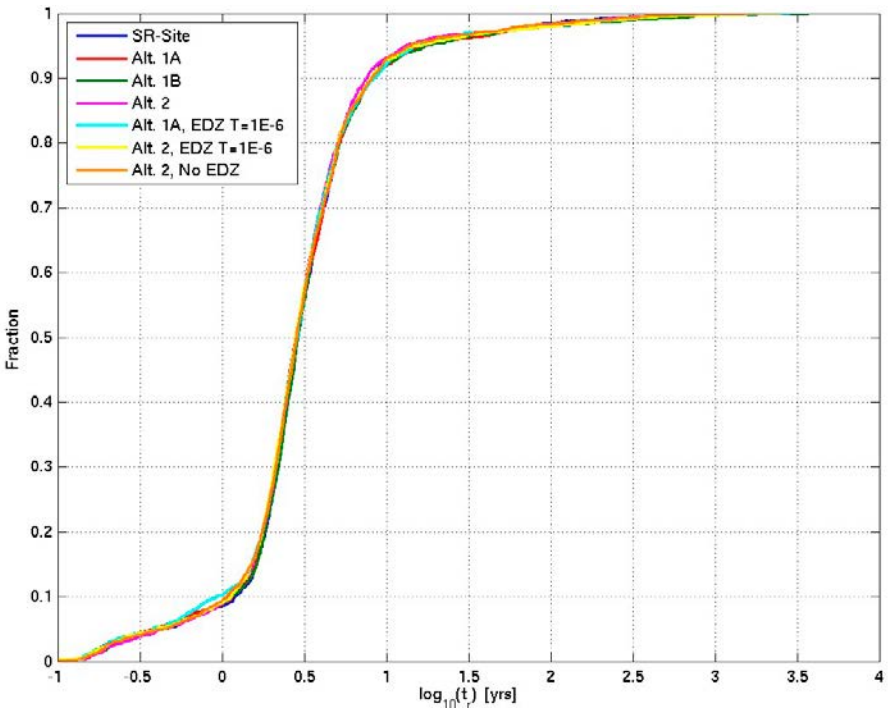


***Figure 3-16.*** *Travel time in the rock, $t_r$, normalised CDF plots for Q2 discharge particles released for glacial ice front location II and successfully reaching the model boundary (~90 %).*

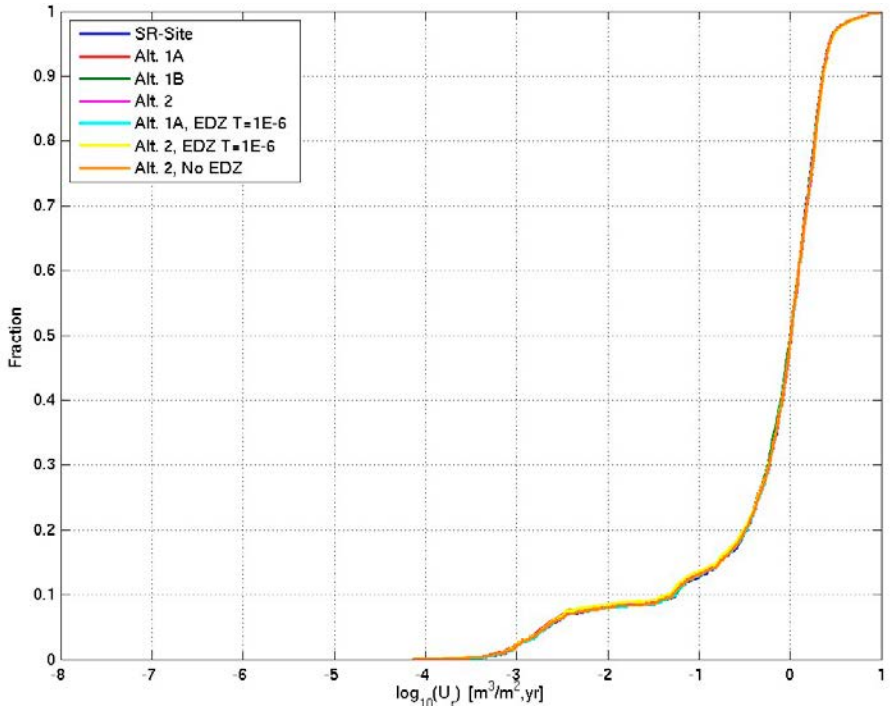


***Figure 3-17.*** *Initial equivalent Darcy flux in the rock, $U_r$, normalised CDF plots for Q2 discharge particles released for glacial ice front location II and successfully reaching the model boundary (~90 %).*

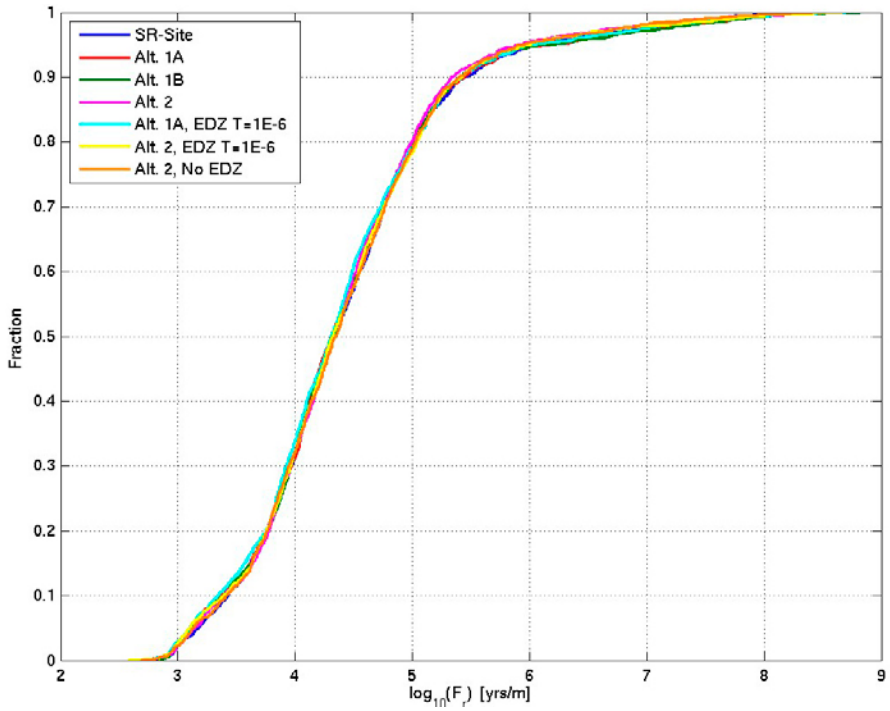


***Figure 3-18.*** *Flow-related transport resistance in the rock, $F_r$, normalised CDF plots for Q2 discharge particles released for glacial ice front location II and successfully reaching the model boundary (~90 %).*

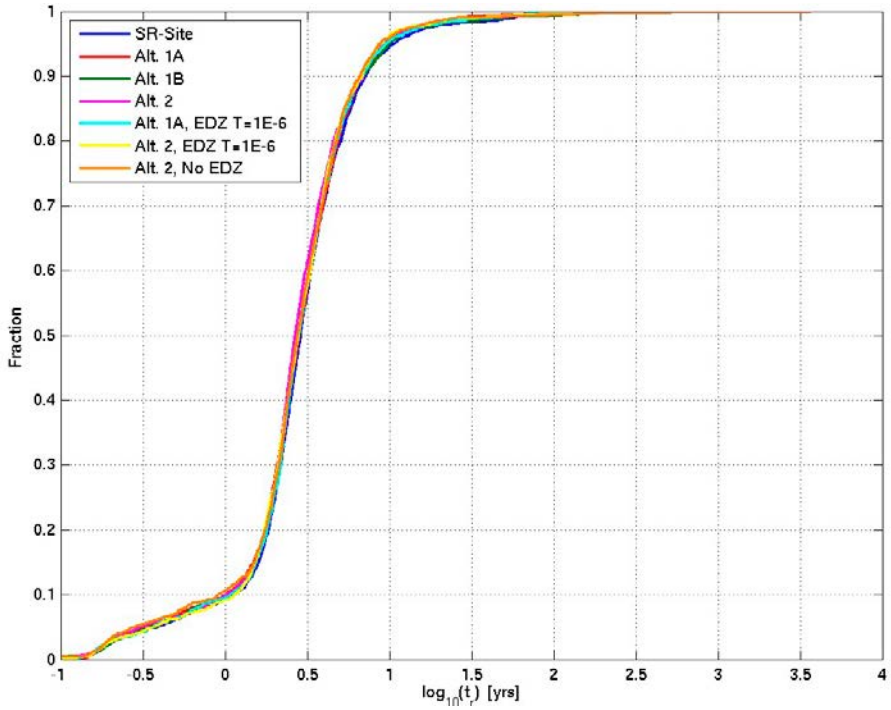


***Figure 3-19.*** *Travel time in the rock, $t_r$, normalised CDF plots for Q3 discharge particles released for glacial ice front location II and successfully reaching the model boundary (~84 %).*

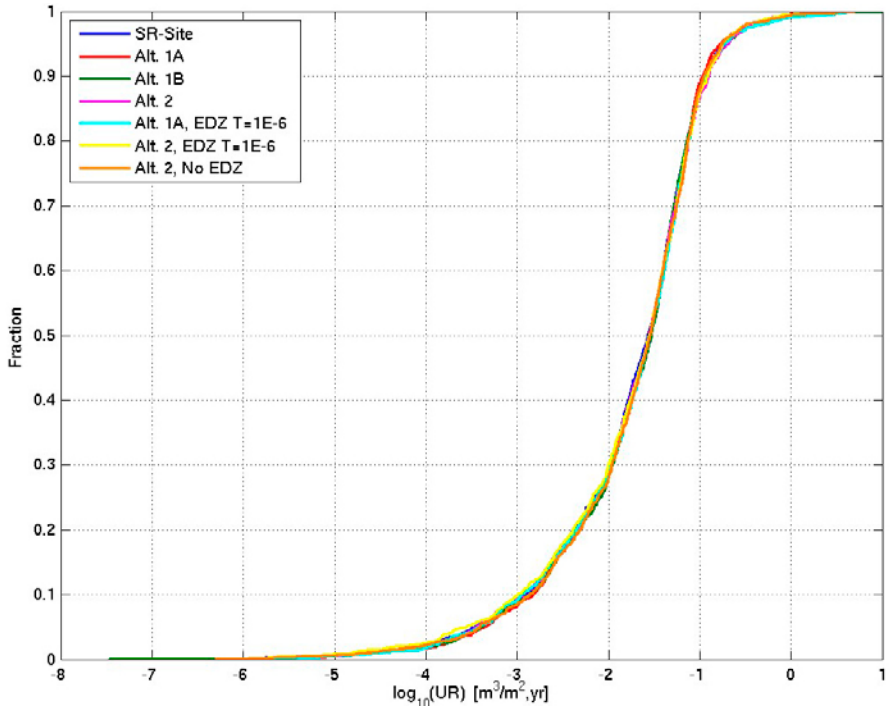


***Figure 3-20.*** *Initial equivalent Darcy flux in the rock, $U_r$, normalised CDF plots for Q3 discharge particles released for glacial ice front location II and successfully reaching the model boundary (~84 %).*

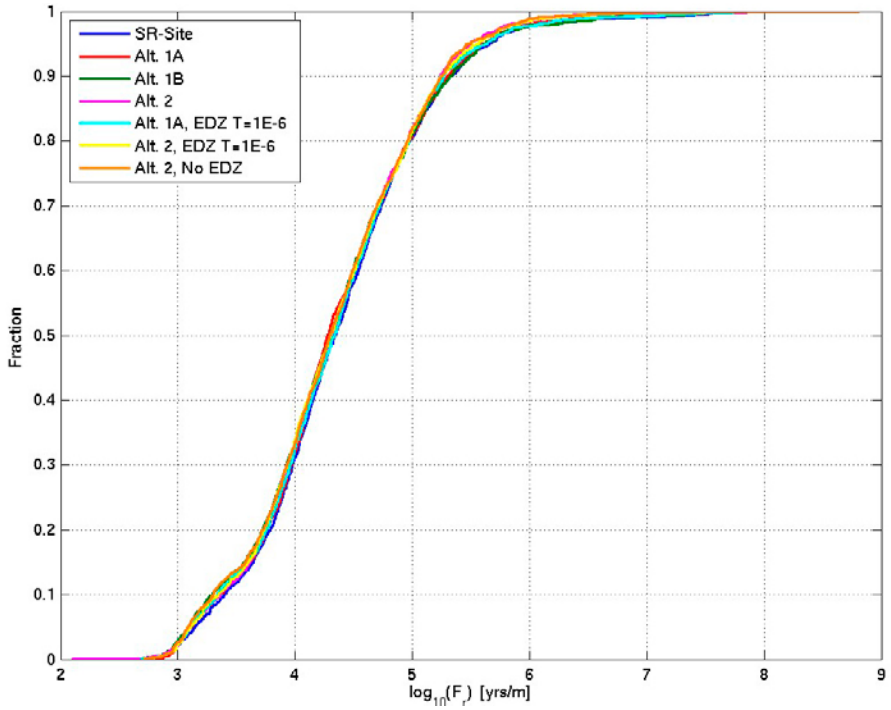


***Figure 3-21.*** *Flow-related transport resistance in the rock, $F_r$, normalised CDF plots for Q3 discharge particles released for glacial ice front location II and successfully reaching the model boundary (~84 %).*

### *Recharge glacial conditions*

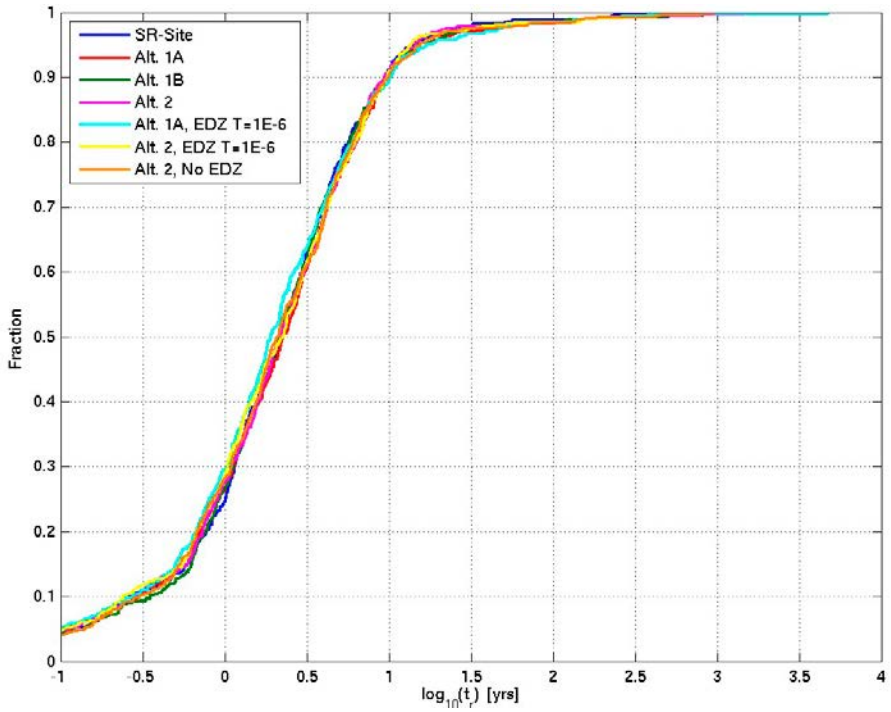


***Figure 3-22.*** *Travel time in the rock, $t_r$, normalised CDF plots for Q1 recharge particles released for glacial ice front location II and successfully tracked back to the model boundary (~29 %).*

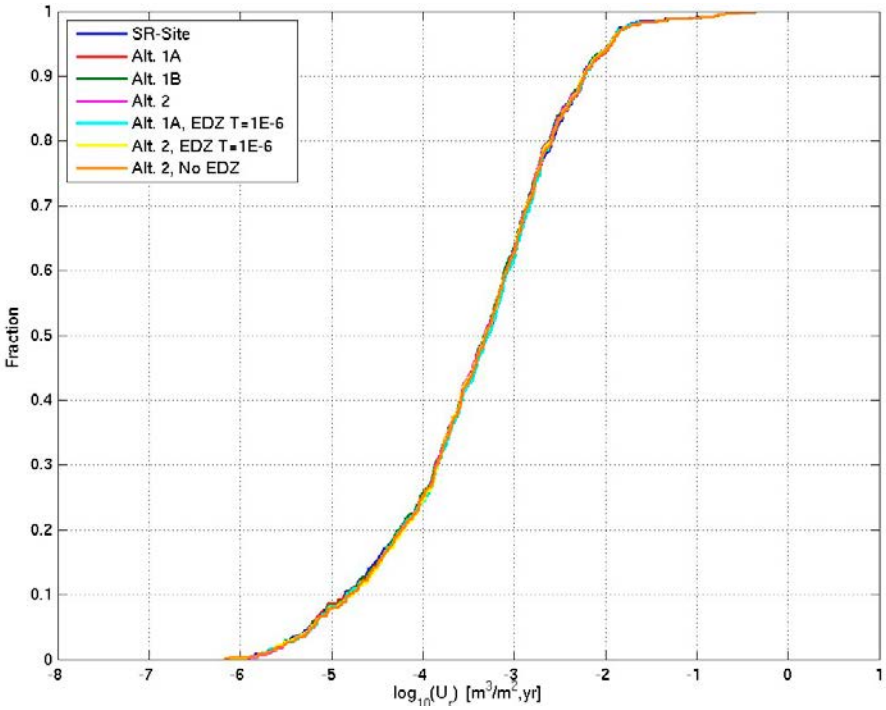


***Figure 3-23.*** *Initial equivalent Darcy flux in the rock, $U_p$, normalised CDF plots for Q1 recharge particles released for glacial ice front location II and successfully tracked back to the model boundary (~29 %).*

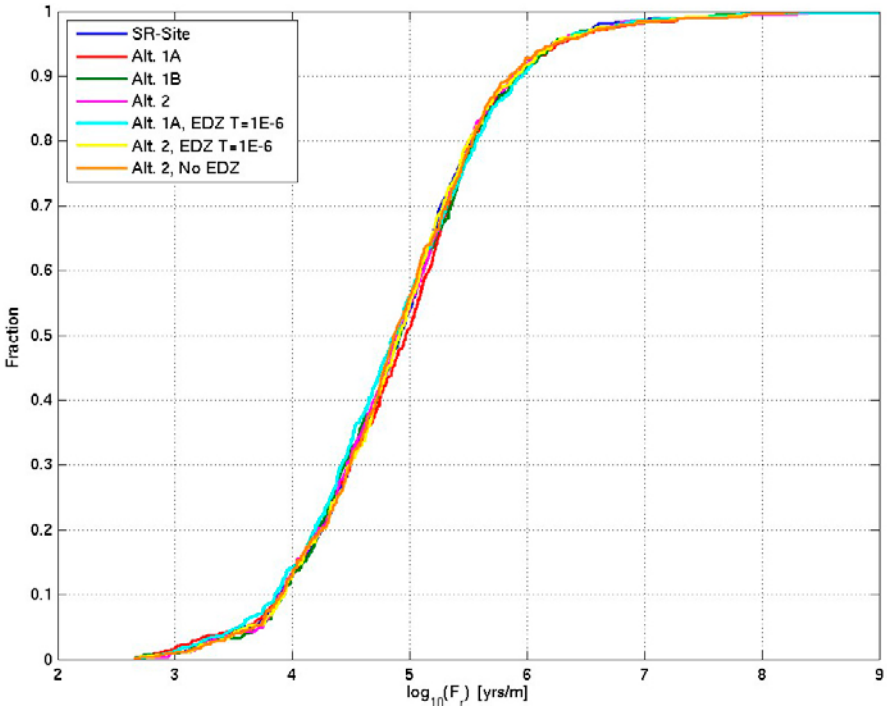


***Figure 3-24.*** *Flow-related transport resistance in the rock, $F_p$, normalised CDF plots for Q1 recharge particles released for glacial ice front location II and successfully tracked back to the model boundary (~29 %).*

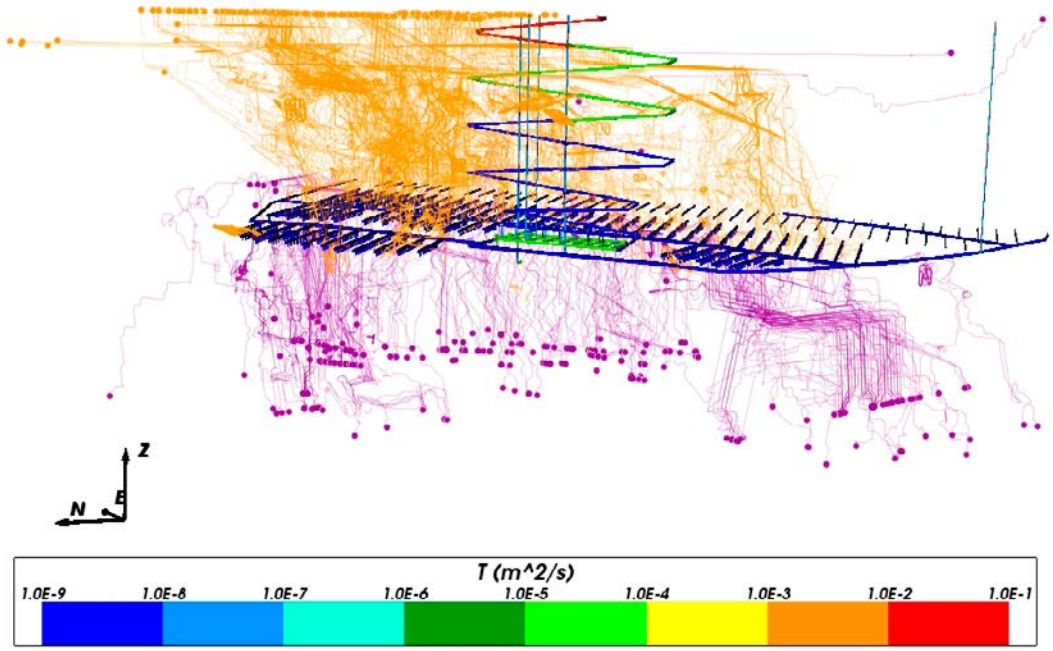


***Figure 3-25.*** *Recharge (purple) and discharge (orange) pathways for the Q1 particles released at 2000 AD and successfully reaching the model boundary (~24 %) of the Alternative 1A case.*

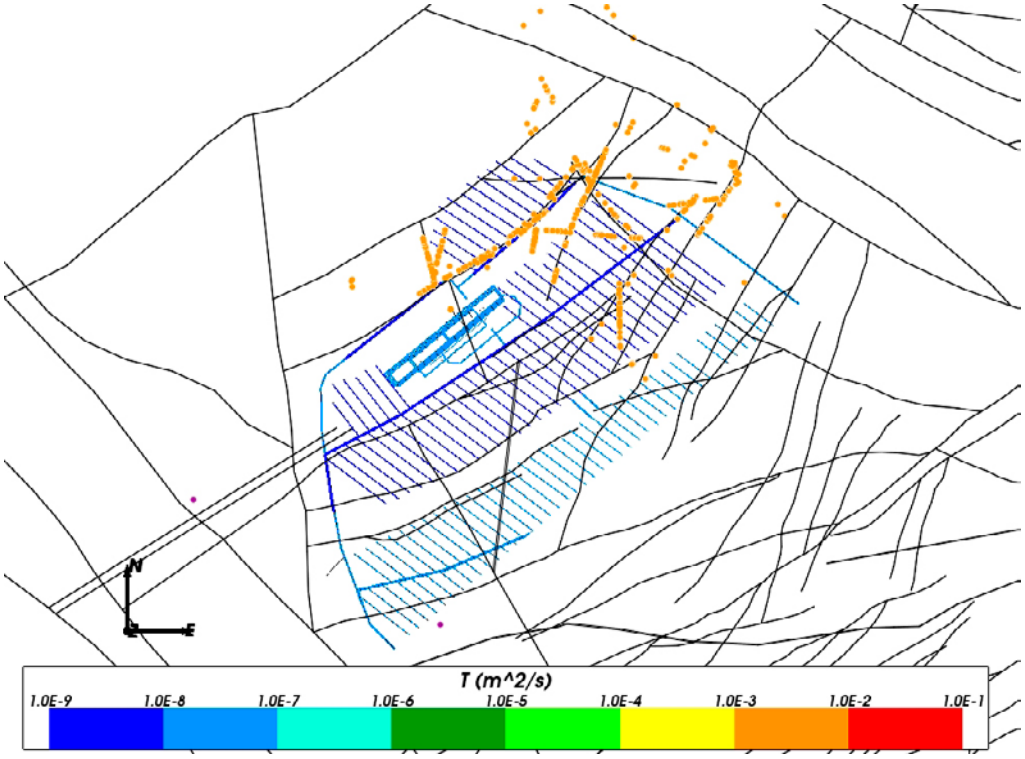


***Figure 3-26.*** *Recharge (purple) and discharge (orange) exit locations for the Q1 particles released at 2000 AD and successfully reaching the model top surface (~24 %) of the Alternative 1A case. Deformation zones at −50 m are black.*

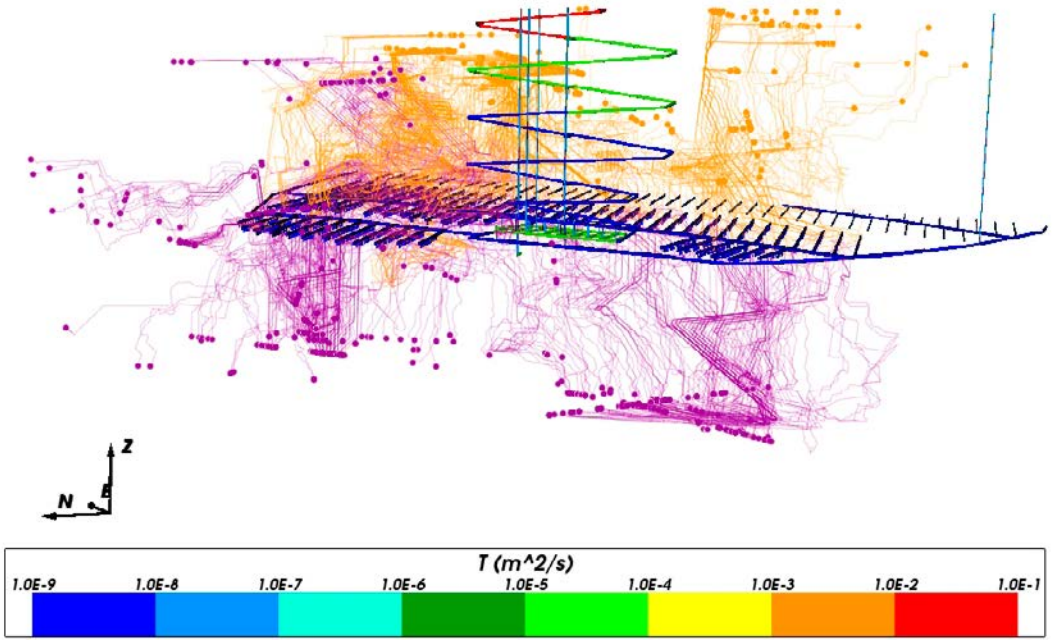


***Figure 3-27.*** *Recharge (purple) and discharge (orange) pathways for the Q1 particles released for glacial ice front location II and successfully reaching the model boundary (~29 %) of the Alternative 1A case.*

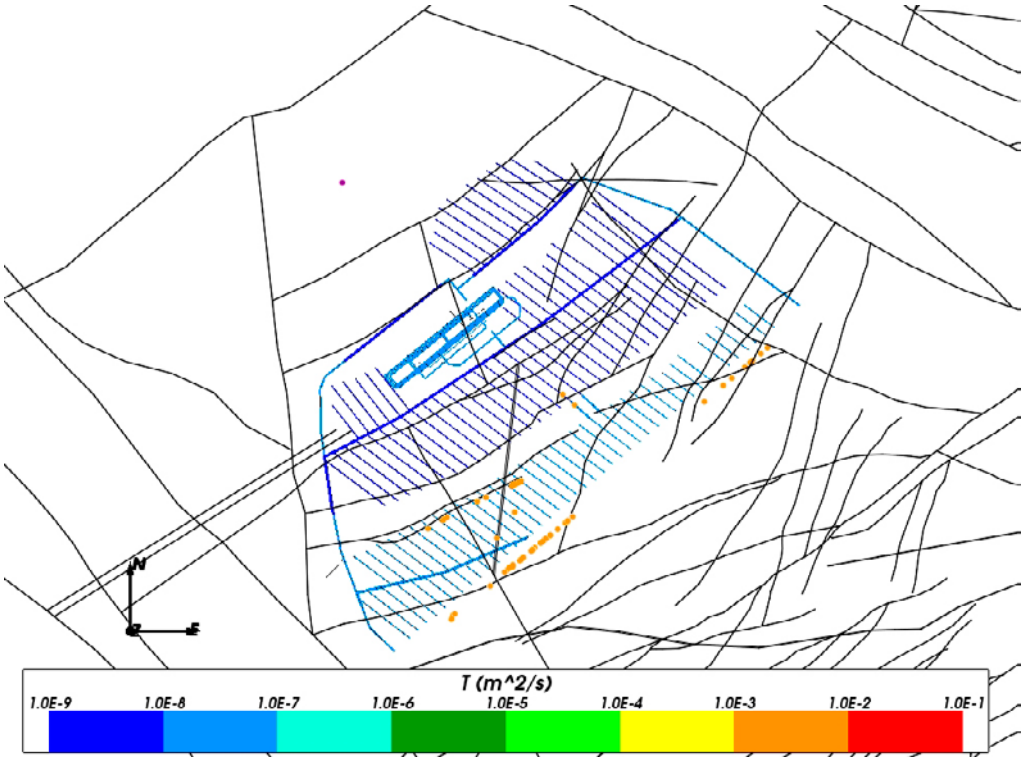


***Figure 3-28.*** *Recharge (purple) and discharge (orange) exit locations for the Q1 particles released for glacial ice front location II and successfully reaching the model top surface (~4 %) of the Alternative 1A case. Deformation zones at −50 m are black.*

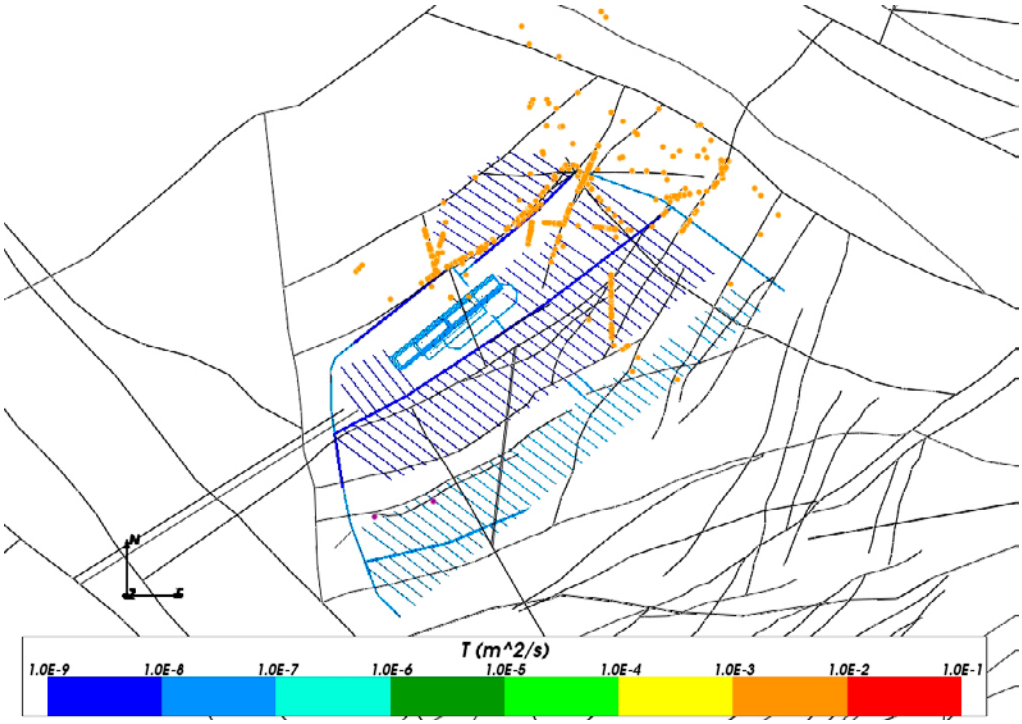


***Figure 3-29.*** *Recharge (purple) and discharge (orange) exit locations for the Q1 particles released at 2000 AD and successfully reaching the model top surface (~24 %) of the Alternative 2 case. Deformation zones at −50 m are black.*

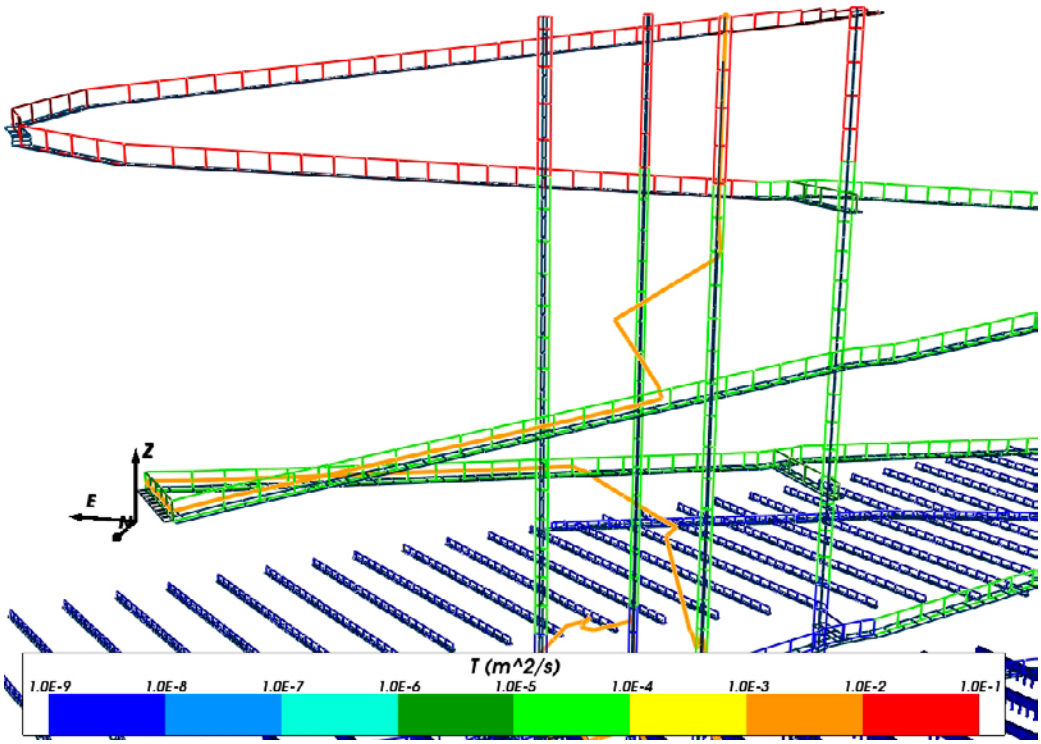


***Figure 3-30.*** *Discharge pathway for a Q1 particle released at 2000 AD and travelling along part of the ramp and a shaft in the Alternative 1A case.*

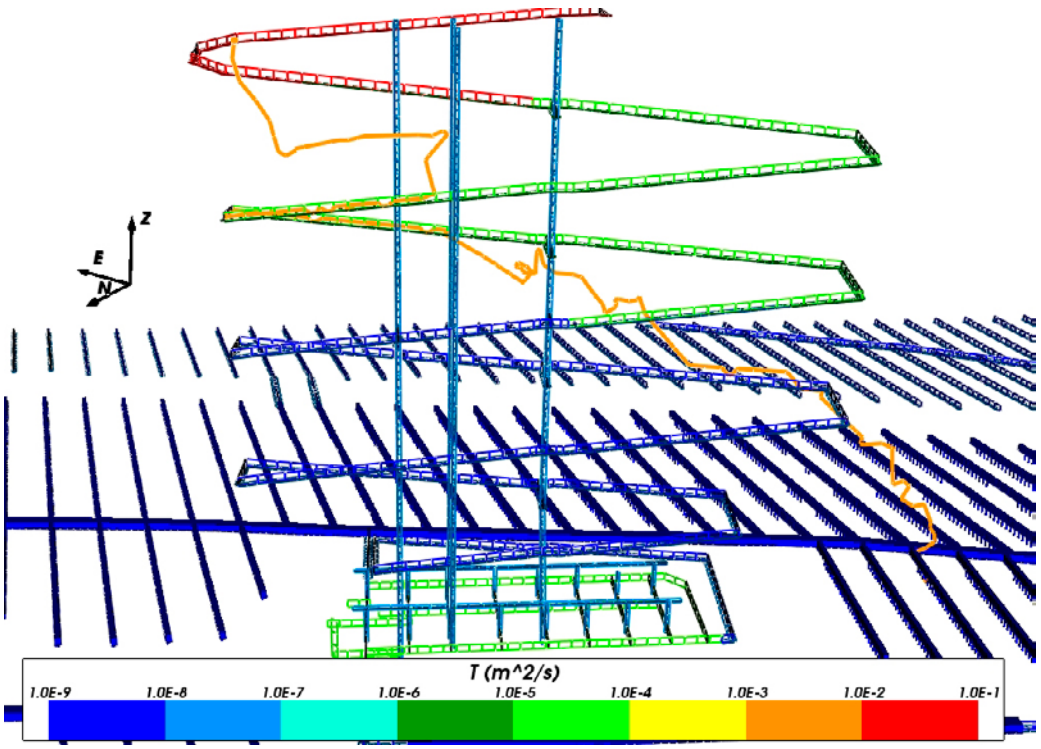


***Figure 3-31.*** *Discharge pathway for a Q1 particle released at 2000 AD and travelling along part of the ramp in the Alternative 1B case.*

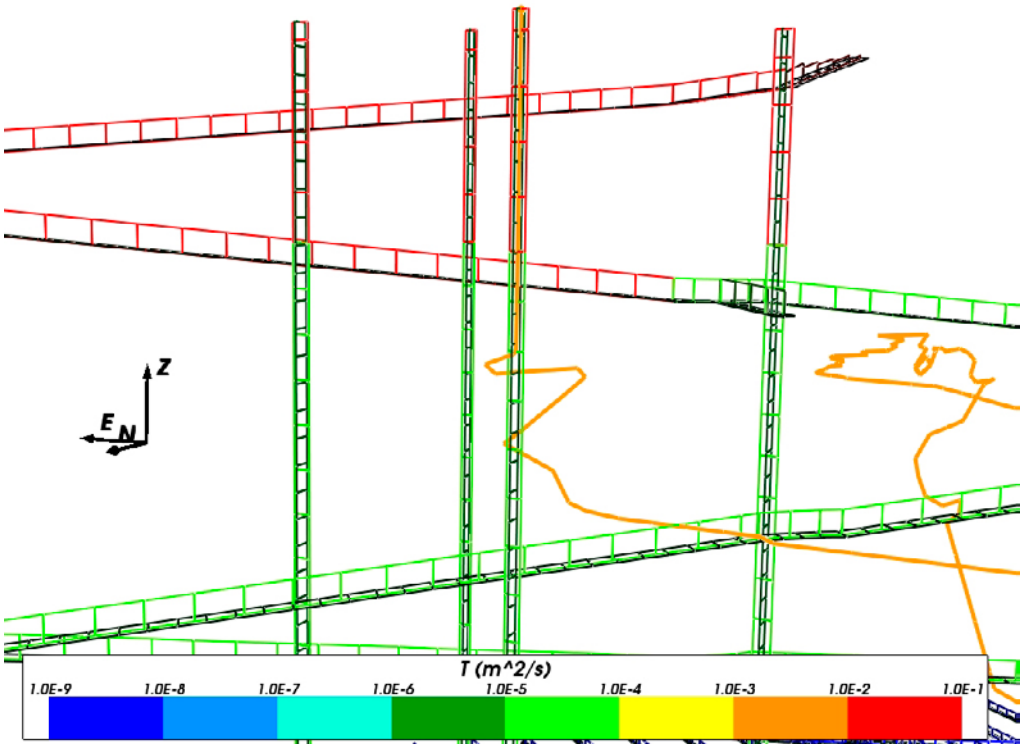


***Figure 3-32.*** *Discharge pathway for a Q1 particle released at 2000 AD and travelling along the upper part of a shaft in the Alternative 2 case.*

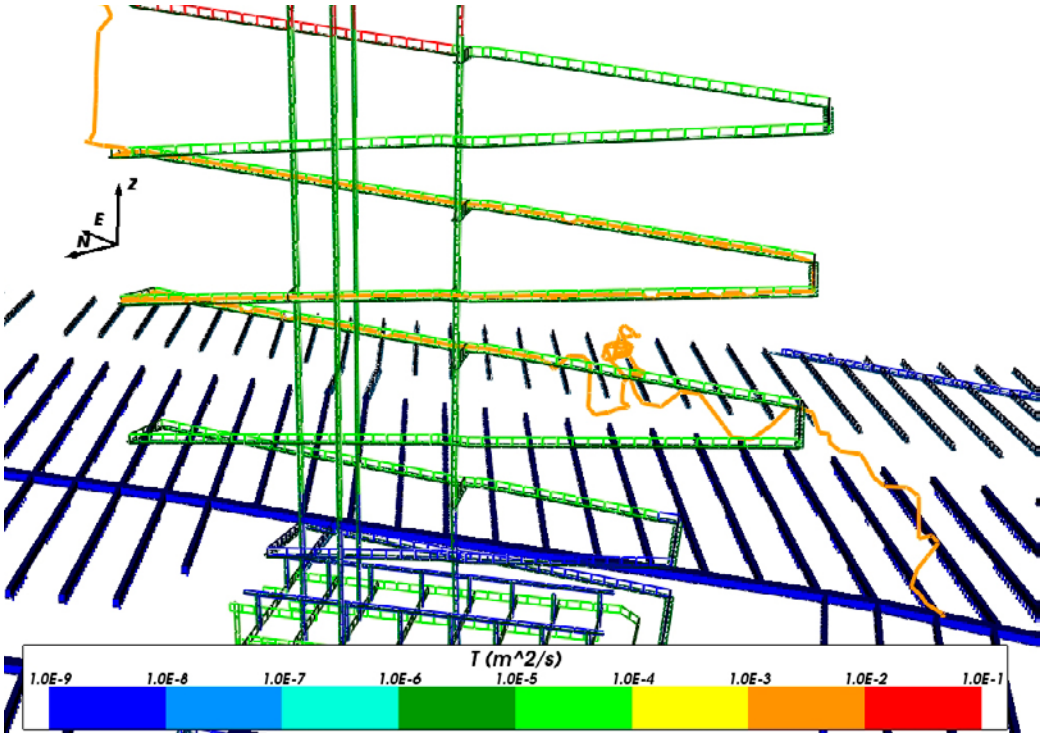


***Figure 3-33.*** *Discharge pathway for a Q1 particle released at 2000 AD and travelling along part of the ramp in the Alternative 2 case with a ramp and shaft EDZ transmissivity of $1.0 \times 10^{-6}$ $m^2/s$.*

## 3.2 Sealing of investigation boreholes

A summary of the modelled borehole cases and the used borehole properties is given in Table 3-25. The table also shows the number of discharge and recharge particles entering the boreholes from release location Q1, Q2 and Q3 for temperate (2000 AD) and glacial (ice front location II) climate conditions. For each release location Q1, Q2 and Q3 there is given: the total number of particles entering boreholes, the number of particles entering KFM boreholes, the number of particles entering HFM boreholes. Table 3-26 shows the corresponding results for realisations 2 and 3 for temperate conditions.

It is clear that there is little or no effect from the boreholes on the particle pathways when the borehole conductivity is less than $10^{-6}$ m/s. In order to have a significant impact on the pathways, at least in the sense of particles entering boreholes, the borehole conductivity needs to be greater than $10^{-4}$ m/s. It is also clear that most of the particles enter KFM boreholes rather than HFM boreholes. This could be explained by the HFM boreholes being shorter and therefore higher up in the rock. This makes them less likely to become a preferred pathway since there are many other highly conductive structures encountered by the particles before they reach the HFM elevations. The results also show that Q1 release locations produce less particles that enter boreholes compared to Q2 and Q3. For temperate conditions, generally fewer recharge particles enter the boreholes compared to discharge particles, although only Q1 is analysed for recharge particles. For glacial conditions the opposite situation prevails. Almost no discharge particles enter the boreholes for glacial conditions but quite a few recharge particles do. Table 3-26 shows that there are some differences in the number of particles entering boreholes between the different realisations. More than twice as many particles enter the boreholes in realisation 2 compared to realisation 3 for Case 8 indicating that there is some sensitivity to the realisation considered. However, since only two additional realisations were studied, it is difficult to draw any general conclusion about the variation between realisations.

The boreholes that attract most particles are KFM07B, KFM07C and KFM08C. Also the HFM boreholes and a few of the other KFM boreholes are to some extent active in terms of attracting released particles but not to the same degree. For glacial conditions KFM07B and KFM09B are the most frequently visited boreholes.

Statistical summaries of various performance measures for the ensemble of discharge particles released at 2000 AD for the Q1, Q2 and Q3 release locations are given in Table 3-27 to Table 3-29, respectively. The corresponding statistical summaries for realisations 2 and 3 are given in Table 3-30 to Table 3-35. Also, for each performance measure the fraction, *OK frac*, of particles successfully reaching the model boundary (for $t_r$ and $F_r$) or successfully starting (for $U_r$) is given. In each table, a comparison between the SR-Site Hydrogeological base case and five different borehole sealing variants is made. The five borehole sealing variants represent the two suggested cases ($K = 10^{-10}$ m/s and $K = 10^{-8}$ m/s) and three additional sensitivities that cover the upper range of modelled conductivities ($K = 10^{-6}$ m/s, $K = 10^{-4}$ m/s and $K = 10^{-2}$ m/s).

Figure 3-34 to Figure 3-51 show the corresponding bar and whisker plots and normalised cumulative distribution function (CDF) plots of the performance measures for the ensemble of discharge particles released at 2000 AD for the Q1, Q2 and Q3 release locations respectively. Figure 3-52 to Figure 3-69 show the corresponding results for realisations 2 and 3. In these figures, the three realisations of the SR-Site Hydrogeological base case are compared to the three realisations of the borehole sealing variant, Case 8 ($K = 10^{-2}$ m/s).

The results for temperate conditions for the ensemble of discharge particles show that including the sealed boreholes into the model has little effect on the performance measure statistics or the distribution of performance measures compared to the SR-Site Hydrogeological base case. Further, changing the properties of the sealed boreholes shows the same small difference in results, at least for borehole conductivities below $10^{-4}$ m/s. The differences in median and 10$^{th}$ percentile values for all three release locations stay within 28 % and are usually much less when comparing the ensemble results. The same conclusion can be drawn for the additional two realisations comparing the variants within each of the realisations. The difference between different realisations for a given variant is of the same magnitude. Some decrease in performance measures can be seen for realisation 3 compared to the other two realisations.

In Table 3-36, a statistical summary of various performance measures for the ensemble of recharge particles released at 2000 AD for the Q1 release locations is given. Table 3-37 and Table 3-38 show the corresponding results for realisations 2 and 3.

In Figure 3-70 to Figure 3-73, the corresponding bar and whisker plots and normalised cumulative distribution function (CDF) plots of the performance measures for the ensemble of recharge particles released at 2000 AD for the Q1 release locations are shown. Figure 3-74 to Figure 3-77 show the corresponding results for realisations 2 and 3.

The recharge particle results for the temperate conditions show that there is a slight decrease in $t_r$ and $F_r$ for some of the cases compared to the SR-Site Hydrogeological base case. One possible explanation for this is the small number of successful particles which could skew the distributions. Even so, the differences are not very pronounced. For $U_r$, the difference in median and 10$^{th}$ percentile values between the cases are very small. Comparing the different realisations again shows that there is a decrease in performance measures for realisation 3.

For the variants at glacial conditions, statistical summaries are given in Table 3-39 to Table 3-42 (these correspond to Table 3-27 to Table 3-38 at temperate conditions) and in Figure 3-78 to Figure 3-99 (these correspond to Figure 3-34 to Figure 3-77 at temperate conditions).

Even though the particle results for the glacial conditions are of a different magnitude compared to the temperate results, the differences are still very small between the cases. The median value for discharge particles differs at most by 10 % between the cases. For the recharge particles, the difference again is slightly larger between the cases but still not very pronounced when analysing the ensemble results.

Since the number of released particles is quite high (1,994) and the number of particles entering the boreholes relatively small, there is a risk that the effect the sealed boreholes have on the ensemble performance measures might be hidden, depending on the number of particles that enter the boreholes and how the performance measures vary for these particles. In order to extract the effect from the sealed boreholes on the flow field and performance measures, as an additional analysis, only the subset of particles that entered the boreholes were selected for statistical analysis of the Q3

release locations. The statistical summaries are given in Table 3-43 to Table 3-45, for all realisations at temperate conditions, and in Table 3-46 for glacial conditions. Bar and whisker plots and CDF plots are shown in Figure 3-100 to Figure 3-105 for temperate conditions. Bar and whisker plots are shown in Figure 3-106 to Figure 3-108 for glacial conditions.

These results take into account all unique particles that enter the boreholes even if the path length along the borehole is short. The three cases with the highest borehole conductivities ($K = 10^{-4}$, $10^{-3}$ and $10^{-2}$ m/s) were chosen for presentation in the figures. The reason for choosing these particular cases is that, for the cases with lower conductivities, there are not enough data since the number of particles entering the boreholes are too low. Even in the three most conductive cases, the data is quite sparse, which explains the slightly rough curves in the CDF plots.

In order to make the comparison as relevant as possible, the same selection of particles found in the sealed boreholes was extracted from the SR-Site Hydrogeological base case and the corresponding statistical analysis was performed. Thus, each borehole case has a corresponding selection of particles in the SR-Site Hydrogeological base case such that BC1 (base case selection 1) corresponds to Case 6 ($K = 10^{-4}$ m/s), BC2 (base case selection 2) to Case 7 ($K = 10^{-3}$ m/s) and BC3 (base case selection 3) to Case 8 ($K = 10^{-2}$ m/s).

The results show that when the statistical analysis is performed on only the particles that enter the sealed boreholes and the statistical results are compared to the corresponding selection of particles in the SR-Site Hydrogeological base case, the effect on the performance measures is larger. For temperate conditions the median values differ between 25 and 50 % while the $10^{th}$ percentile indicates a large spread between the single particles, with a difference of as much as several orders of magnitude. The variation between different realisations is slightly higher indicating some sensitivity to the choice of realisation. For the glacial conditions the difference in performance measure statistics is even greater. The median and $10^{th}$ percentile values for the performance measures differ up to a factor 7 between the cases.

Figure 3-109 shows discharge pathways for 21 particles released from starting positions 950−970 in Case 6. Figure 3-110 shows three selected discharge pathways from Figure 3-109, released from starting positions 958−960. The figures show how some of the released particles enter borehole KFM07C through the deposition tunnel. They follow KFM07C for a few hundred meters upwards and then continue into the fracture system. At higher elevations, the sheet joints in the upper bedrock attract many of the particles that initially follow the boreholes upwards and eventually exit through the model top surface further away from the borehole. Some of the particles enter the boreholes at higher elevations, near the surface. These figures show that there tends to be substantial paths in the bedrock near the start and at the end, but the borehole provides a shortcut between the main transport pathways at depth and the sheet joints.

Figure 3-111 and Figure 3-112 show the recharge pathways in Case 6 from two views. It is clear that most of the particle trajectories are vertical and from below the repository. Only a few particles originate from the top surface, indicating that the sealed boreholes are not likely to draw oxygenated surface water down to repository depths.

**Table 3-25. Summary of modelled cases with borehole properties and the number of discharge and recharge particles entering the boreholes from release locations Q1, Q2 and Q3 for temperate and glacial climate conditions. For each Q1, Q2 and Q3 is given: the total number of particles entering boreholes, the number of particles entering KFM boreholes, the number of particles entering HFM boreholes.**

| Case | Borehole property | Temperate conditions (2000 AD) | | | | | | | | Glacial conditions (ice front location II) | | | | | | | |
|---|---|---|---|---|---|---|---|---|---|---|---|---|---|---|---|---|---|
| | | Discharge | | | | Recharge | | | | Discharge | | | | Recharge | | | |
| | | | Total | KFM | HFM | | Total | KFM | HFM | | Total | KFM | HFM | | Total | KFM | HFM |
| Case 1 | $K = 10^{-10}$ m/s porosity = 0.41 | Q1 | 0 | 0 | 0 | Q1 | 0 | 0 | 0 | Q1 | 0 | 0 | 0 | Q1 | 0 | 0 | 0 |
| | | Q2 | 0 | 0 | 0 | | | | | Q2 | 0 | 0 | 0 | | | | |
| | | Q3 | 0 | 0 | 0 | | | | | Q3 | 0 | 0 | 0 | | | | |
| Case 2 | $K = 10^{-8}$ m/s porosity = 0.2 | Q1 | 0 | 0 | 0 | Q1 | 0 | 0 | 0 | Q1 | 0 | 0 | 0 | Q1 | 0 | 0 | 0 |
| | | Q2 | 1 | 1 | 0 | | | | | Q2 | 0 | 0 | 0 | | | | |
| | | Q3 | 1 | 0 | 1 | | | | | Q3 | 0 | 0 | 0 | | | | |
| Case 3 | $K = 10^{-7}$ m/s porosity = 0.2 | Q1 | 0 | 0 | 0 | Q1 | 0 | 0 | 0 | Q1 | 0 | 0 | 0 | Q1 | 0 | 0 | 0 |
| | | Q2 | 0 | 0 | 0 | | | | | Q2 | 0 | 0 | 0 | | | | |
| | | Q3 | 1 | 1 | 0 | | | | | Q3 | 0 | 0 | 0 | | | | |
| Case 4 | $K = 10^{-6}$ m/s porosity = 0.2 | Q1 | 1 | 0 | 1 | Q1 | 1 | 1 | 0 | Q1 | 0 | 0 | 0 | Q1 | 0 | 0 | 0 |
| | | Q2 | 5 | 5 | 0 | | | | | Q2 | 0 | 0 | 0 | | | | |
| | | Q3 | 0 | 0 | 0 | | | | | Q3 | 0 | 0 | 0 | | | | |
| Case 5 | $K = 10^{-5}$ m/s porosity = 0.2 | Q1 | 2 | 2 | 0 | Q1 | 8 | 8 | 0 | Q1 | 0 | 0 | 0 | Q1 | 3 | 3 | 0 |
| | | Q2 | 7 | 5 | 2 | | | | | Q2 | 0 | 0 | 0 | | | | |
| | | Q3 | 7 | 6 | 1 | | | | | Q3 | 1 | 1 | 0 | | | | |
| Case 6 | $K = 10^{-4}$ m/s porosity = 0.2 | Q1 | 9 | 8 | 1 | Q1 | 12 | 12 | 0 | Q1 | 1 | 1 | 0 | Q1 | 13 | 13 | 0 |
| | | Q2 | 21 | 16 | 5 | | | | | Q2 | 2 | 2 | 0 | | | | |
| | | Q3 | 19 | 15 | 4 | | | | | Q3 | 2 | 2 | 0 | | | | |
| Case 7 | $K = 10^{-3}$ m/s porosity = 0.2 | Q1 | 31 | 28 | 3 | Q1 | 20 | 20 | 0 | Q1 | 2 | 2 | 0 | Q1 | 54 | 54 | 0 |
| | | Q2 | 85 | 66 | 19 | | | | | Q2 | 3 | 3 | 0 | | | | |
| | | Q3 | 77 | 60 | 17 | | | | | Q3 | 3 | 3 | 0 | | | | |
| Case 8 | $K = 10^{-2}$ m/s porosity = 0.2 | Q1 | 78 | 62 | 16 | Q1 | 40 | 40 | 0 | Q1 | 1 | 1 | 0 | Q1 | 96 | 96 | 0 |
| | | Q2 | 196 | 155 | 41 | | | | | Q2 | 1 | 1 | 0 | | | | |
| | | Q3 | 200 | 170 | 30 | | | | | Q3 | 3 | 3 | 0 | | | | |

**Table 3-26. Summary of modelled cases with borehole properties and the number of discharge and recharge particles entering the boreholes from release location Q1, Q2 and Q3 for realisations 2 and 3 at temperate conditions (2000 AD). For each Q1, Q2 and Q3 is given: the total number of particles entering boreholes, the number of particles entering KFM boreholes, the number of particles entering HFM boreholes.**

| Case | Borehole property | Realisation 2 (2000 AD) | | | | | | | | Realisation 3 (2000 AD) | | | | | | | |
|---|---|---|---|---|---|---|---|---|---|---|---|---|---|---|---|---|---|
| | | Discharge | | | | Recharge | | | | Discharge | | | | Recharge | | | |
| | | | Total | KFM | HFM | | Total | KFM | HFM | | Total | KFM | HFM | | Total | KFM | HFM |
| Case 1 | $K = 10^{-10}$ m/s porosity = 0.41 | Q1 | 0 | 0 | 0 | Q1 | 0 | 0 | 0 | Q1 | 0 | 0 | 0 | Q1 | 0 | 0 | 0 |
| | | Q2 | 0 | 0 | 0 | | | | | Q2 | 0 | 0 | 0 | | | | |
| | | Q3 | 0 | 0 | 0 | | | | | Q3 | 0 | 0 | 0 | | | | |
| Case 2 | $K = 10^{-8}$ m/s porosity = 0.2 | Q1 | 0 | 0 | 0 | Q1 | 3 | 3 | 0 | Q1 | 0 | 0 | 0 | Q1 | 1 | 1 | 0 |
| | | Q2 | 1 | 1 | 0 | | | | | Q2 | 1 | 0 | 1 | | | | |
| | | Q3 | 3 | 3 | 0 | | | | | Q3 | 1 | 1 | 0 | | | | |
| Case 3 | $K = 10^{-7}$ m/s porosity = 0.2 | Q1 | 0 | 0 | 0 | Q1 | 3 | 3 | 0 | Q1 | 0 | 0 | 0 | Q1 | 3 | 3 | 0 |
| | | Q2 | 9 | 9 | 0 | | | | | Q2 | 2 | 2 | 0 | | | | |
| | | Q3 | 8 | 8 | 0 | | | | | Q3 | 2 | 2 | 0 | | | | |
| Case 4 | $K = 10^{-6}$ m/s porosity = 0.2 | Q1 | 1 | 1 | 0 | Q1 | 8 | 8 | 0 | Q1 | 5 | 5 | 0 | Q1 | 3 | 3 | 0 |
| | | Q2 | 11 | 11 | 0 | | | | | Q2 | 6 | 5 | 1 | | | | |
| | | Q3 | 3 | 3 | 0 | | | | | Q3 | 10 | 9 | 1 | | | | |
| Case 5 | $K = 10^{-5}$ m/s porosity = 0.2 | Q1 | 3 | 3 | 0 | Q1 | 13 | 13 | 0 | Q1 | 23 | 22 | 1 | Q1 | 10 | 10 | 0 |
| | | Q2 | 18 | 18 | 0 | | | | | Q2 | 28 | 27 | 1 | | | | |
| | | Q3 | 14 | 14 | 0 | | | | | Q3 | 28 | 28 | 1 | | | | |
| Case 6 | $K = 10^{-4}$ m/s porosity = 0.2 | Q1 | 16 | 16 | 0 | Q1 | 9 | 9 | 0 | Q1 | 29 | 29 | 0 | Q1 | 11 | 11 | 0 |
| | | Q2 | 56 | 55 | 1 | | | | | Q2 | 54 | 52 | 2 | | | | |
| | | Q3 | 47 | 46 | 1 | | | | | Q3 | 43 | 40 | 3 | | | | |
| Case 7 | $K = 10^{-3}$ m/s porosity = 0.2 | Q1 | 56 | 55 | 1 | Q1 | 17 | 17 | 0 | Q1 | 46 | 45 | 1 | Q1 | 29 | 29 | 0 |
| | | Q2 | 158 | 158 | 0 | | | | | Q2 | 79 | 74 | 5 | | | | |
| | | Q3 | 155 | 148 | 7 | | | | | Q3 | 92 | 80 | 14 | | | | |
| Case 8 | $K = 10^{-2}$ m/s porosity = 0.2 | Q1 | 109 | 102 | 7 | Q1 | 40 | 40 | 0 | Q1 | 75 | 58 | 17 | Q1 | 33 | 33 | 0 |
| | | Q2 | 300 | 293 | 7 | | | | | Q2 | 120 | 103 | 17 | | | | |
| | | Q3 | 300 | 292 | 8 | | | | | Q3 | 134 | 102 | 32 | | | | |

### *Discharge temperate conditions*

**Table 3-27. Statistical summary of various performance measures for the ensemble of particles. Comparison between the SR-Site Hydrogeological base case and five different borehole sealing variants. Statistics for Q1 discharge particles released at 2000 AD.**

| Case | $\log_{10}(t_r)$ [y] | | | | | $\log_{10}(U_r)$ [m/y] | | | | | $\log_{10}(F_r)$ [y/m] | | | | |
|---|---|---|---|---|---|---|---|---|---|---|---|---|---|---|---|
| | Median | Std. dev. | 10 % | 90 % | OK frac | Median | Std. dev. | 10 % | 90 % | OK frac | Median | Std. dev. | 10 % | 90 % | OK frac |
| SR-Site base case | 2.285 | 0.397 | 1.772 | 2.719 | 0.244 | −5.321 | 1.039 | −6.719 | −4.135 | 0.407 | 6.497 | 0.695 | 5.728 | 7.278 | 0.244 |
| Case 1 K = $10^{-10}$ m/s | 2.296 | 0.389 | 1.817 | 2.721 | 0.243 | −5.322 | 1.037 | −6.712 | −4.132 | 0.406 | 6.495 | 0.690 | 5.727 | 7.397 | 0.243 |
| Case 2 K = $10^{-8}$ m/s | 2.298 | 0.390 | 1.818 | 2.721 | 0.243 | −5.322 | 1.037 | −6.712 | −4.132 | 0.406 | 6.493 | 0.691 | 5.728 | 7.410 | 0.243 |
| Case 4 K = $10^{-6}$ m/s | 2.289 | 0.378 | 1.760 | 2.698 | 0.245 | −5.326 | 1.036 | −6.713 | −4.141 | 0.406 | 6.516 | 0.667 | 5.758 | 7.383 | 0.245 |
| Case 6 K = $10^{-4}$ m/s | 2.254 | 0.389 | 1.766 | 2.663 | 0.240 | −5.335 | 1.034 | −6.702 | −4.138 | 0.405 | 6.523 | 0.717 | 5.750 | 7.404 | 0.240 |
| Case 8 K = $10^{-2}$ m/s | 2.192 | 0.398 | 1.722 | 2.616 | 0.242 | −5.345 | 1.034 | −6.719 | −4.150 | 0.406 | 6.510 | 0.703 | 5.679 | 7.364 | 0.242 |

**Table 3-28. Statistical summary of various performance measures for the ensemble of particles. Comparison between the SR-Site Hydrogeological base case and five different borehole sealing variants. Statistics for Q2 discharge particles released at 2000 AD.**

| Case | $\log_{10}(t_r)$ [y] | | | | | $\log_{10}(U_r)$ [m/y] | | | | | $\log_{10}(F_r)$ [y/m] | | | | |
|---|---|---|---|---|---|---|---|---|---|---|---|---|---|---|---|
| | Median | Std. dev. | 10 % | 90 % | OK frac | Median | Std. dev. | 10 % | 90 % | OK frac | Median | Std. dev. | 10 % | 90 % | OK frac |
| SR-Site base case | 2.242 | 0.377 | 1.747 | 2.671 | 0.892 | −2.100 | 0.373 | −2.483 | −1.559 | 1.000 | 6.157 | 0.773 | 5.172 | 7.112 | 0.892 |
| Case 1 K = $10^{-10}$ m/s | 2.238 | 0.363 | 1.776 | 2.685 | 0.895 | −2.100 | 0.373 | −2.483 | −1.558 | 1.000 | 6.223 | 0.757 | 5.198 | 7.155 | 0.895 |
| Case 2 K = $10^{-8}$ m/s | 2.240 | 0.376 | 1.745 | 2.683 | 0.894 | −2.100 | 0.373 | −2.483 | −1.558 | 1.000 | 6.206 | 0.786 | 5.188 | 7.164 | 0.894 |
| Case 4 K = $10^{-6}$ m/s | 2.232 | 0.365 | 1.762 | 2.654 | 0.902 | −2.100 | 0.373 | −2.482 | −1.559 | 1.000 | 6.253 | 0.760 | 5.219 | 7.153 | 0.902 |
| Case 6 K = $10^{-4}$ m/s | 2.215 | 0.356 | 1.746 | 2.629 | 0.893 | −2.101 | 0.372 | −2.481 | −1.562 | 1.000 | 6.227 | 0.766 | 5.195 | 7.143 | 0.893 |
| Case 8 K = $10^{-2}$ m/s | 2.179 | 0.351 | 1.733 | 2.593 | 0.894 | −2.093 | 0.369 | −2.480 | −1.570 | 1.000 | 6.214 | 0.728 | 5.262 | 7.089 | 0.894 |

**Table 3-29. Statistical summary of various performance measures for the ensemble of particles. Comparison between the SR-Site Hydrogeological base case and five different borehole sealing variants. Statistics for Q3 discharge particles released at 2000 AD.**

| Case | $\log_{10}(t_r)$ [y] | | | | | $\log_{10}(U_r)$ [m/y] | | | | | $\log_{10}(F_r)$ [y/m] | | | | |
|---|---|---|---|---|---|---|---|---|---|---|---|---|---|---|---|
| | Median | Std. dev. | 10 % | 90 % | OK frac | Median | Std. dev. | 10 % | 90 % | OK frac | Median | Std. dev. | 10 % | 90 % | OK frac |
| SR-Site base case | 2.229 | 0.366 | 1.739 | 2.635 | 0.780 | −3.384 | 0.701 | −4.278 | −2.725 | 0.780 | 6.188 | 0.727 | 5.162 | 6.989 | 0.780 |
| Case 1 $K = 10^{-10}$ m/s | 2.234 | 0.358 | 1.761 | 2.637 | 0.783 | −3.368 | 0.714 | −4.248 | −2.706 | 0.783 | 6.164 | 0.739 | 5.154 | 7.013 | 0.783 |
| Case 2 $K = 10^{-8}$ m/s | 2.221 | 0.361 | 1.739 | 2.615 | 0.778 | −3.396 | 0.692 | −4.254 | −2.741 | 0.778 | 6.158 | 0.726 | 5.100 | 6.945 | 0.778 |
| Case 4 $K = 10^{-6}$ m/s | 2.220 | 0.362 | 1.752 | 2.638 | 0.787 | −3.361 | 0.676 | −4.236 | −2.717 | 0.787 | 6.178 | 0.740 | 5.140 | 7.039 | 0.787 |
| Case 6 $K = 10^{-4}$ m/s | 2.205 | 0.357 | 1.736 | 2.603 | 0.785 | −3.377 | 0.703 | −4.286 | −2.716 | 0.785 | 6.185 | 0.736 | 5.141 | 7.010 | 0.785 |
| Case 8 $K = 10^{-2}$ m/s | 2.155 | 0.358 | 1.722 | 2.563 | 0.786 | −3.394 | 0.711 | −4.318 | −2.726 | 0.786 | 6.170 | 0.723 | 5.138 | 6.974 | 0.786 |

**Table 3-30. Statistical summary of various performance measures for the ensemble of particles. Comparison between the SR-Site Hydrogeological base case and five different borehole sealing variants for realisation 2. Statistics for Q1 discharge particles released at 2000 AD.**

| Case | $\log_{10}(t_r)$ [y] | | | | | $\log_{10}(U_r)$ [m/y] | | | | | $\log_{10}(F_r)$ [y/m] | | | | |
|---|---|---|---|---|---|---|---|---|---|---|---|---|---|---|---|
| | Median | Std. dev. | 10 % | 90 % | OK frac | Median | Std. dev. | 10 % | 90 % | OK frac | Median | Std. dev. | 10 % | 90 % | OK frac |
| SR-Site base case, r2 | 2.221 | 0.461 | 1.760 | 2.641 | 0.244 | −5.419 | 1.147 | −6.753 | −3.924 | 0.398 | 6.626 | 0.792 | 5.648 | 7.473 | 0.244 |
| Case 1 $K = 10^{-10}$ m/s | 2.196 | 0.495 | 1.781 | 2.675 | 0.240 | −5.419 | 1.147 | −6.753 | −3.924 | 0.398 | 6.654 | 0.831 | 5.604 | 7.554 | 0.240 |
| Case 2 $K = 10^{-8}$ m/s | 2.185 | 0.461 | 1.742 | 2.591 | 0.243 | −5.419 | 1.147 | −6.753 | −3.924 | 0.398 | 6.604 | 0.776 | 5.684 | 7.398 | 0.243 |
| Case 4 $K = 10^{-6}$ m/s | 2.203 | 0.474 | 1.750 | 2.655 | 0.240 | −5.424 | 1.149 | −6.763 | −3.924 | 0.398 | 6.646 | 0.794 | 5.700 | 7.428 | 0.240 |
| Case 6 $K = 10^{-4}$ m/s | 2.213 | 0.460 | 1.733 | 2.610 | 0.242 | −5.413 | 1.147 | −6.756 | −3.924 | 0.398 | 6.608 | 0.802 | 5.590 | 7.487 | 0.242 |
| Case 8 $K = 10^{-2}$ m/s | 2.162 | 0.508 | 1.624 | 2.561 | 0.238 | −5.426 | 1.160 | −6.777 | −3.932 | 0.396 | 6.558 | 0.811 | 5.573 | 7.487 | 0.238 |

**Table 3-31. Statistical summary of various performance measures for the ensemble of particles. Comparison between the SR-Site Hydrogeological base case and five different borehole sealing variants for realisation 2. Statistics for Q2 discharge particles released at 2000 AD.**

| Case | $\log_{10}(t_r)$ [y] | | | | | $\log_{10}(U_r)$ [m/y] | | | | | $\log_{10}(F_r)$ [y/m] | | | | |
|---|---|---|---|---|---|---|---|---|---|---|---|---|---|---|---|
| | Median | Std. dev. | 10 % | 90 % | OK frac | Median | Std. dev. | 10 % | 90 % | OK frac | Median | Std. dev. | 10 % | 90 % | OK frac |
| SR-Site base case, r2 | 2.177 | 0.421 | 1.748 | 2.546 | 0.921 | −2.127 | 0.312 | −2.492 | −1.770 | 1.000 | 6.309 | 0.807 | 5.298 | 7.189 | 0.921 |
| Case 1 K = $10^{-10}$ m/s | 2.188 | 0.423 | 1.771 | 2.563 | 0.936 | −2.127 | 0.312 | −2.492 | −1.770 | 1.000 | 6.311 | 0.811 | 5.242 | 7.169 | 0.936 |
| Case 2 K = $10^{-8}$ m/s | 2.175 | 0.420 | 1.754 | 2.560 | 0.938 | −2.127 | 0.312 | −2.493 | −1.770 | 1.000 | 6.272 | 0.819 | 5.247 | 7.177 | 0.938 |
| Case 4 K = $10^{-6}$ m/s | 2.170 | 0.425 | 1.743 | 2.559 | 0.934 | −2.126 | 0.312 | −2.492 | −1.771 | 1.000 | 6.307 | 0.795 | 5.301 | 7.166 | 0.934 |
| Case 6 K = $10^{-4}$ m/s | 2.171 | 0.425 | 1.745 | 2.553 | 0.932 | −2.126 | 0.313 | −2.491 | −1.776 | 1.000 | 6.293 | 0.808 | 5.277 | 7.192 | 0.932 |
| Case 8 K = $10^{-2}$ m/s | 2.106 | 0.468 | 1.552 | 2.528 | 0.930 | −2.133 | 0.320 | −2.493 | −1.769 | 1.000 | 6.236 | 0.805 | 5.220 | 7.185 | 0.930 |

**Table 3-32. Statistical summary of various performance measures for the ensemble of particles. Comparison between the SR-Site Hydrogeological base case and five different borehole sealing variants for realisation 2. Statistics for Q3 discharge particles released at 2000 AD.**

| Case | $\log_{10}(t_r)$ [y] | | | | | $\log_{10}(U_r)$ [m/y] | | | | | $\log_{10}(F_r)$ [y/m] | | | | |
|---|---|---|---|---|---|---|---|---|---|---|---|---|---|---|---|
| | Median | Std. dev. | 10 % | 90 % | OK frac | Median | Std. dev. | 10 % | 90 % | OK frac | Median | Std. dev. | 10 % | 90 % | OK frac |
| SR-Site base case, r2 | 2.171 | 0.426 | 1.739 | 2.541 | 0.778 | −3.414 | 0.719 | −4.376 | −2.785 | 0.778 | 6.239 | 0.796 | 5.216 | 7.113 | 0.778 |
| Case 1 K = $10^{-10}$ m/s | 2.165 | 0.423 | 1.751 | 2.541 | 0.786 | −3.420 | 0.725 | −4.366 | −2.795 | 0.786 | 6.240 | 0.766 | 5.233 | 7.082 | 0.786 |
| Case 2 K = $10^{-8}$ m/s | 2.170 | 0.419 | 1.739 | 2.545 | 0.787 | −3.398 | 0.705 | −4.327 | −2.788 | 0.787 | 6.242 | 0.764 | 5.193 | 7.050 | 0.787 |
| Case 4 K = $10^{-6}$ m/s | 2.157 | 0.426 | 1.728 | 2.525 | 0.789 | −3.425 | 0.742 | −4.382 | −2.758 | 0.789 | 6.230 | 0.759 | 5.235 | 7.035 | 0.789 |
| Case 6 K = $10^{-4}$ m/s | 2.145 | 0.434 | 1.723 | 2.536 | 0.780 | −3.436 | 0.738 | −4.376 | −2.756 | 0.780 | 6.235 | 0.770 | 5.249 | 7.055 | 0.780 |
| Case 8 K = $10^{-2}$ m/s | 2.110 | 0.478 | 1.491 | 2.498 | 0.764 | −3.422 | 0.750 | −4.350 | −2.764 | 0.764 | 6.193 | 0.760 | 5.231 | 6.943 | 0.764 |

**Table 3-33. Statistical summary of various performance measures for the ensemble of particles. Comparison between the SR-Site Hydrogeological base case and five different borehole sealing variants for realisation 3. Statistics for Q1 discharge particles released at 2000 AD.**

| Case | $\log_{10}(t_r)$ [y] | | | | | $\log_{10}(U_r)$ [m/y] | | | | | $\log_{10}(F_r)$ [y/m] | | | | |
|---|---|---|---|---|---|---|---|---|---|---|---|---|---|---|---|
| | Median | Std. dev. | 10 % | 90 % | OK frac | Median | Std. dev. | 10 % | 90 % | OK frac | Median | Std. dev. | 10 % | 90 % | OK frac |
| SR-Site base case, r3 | 2.128 | 0.413 | 1.595 | 2.662 | 0.277 | −5.164 | 1.196 | −6.655 | −3.443 | 0.432 | 6.465 | 0.737 | 5.559 | 7.410 | 0.277 |
| Case 1 $K = 10^{-10}$ m/s | 2.129 | 0.396 | 1.641 | 2.580 | 0.285 | −5.159 | 1.196 | −6.656 | −3.444 | 0.432 | 6.443 | 0.726 | 5.491 | 7.321 | 0.285 |
| Case 2 $K = 10^{-8}$ m/s | 2.109 | 0.417 | 1.651 | 2.610 | 0.285 | −5.159 | 1.196 | −6.656 | −3.444 | 0.432 | 6.408 | 0.734 | 5.594 | 7.342 | 0.285 |
| Case 4 $K = 10^{-6}$ m/s | 2.112 | 0.426 | 1.592 | 2.632 | 0.286 | −5.159 | 1.197 | −6.655 | −3.444 | 0.432 | 6.434 | 0.724 | 5.560 | 7.327 | 0.286 |
| Case 6 $K = 10^{-4}$ m/s | 2.097 | 0.423 | 1.584 | 2.658 | 0.283 | −5.156 | 1.200 | −6.649 | −3.443 | 0.432 | 6.392 | 0.733 | 5.584 | 7.419 | 0.283 |
| Case 8 $K = 10^{-2}$ m/s | 2.077 | 0.420 | 1.539 | 2.545 | 0.283 | −5.149 | 1.210 | −6.645 | −3.410 | 0.432 | 6.419 | 0.738 | 5.512 | 7.290 | 0.283 |

**Table 3-34. Statistical summary of various performance measures for the ensemble of particles. Comparison between the SR-Site Hydrogeological base case and five different borehole sealing variants for realisation 3. Statistics for Q2 discharge particles released at 2000 AD.**

| Case | $\log_{10}(t_r)$ [y] | | | | | $\log_{10}(U_r)$ [m/y] | | | | | $\log_{10}(F_r)$ [y/m] | | | | |
|---|---|---|---|---|---|---|---|---|---|---|---|---|---|---|---|
| | Median | Std. dev. | 10 % | 90 % | OK frac | Median | Std. dev. | 10 % | 90 % | OK frac | Median | Std. dev. | 10 % | 90 % | OK frac |
| SR-Site base case, r3 | 2.056 | 0.409 | 1.572 | 2.584 | 0.892 | −2.082 | 0.363 | −2.551 | −1.634 | 1.000 | 6.134 | 0.794 | 5.104 | 7.157 | 0.892 |
| Case 1 $K = 10^{-10}$ m/s | 2.080 | 0.415 | 1.585 | 2.615 | 0.920 | −2.083 | 0.363 | −2.551 | −1.635 | 1.000 | 6.144 | 0.807 | 5.106 | 7.129 | 0.920 |
| Case 2 $K = 10^{-8}$ m/s | 2.072 | 0.415 | 1.582 | 2.617 | 0.919 | −2.083 | 0.363 | −2.551 | −1.635 | 1.000 | 6.130 | 0.817 | 5.099 | 7.238 | 0.919 |
| Case 4 $K = 10^{-6}$ m/s | 2.081 | 0.414 | 1.572 | 2.618 | 0.919 | −2.082 | 0.363 | −2.552 | −1.635 | 1.000 | 6.153 | 0.807 | 5.124 | 7.128 | 0.919 |
| Case 6 $K = 10^{-4}$ m/s | 2.066 | 0.414 | 1.562 | 2.572 | 0.923 | −2.082 | 0.365 | −2.553 | −1.631 | 1.000 | 6.177 | 0.798 | 5.115 | 7.144 | 0.923 |
| Case 8 $K = 10^{-2}$ m/s | 2.050 | 0.403 | 1.571 | 2.564 | 0.922 | −2.084 | 0.370 | −2.556 | −1.614 | 1.000 | 6.155 | 0.813 | 5.094 | 7.196 | 0.922 |

**Table 3-35. Statistical summary of various performance measures for the ensemble of particles. Comparison between the SR-Site Hydrogeological base case and five different borehole sealing variants for realisation 3. Statistics for Q3 discharge particles released at 2000 AD.**

| Case | $\log_{10}(t_r)$ [y] | | | | | $\log_{10}(U_r)$ [m/y] | | | | | $\log_{10}(F_r)$ [y/m] | | | | |
|---|---|---|---|---|---|---|---|---|---|---|---|---|---|---|---|
| | Median | Std. dev. | 10 % | 90 % | OK frac | Median | Std. dev. | 10 % | 90 % | OK frac | Median | Std. dev. | 10 % | 90 % | OK frac |
| SR-Site base case, r3 | 2.042 | 0.396 | 1.549 | 2.534 | 0.750 | −3.371 | 0.719 | −4.379 | −2.771 | 0.750 | 6.064 | 0.777 | 5.001 | 6.973 | 0.750 |
| Case 1 $K = 10^{-10}$ m/s | 2.046 | 0.391 | 1.558 | 2.537 | 0.771 | −3.374 | 0.731 | −4.466 | −2.794 | 0.771 | 6.087 | 0.743 | 5.071 | 6.973 | 0.771 |
| Case 2 $K = 10^{-8}$ m/s | 2.041 | 0.397 | 1.546 | 2.560 | 0.767 | −3.355 | 0.735 | −4.452 | −2.744 | 0.767 | 6.084 | 0.760 | 5.023 | 6.958 | 0.767 |
| Case 4 $K = 10^{-6}$ m/s | 2.049 | 0.396 | 1.559 | 2.560 | 0.768 | −3.353 | 0.730 | −4.356 | −2.767 | 0.768 | 6.082 | 0.762 | 5.074 | 7.001 | 0.768 |
| Case 6 $K = 10^{-4}$ m/s | 2.040 | 0.392 | 1.563 | 2.551 | 0.767 | −3.387 | 0.738 | −4.383 | −2.763 | 0.767 | 6.106 | 0.746 | 5.068 | 6.976 | 0.767 |
| Case 8 $K = 10^{-2}$ m/s | 2.026 | 0.402 | 1.546 | 2.543 | 0.760 | −3.357 | 0.700 | −4.295 | −2.750 | 0.760 | 6.104 | 0.750 | 5.085 | 6.987 | 0.760 |

### *Recharge temperate conditions*

**Table 3-36. Statistical summary of various performance measures for the ensemble of particles. Comparison between the SR-Site Hydrogeological base case and five different borehole sealing variants. Statistics for Q1 recharge particles released at 2000 AD.**

| Case | $\log_{10}(t_r)$ [y] | | | | | $\log_{10}(U_r)$ [m/y] | | | | | $\log_{10}(F_r)$ [y/m] | | | | |
|---|---|---|---|---|---|---|---|---|---|---|---|---|---|---|---|
| | Median | Std. dev. | 10 % | 90 % | OK frac | Median | Std. dev. | 10 % | 90 % | OK frac | Median | Std. dev. | 10 % | 90 % | OK frac |
| SR-Site base case | 1.852 | 0.674 | 0.831 | 2.480 | 0.187 | −5.298 | 1.070 | −6.702 | −4.087 | 0.345 | 6.428 | 0.819 | 5.430 | 7.568 | 0.187 |
| Case 1 $K = 10^{-10}$ m/s | 1.892 | 0.697 | 0.853 | 2.506 | 0.186 | −5.299 | 1.068 | −6.701 | −4.079 | 0.347 | 6.467 | 0.850 | 5.482 | 7.561 | 0.186 |
| Case 2 $K = 10^{-8}$ m/s | 1.892 | 0.690 | 0.849 | 2.504 | 0.186 | −5.299 | 1.068 | −6.701 | −4.079 | 0.347 | 6.471 | 0.842 | 5.480 | 7.564 | 0.186 |
| Case 4 $K = 10^{-6}$ m/s | 1.901 | 0.640 | 1.008 | 2.490 | 0.186 | −5.299 | 1.067 | −6.698 | −4.068 | 0.348 | 6.584 | 0.795 | 5.500 | 7.466 | 0.186 |
| Case 6 $K = 10^{-4}$ m/s | 1.824 | 0.670 | 0.869 | 2.515 | 0.186 | −5.304 | 1.067 | −6.700 | −4.066 | 0.346 | 6.458 | 0.838 | 5.416 | 7.493 | 0.186 |
| Case 8 $K = 10^{-2}$ m/s | 1.717 | 0.704 | 0.688 | 2.488 | 0.181 | −5.307 | 1.069 | −6.686 | −4.087 | 0.346 | 6.475 | 0.826 | 5.436 | 7.460 | 0.181 |

**Table 3-37. Statistical summary of various performance measures for the ensemble of particles. Comparison between the SR-Site Hydrogeological base case and five different borehole sealing variants for realisation 2. Statistics for Q1 recharge particles released at 2000 AD.**

| Case | $\log_{10}(t_r)$ [y] | | | | | $\log_{10}(U_r)$ [m/y] | | | | | $\log_{10}(F_r)$ [y/m] | | | | |
|---|---|---|---|---|---|---|---|---|---|---|---|---|---|---|---|
| | Median | Std. dev. | 10 % | 90 % | OK frac | Median | Std. dev. | 10 % | 90 % | OK frac | Median | Std. dev. | 10 % | 90 % | OK frac |
| SR-Site base case, r2 | 1.840 | 0.682 | 1.008 | 2.478 | 0.166 | −5.482 | 1.229 | −6.800 | −3.755 | 0.325 | 6.566 | 0.901 | 5.552 | 7.491 | 0.166 |
| Case 1 $K = 10^{-10}$ m/s | 1.861 | 0.682 | 0.860 | 2.502 | 0.169 | −5.484 | 1.230 | −6.796 | −3.755 | 0.325 | 6.532 | 0.869 | 5.581 | 7.471 | 0.169 |
| Case 2 $K = 10^{-8}$ m/s | 1.861 | 0.680 | 0.846 | 2.491 | 0.169 | −5.482 | 1.229 | −6.796 | −3.755 | 0.325 | 6.536 | 0.896 | 5.588 | 7.491 | 0.169 |
| Case 4 $K = 10^{-6}$ m/s | 1.899 | 0.668 | 0.839 | 2.450 | 0.167 | −5.482 | 1.228 | −6.794 | −3.757 | 0.326 | 6.600 | 0.876 | 5.550 | 7.519 | 0.167 |
| Case 6 $K = 10^{-4}$ m/s | 1.896 | 0.686 | 0.847 | 2.490 | 0.169 | −5.479 | 1.225 | −6.794 | −3.751 | 0.326 | 6.590 | 0.909 | 5.528 | 7.472 | 0.169 |
| Case 8 $K = 10^{-2}$ m/s | 1.912 | 0.720 | 0.948 | 2.591 | 0.173 | −5.482 | 1.227 | −6.764 | −3.749 | 0.327 | 6.626 | 0.938 | 5.502 | 7.665 | 0.173 |

**Table 3-38. Statistical summary of various performance measures for the ensemble of particles. Comparison between the SR-Site Hydrogeological base case and five different borehole sealing variants for realisation 3. Statistics for Q1 recharge particles released at 2000 AD.**

| Case | $\log_{10}(t_r)$ [y] | | | | | $\log_{10}(U_r)$ [m/y] | | | | | $\log_{10}(F_r)$ [y/m] | | | | |
|---|---|---|---|---|---|---|---|---|---|---|---|---|---|---|---|
| | Median | Std. dev. | 10 % | 90 % | OK frac | Median | Std. dev. | 10 % | 90 % | OK frac | Median | Std. dev. | 10 % | 90 % | OK frac |
| SR-Site base case, r3 | 1.589 | 0.656 | 0.764 | 2.300 | 0.232 | −5.136 | 1.241 | −6.615 | −3.345 | 0.370 | 6.426 | 0.771 | 5.608 | 7.316 | 0.232 |
| Case 1 $K = 10^{-10}$ m/s | 1.599 | 0.691 | 0.735 | 2.383 | 0.230 | −5.135 | 1.241 | −6.614 | −3.346 | 0.370 | 6.445 | 0.767 | 5.669 | 7.286 | 0.230 |
| Case 2 $K = 10^{-8}$ m/s | 1.594 | 0.684 | 0.741 | 2.382 | 0.231 | −5.135 | 1.241 | −6.614 | −3.346 | 0.370 | 6.445 | 0.754 | 5.670 | 7.257 | 0.231 |
| Case 4 $K = 10^{-6}$ m/s | 1.584 | 0.638 | 0.767 | 2.287 | 0.227 | −5.135 | 1.241 | −6.614 | −3.345 | 0.370 | 6.394 | 0.737 | 5.651 | 7.256 | 0.227 |
| Case 6 $K = 10^{-4}$ m/s | 1.613 | 0.673 | 0.712 | 2.248 | 0.231 | −5.133 | 1.244 | −6.612 | −3.336 | 0.371 | 6.389 | 0.739 | 5.634 | 7.243 | 0.231 |
| Case 8 $K = 10^{-2}$ m/s | 1.511 | 0.701 | 0.590 | 2.278 | 0.228 | −5.134 | 1.252 | −6.608 | −3.291 | 0.371 | 6.340 | 0.790 | 5.391 | 7.235 | 0.228 |

### *Discharge glacial conditions*

**Table 3-39. Statistical summary of various performance measures for the ensemble of particles. Comparison between the SR-Site Hydrogeological base case and five different borehole sealing variants. Statistics for Q1 discharge particles released for glacial ice front location II.**

| Case | $\log_{10}(t_r)$ [y] | | | | | $\log_{10}(U_r)$ [m/y] | | | | | $\log_{10}(F_r)$ [y/m] | | | | |
|---|---|---|---|---|---|---|---|---|---|---|---|---|---|---|---|
| | Median | Std. dev. | 10 % | 90 % | OK frac | Median | Std. dev. | 10 % | 90 % | OK frac | Median | Std. dev. | 10 % | 90 % | OK frac |
| SR-Site base case | 0.470 | 0.512 | 0.118 | 0.960 | 0.289 | −3.578 | 1.342 | −5.716 | −2.254 | 0.378 | 4.861 | 0.890 | 3.913 | 6.021 | 0.289 |
| Case 1 K = $10^{-10}$ m/s | 0.495 | 0.442 | 0.142 | 0.937 | 0.294 | −3.576 | 1.340 | −5.693 | −2.258 | 0.378 | 4.857 | 0.838 | 3.976 | 6.001 | 0.294 |
| Case 2 K = $10^{-8}$ m/s | 0.492 | 0.443 | 0.142 | 0.931 | 0.293 | −3.576 | 1.340 | −5.693 | −2.257 | 0.378 | 4.849 | 0.837 | 3.990 | 5.992 | 0.293 |
| Case 4 K = $10^{-6}$ m/s | 0.516 | 0.433 | 0.163 | 0.915 | 0.293 | −3.576 | 1.341 | −5.693 | −2.246 | 0.378 | 4.849 | 0.817 | 4.004 | 5.984 | 0.293 |
| Case 6 K = $10^{-4}$ m/s | 0.498 | 0.499 | 0.110 | 1.029 | 0.291 | −3.576 | 1.342 | −5.697 | −2.235 | 0.378 | 4.819 | 0.883 | 3.934 | 6.069 | 0.291 |
| Case 8 K = $10^{-2}$ m/s | 0.496 | 0.435 | 0.182 | 0.908 | 0.287 | −3.575 | 1.345 | −5.708 | −2.234 | 0.379 | 4.830 | 0.825 | 4.013 | 5.911 | 0.287 |

**Table 3-40. Statistical summary of various performance measures for the ensemble of particles. Comparison between the SR-Site Hydrogeological base case and five different borehole sealing variants. Statistics for Q2 discharge particles released for glacial ice front location II.**

| Case | $\log_{10}(t_r)$ [y] | | | | | $\log_{10}(U_r)$ [m/y] | | | | | $\log_{10}(F_r)$ [y/m] | | | | |
|---|---|---|---|---|---|---|---|---|---|---|---|---|---|---|---|
| | Median | Std. dev. | 10 % | 90 % | OK frac | Median | Std. dev. | 10 % | 90 % | OK frac | Median | Std. dev. | 10 % | 90 % | OK frac |
| SR-Site base case | 0.462 | 0.486 | 0.078 | 0.915 | 0.896 | −0.021 | 1.003 | −2.489 | 0.356 | 1.000 | 4.316 | 0.899 | 3.430 | 5.452 | 0.896 |
| Case 1 K = $10^{-10}$ m/s | 0.456 | 0.503 | −0.008 | 0.935 | 0.896 | −0.022 | 1.003 | −2.489 | 0.357 | 1.000 | 4.346 | 0.913 | 3.366 | 5.544 | 0.896 |
| Case 2 K = $10^{-8}$ m/s | 0.452 | 0.504 | −0.011 | 0.935 | 0.897 | −0.022 | 1.003 | −2.489 | 0.357 | 1.000 | 4.339 | 0.913 | 3.355 | 5.524 | 0.897 |
| Case 4 K = $10^{-6}$ m/s | 0.458 | 0.506 | −0.002 | 0.905 | 0.899 | −0.022 | 1.003 | −2.489 | 0.357 | 1.000 | 4.341 | 0.926 | 3.368 | 5.423 | 0.899 |
| Case 6 K = $10^{-4}$ m/s | 0.455 | 0.509 | −0.020 | 0.915 | 0.902 | −0.019 | 1.003 | −2.489 | 0.357 | 1.000 | 4.336 | 0.954 | 3.355 | 5.497 | 0.902 |
| Case 8 K = $10^{-2}$ m/s | 0.444 | 0.510 | 0.048 | 0.920 | 0.897 | −0.023 | 1.007 | −2.485 | 0.360 | 1.000 | 4.312 | 0.936 | 3.327 | 5.499 | 0.897 |

**Table 3-41. Statistical summary of various performance measures for the ensemble of particles. Comparison between the SR-Site Hydrogeological base case and five different borehole sealing variants. Statistics for Q3 discharge particles released for glacial ice front location II.**

| Case | $\log_{10}(t_r)$ [y] | | | | | $\log_{10}(U_r)$ [m/y] | | | | | $\log_{10}(F_r)$ [y/m] | | | | |
|---|---|---|---|---|---|---|---|---|---|---|---|---|---|---|---|
| | Median | Std. dev. | 10 % | 90 % | OK frac | Median | Std. dev. | 10 % | 90 % | OK frac | Median | Std. dev. | 10 % | 90 % | OK frac |
| SR-Site base case | 0.459 | 0.427 | 0.057 | 0.855 | 0.841 | −1.565 | 0.869 | −2.899 | −0.951 | 0.842 | 4.340 | 0.774 | 3.403 | 5.342 | 0.841 |
| Case 1 $K = 10^{-10}$ m/s | 0.451 | 0.413 | 0.019 | 0.829 | 0.841 | −1.539 | 0.870 | −2.961 | −0.899 | 0.842 | 4.290 | 0.761 | 3.338 | 5.297 | 0.841 |
| Case 2 $K = 10^{-8}$ m/s | 0.451 | 0.407 | 0.020 | 0.823 | 0.842 | −1.541 | 0.867 | −2.917 | −0.899 | 0.842 | 4.286 | 0.757 | 3.333 | 5.293 | 0.842 |
| Case 4 $K = 10^{-6}$ m/s | 0.442 | 0.404 | 0.019 | 0.830 | 0.840 | −1.549 | 0.864 | −2.901 | −0.911 | 0.840 | 4.287 | 0.754 | 3.336 | 5.300 | 0.840 |
| Case 6 $K = 10^{-4}$ m/s | 0.462 | 0.419 | 0.080 | 0.833 | 0.843 | −1.536 | 0.873 | −2.954 | −0.969 | 0.843 | 4.332 | 0.769 | 3.394 | 5.299 | 0.843 |
| Case 8 $K = 10^{-2}$ m/s | 0.444 | 0.425 | −0.029 | 0.839 | 0.846 | −1.559 | 0.909 | −3.011 | −0.959 | 0.846 | 4.313 | 0.782 | 3.345 | 5.316 | 0.846 |

### *Recharge glacial conditions*

**Table 3-42. Statistical summary of various performance measures for the ensemble of particles. Comparison between the SR-Site Hydrogeological base case and five different borehole sealing variants. Statistics for Q1 recharge particles released for glacial ice front location II.**

| Case | $\log_{10}(t_r)$ [y] | | | | | $\log_{10}(U_r)$ [m/y] | | | | | $\log_{10}(F_r)$ [y/m] | | | | |
|---|---|---|---|---|---|---|---|---|---|---|---|---|---|---|---|
| | Median | Std. dev. | 10 % | 90 % | OK frac | Median | Std. dev. | 10 % | 90 % | OK frac | Median | Std. dev. | 10 % | 90 % | OK frac |
| SR-Site base case | 0.345 | 0.636 | −0.614 | 0.988 | 0.291 | −3.562 | 1.282 | −5.548 | −2.278 | 0.375 | 4.916 | 0.835 | 3.892 | 5.938 | 0.291 |
| Case 1 $K = 10^{-10}$ m/s | 0.330 | 0.655 | −0.597 | 1.013 | 0.286 | −3.562 | 1.280 | −5.548 | −2.283 | 0.374 | 4.887 | 0.843 | 3.885 | 5.973 | 0.286 |
| Case 2 $K = 10^{-8}$ m/s | 0.330 | 0.655 | −0.597 | 1.013 | 0.286 | −3.562 | 1.280 | −5.548 | −2.283 | 0.374 | 4.887 | 0.842 | 3.891 | 5.973 | 0.286 |
| Case 4 $K = 10^{-6}$ m/s | 0.313 | 0.677 | −0.479 | 1.009 | 0.287 | −3.563 | 1.280 | −5.548 | −2.293 | 0.374 | 4.891 | 0.871 | 3.867 | 5.958 | 0.287 |
| Case 6 $K = 10^{-4}$ m/s | 0.351 | 0.666 | −0.582 | 0.998 | 0.292 | −3.568 | 1.281 | −5.551 | −2.299 | 0.373 | 4.878 | 0.835 | 3.931 | 5.979 | 0.292 |
| Case 8 $K = 10^{-2}$ m/s | 0.216 | 0.729 | −0.802 | 0.954 | 0.282 | −3.568 | 1.284 | −5.585 | −2.295 | 0.373 | 4.828 | 0.873 | 3.824 | 5.898 | 0.282 |

### *Selection of particles entering the sealed boreholes*

**Table 3-43. Statistical summary of various performance measures for the particles entering the boreholes. Comparison between the SR-Site Hydrogeological base case and three different borehole sealing variants. For each borehole sealing variant the corresponding selection of particles were selected from the SR-Site base case. Statistics for Q3 discharge particles released at 2000 AD.**

| Case | $\log_{10}(t_r)$ [y] | | | | | $\log_{10}(U_r)$ [m/y] | | | | | $\log_{10}(F_r)$ [y/m] | | | | |
|---|---|---|---|---|---|---|---|---|---|---|---|---|---|---|---|
| | Median | Std. dev. | 10 % | 90 % | OK frac | Median | Std. dev. | 10 % | 90 % | OK frac | Median | Std. dev. | 10 % | 90 % | OK frac |
| SR-Site base case (BC1) | 2.314 | 0.267 | 1.986 | 2.748 | 0.737 | −3.461 | 1.175 | −6.009 | −2.712 | 0.737 | 6.442 | 0.759 | 5.341 | 7.182 | 0.737 |
| Case 6 K = $10^{-4}$ m/s | 2.256 | 0.635 | 1.147 | 2.764 | 0.684 | −3.391 | 0.914 | −4.540 | −2.217 | 0.684 | 6.267 | 0.934 | 4.598 | 7.277 | 0.684 |
| SR-Site base case (BC2) | 2.313 | 0.319 | 1.756 | 2.601 | 0.909 | −3.401 | 0.621 | −4.160 | −2.737 | 0.909 | 6.305 | 0.781 | 4.730 | 6.947 | 0.909 |
| Case 7 K = $10^{-3}$ m/s | 2.210 | 0.450 | 1.509 | 2.728 | 0.935 | −3.346 | 0.873 | −4.783 | −2.482 | 0.935 | 6.438 | 0.815 | 5.059 | 7.102 | 0.935 |
| SR-Site base case (BC3) | 2.337 | 0.375 | 1.709 | 2.753 | 0.880 | −3.411 | 0.658 | −4.129 | −2.780 | 0.880 | 6.377 | 0.793 | 4.954 | 6.997 | 0.880 |
| Case 8 K = $10^{-2}$ m/s | 2.233 | 0.400 | 1.677 | 2.637 | 0.920 | −3.348 | 0.747 | −4.252 | −2.742 | 0.920 | 6.287 | 0.745 | 4.938 | 6.901 | 0.920 |

**Table 3-44. Statistical summary of various performance measures for the particles entering the boreholes. Comparison between the SR-Site Hydrogeological base case and three different borehole sealing variants for realisation 2. For each borehole sealing variant the corresponding selection of particles were selected from the SR-Site base case. Statistics for Q3 discharge particles released at 2000 AD.**

| Case | $\log_{10}(t_r)$ [y] | | | | | $\log_{10}(U_r)$ [m/y] | | | | | $\log_{10}(F_r)$ [y/m] | | | | |
|---|---|---|---|---|---|---|---|---|---|---|---|---|---|---|---|
| | Median | Std. dev. | 10 % | 90 % | OK frac | Median | Std. dev. | 10 % | 90 % | OK frac | Median | Std. dev. | 10 % | 90 % | OK frac |
| SR-Site base case (BC1) | 2.357 | 0.237 | 2.115 | 2.702 | 0.894 | −3.393 | 0.828 | −4.819 | −2.873 | 0.894 | 6.817 | 0.406 | 6.193 | 7.280 | 0.894 |
| Case 6 K = $10^{-4}$ m/s | 2.075 | 0.650 | 1.306 | 2.553 | 0.915 | −3.339 | 0.649 | −4.589 | −2.812 | 0.915 | 6.362 | 0.937 | 5.241 | 7.127 | 0.915 |
| SR-Site base case (BC2) | 2.312 | 0.294 | 1.991 | 2.643 | 0.748 | −3.443 | 0.605 | −4.375 | −2.937 | 0.748 | 6.762 | 0.600 | 6.050 | 7.295 | 0.748 |
| Case 7 K = $10^{-3}$ m/s | 2.035 | 0.515 | 1.327 | 2.492 | 0.890 | −3.393 | 0.659 | −4.466 | −2.865 | 0.890 | 6.619 | 0.767 | 5.887 | 7.223 | 0.890 |
| SR-Site base case (BC3) | 2.251 | 0.278 | 1.921 | 2.598 | 0.870 | −3.473 | 0.697 | −4.574 | −2.893 | 0.870 | 6.541 | 0.715 | 5.459 | 7.187 | 0.870 |
| Case 8 K = $10^{-2}$ m/s | 1.950 | 0.555 | 1.041 | 2.413 | 0.860 | −3.385 | 0.716 | −4.286 | −2.885 | 0.860 | 6.352 | 0.696 | 5.459 | 7.027 | 0.860 |

**Table 3-45. Statistical summary of various performance measures for the particles entering the boreholes. Comparison between the SR-Site Hydrogeological base case and three different borehole sealing variants for realisation 3. For each borehole sealing variant the corresponding selection of particles were selected from the SR-Site base case. Statistics for Q3 discharge particles released at 2000 AD.**

| Case | $\log_{10}(t_r)$ [y] | | | | | $\log_{10}(U_r)$ [m/y] | | | | | $\log_{10}(F_r)$ [y/m] | | | | |
|---|---|---|---|---|---|---|---|---|---|---|---|---|---|---|---|
| | Median | Std. dev. | 10 % | 90 % | OK frac | Median | Std. dev. | 10 % | 90 % | OK frac | Median | Std. dev. | 10 % | 90 % | OK frac |
| SR-Site base case (BC1) | 2.210 | 0.354 | 1.733 | 2.630 | 0.535 | −3.559 | 0.751 | −4.480 | −2.879 | 0.535 | 6.258 | 0.718 | 5.504 | 7.308 | 0.535 |
| Case 6 $K = 10^{-4}$ m/s | 2.257 | 0.426 | 1.738 | 2.785 | 0.674 | −3.614 | 0.806 | −4.352 | −2.758 | 0.674 | 6.499 | 0.707 | 5.189 | 7.143 | 0.674 |
| SR-Site base case (BC2) | 2.179 | 0.350 | 1.733 | 2.684 | 0.685 | −3.559 | 0.751 | −4.694 | −2.882 | 0.685 | 6.384 | 0.570 | 5.773 | 6.934 | 0.685 |
| Case 7 $K = 10^{-3}$ m/s | 2.294 | 0.465 | 1.604 | 2.730 | 0.750 | −3.583 | 0.740 | −4.672 | −3.113 | 0.750 | 6.458 | 0.497 | 5.902 | 6.996 | 0.750 |
| SR-Site base case (BC3) | 2.056 | 0.377 | 1.506 | 2.518 | 0.687 | −3.533 | 0.689 | −4.441 | −2.803 | 0.687 | 6.204 | 0.746 | 4.944 | 6.815 | 0.687 |
| Case 8 $K = 10^{-2}$ m/s | 2.158 | 0.579 | 1.087 | 2.511 | 0.739 | −3.478 | 0.621 | −4.331 | −2.868 | 0.739 | 6.312 | 0.795 | 4.885 | 6.733 | 0.739 |

**Table 3-46. Statistical summary of various performance measures for the particles entering the boreholes. Comparison between the SR-Site Hydrogeological base case and three different borehole sealing variants. For each borehole sealing variant the corresponding selection of particles were selected from the SR-Site base case. Statistics for Q3 discharge particles released for glacial ice front location II.**

| Case | $\log_{10}(t_r)$ [y] | | | | | $\log_{10}(U_r)$ [m/y] | | | | | $\log_{10}(F_r)$ [y/m] | | | | |
|---|---|---|---|---|---|---|---|---|---|---|---|---|---|---|---|
| | Median | Std. dev. | 10 % | 90 % | OK frac | Median | Std. dev. | 10 % | 90 % | OK frac | Median | Std. dev. | 10 % | 90 % | OK frac |
| SR-Site base case (BC1) | 0.233 | 0.012 | 0.224 | 0.242 | 1.000 | −0.970 | 0.307 | −1.187 | −0.753 | 1.000 | 4.326 | 0.052 | 4.289 | 4.363 | 1.000 |
| Case 6 $K = 10^{-4}$ m/s | 0.118 | 0.503 | −0.237 | 0.473 | 1.000 | −0.894 | 0.404 | −1.180 | −0.609 | 1.000 | 4.216 | 0.482 | 3.875 | 4.557 | 1.000 |
| SR-Site base case (BC2) | 0.242 | 0.377 | 0.132 | 0.833 | 1.000 | −0.753 | 0.440 | −1.500 | −0.725 | 1.000 | 4.320 | 0.360 | 4.289 | 4.927 | 1.000 |
| Case 7 $K = 10^{-3}$ m/s | −0.194 | 0.155 | −0.400 | −0.097 | 1.000 | −0.702 | 0.328 | −1.221 | −0.614 | 1.000 | 3.671 | 0.188 | 3.423 | 3.792 | 1.000 |
| SR-Site base case (BC3) | 0.091 | 0.027 | 0.080 | 0.132 | 1.000 | −0.725 | 0.153 | −0.991 | −0.725 | 1.000 | 4.223 | 0.424 | 3.542 | 4.320 | 1.000 |
| Case 8 $K = 10^{-2}$ m/s | 0.052 | 0.096 | −0.111 | 0.057 | 1.000 | −0.714 | 0.154 | −0.980 | −0.714 | 1.000 | 3.462 | 0.056 | 3.442 | 3.548 | 1.000 |

### *Discharge temperate conditions*

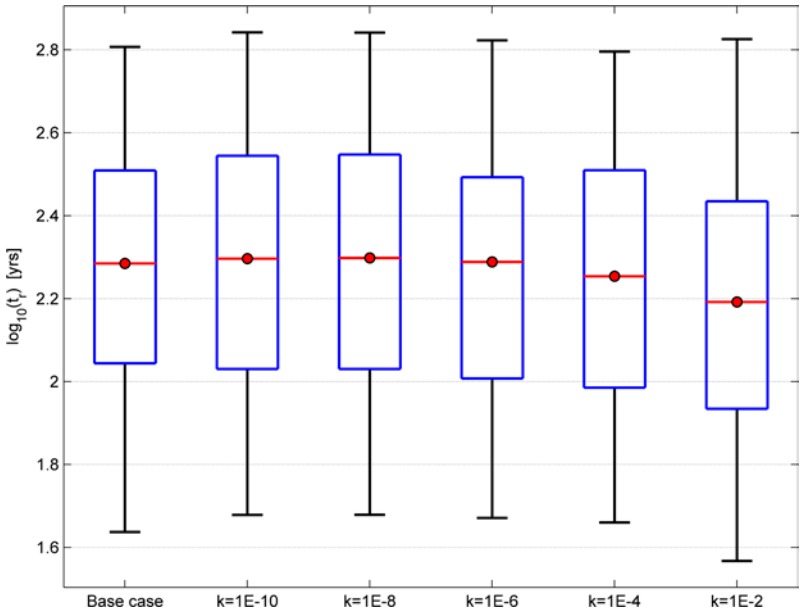


***Figure 3-34.*** *Bar and whisker plot of $t_r$ for the SR-Site Hydrogeological base case (Base case) and five different borehole sealing variants (conductivity in m/s), for all Q1 discharge particles released at 2000 AD and successfully reaching the model boundary. The statistical measures are the median (red), 25$^{th}$ and 75$^{th}$ percentile (blue bar) and the 5$^{th}$ and 95$^{th}$ percentile (black "whiskers").*

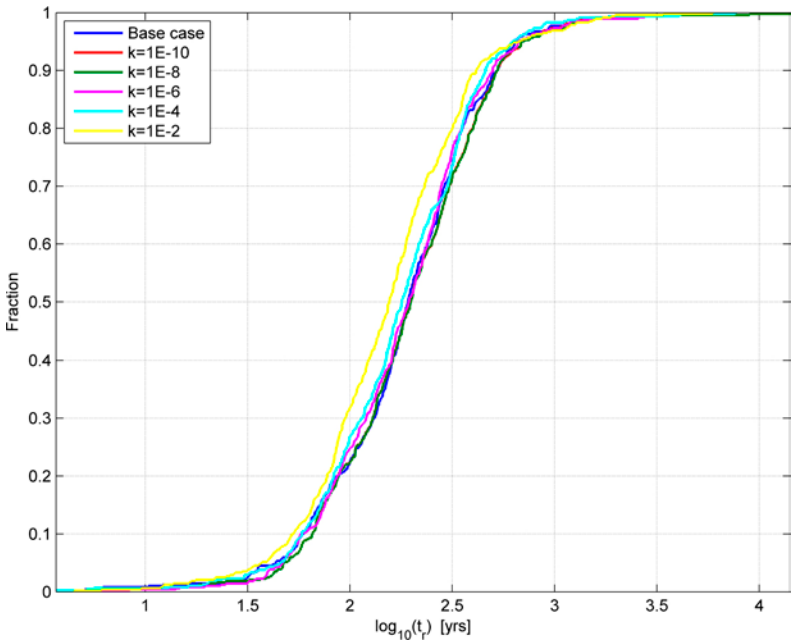


***Figure 3-35.*** *Normalised CDF plot of $t_r$ for the SR-Site Hydrogeological base case (Base case) and five different borehole sealing variants (conductivity in m/s), for all Q1 discharge particles released at 2000 AD and successfully reaching the model boundary.*

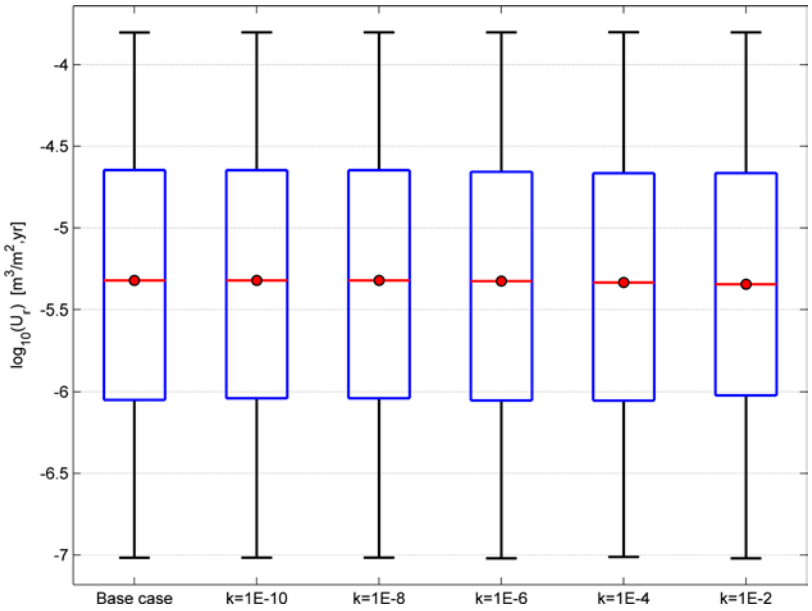


***Figure 3-36.*** *Bar and whisker plot of $U_r$ for the SR-Site Hydrogeological base case (Base case) and five different borehole sealing variants (conductivity in m/s), for all Q1 discharge particles released at 2000 AD and successfully reaching the model boundary. The statistical measures are the median (red), 25$^{th}$ and 75$^{th}$ percentile (blue bar) and the 5$^{th}$ and 95$^{th}$ percentile (black "whiskers").*

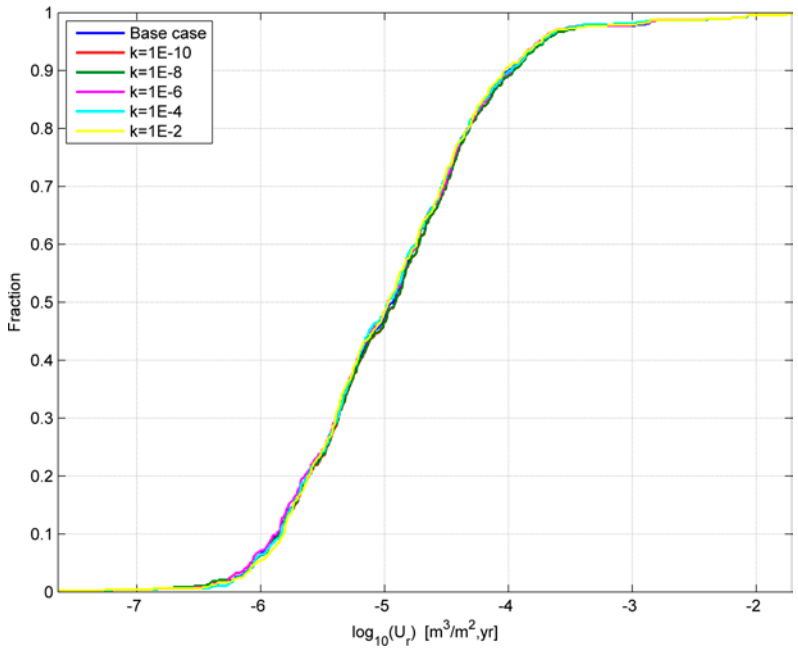


***Figure 3-37.*** *Normalised CDF plot of $U_r$ for the SR-Site Hydrogeological base case (Base case) and five different borehole sealing variants (conductivity in m/s), for all Q1 discharge particles released at 2000 AD and successfully reaching the model boundary.*

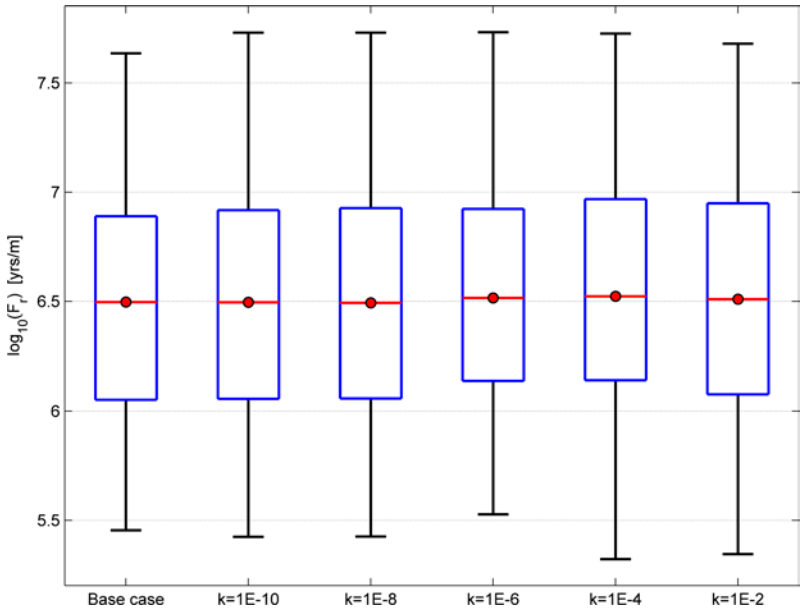


***Figure 3-38.*** *Bar and whisker plot of $F_r$ for the SR-Site Hydrogeological base case (Base case) and five different borehole sealing variants (conductivity in m/s), for all Q1 discharge particles released at 2000 AD and successfully reaching the model boundary. The statistical measures are the median (red), 25$^{th}$ and 75$^{th}$ percentile (blue bar) and the 5$^{th}$ and 95$^{th}$ percentile (black "whiskers").*

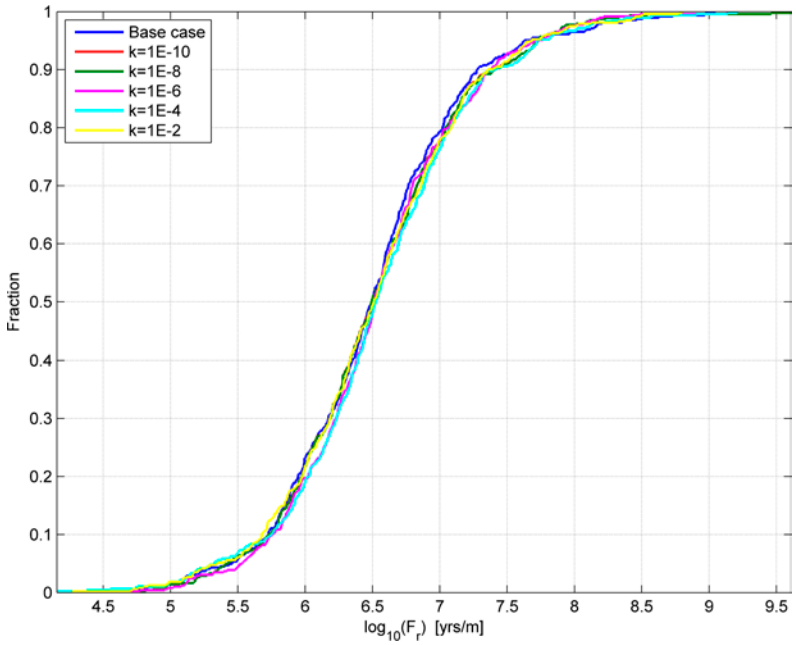


***Figure 3-39.*** *Normalised CDF plot of $F_r$ for the SR-Site Hydrogeological base case (Base case) and five different borehole sealing variants (conductivity in m/s), for all Q1 discharge particles released at 2000 AD and successfully reaching the model boundary.*

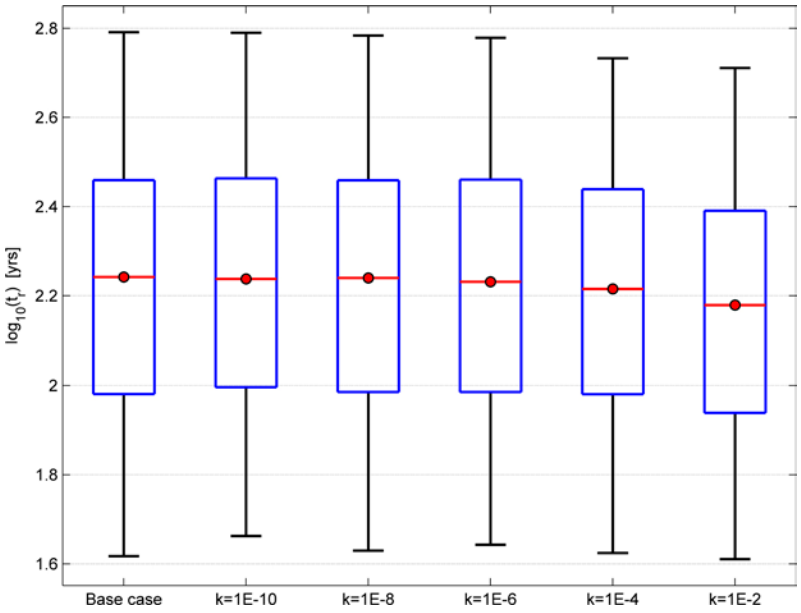


***Figure 3-40.*** *Bar and whisker plot of $t_r$ for the SR-Site Hydrogeological base case (Base case) and five different borehole sealing variants (conductivity in m/s), for all Q2 discharge particles released at 2000 AD and successfully reaching the model boundary. The statistical measures are the median (red), 25$^{th}$ and 75$^{th}$ percentile (blue bar) and the 5$^{th}$ and 95$^{th}$ percentile (black "whiskers").*

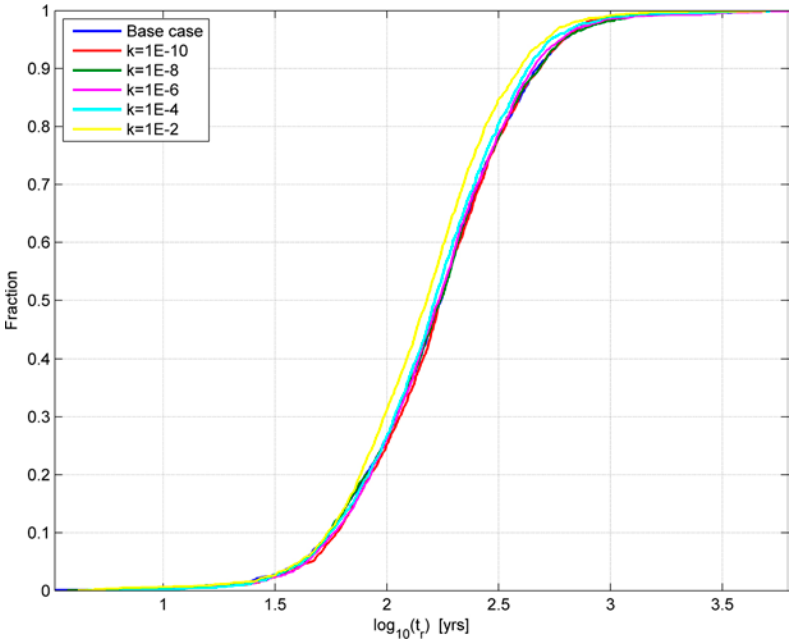


***Figure 3-41.*** *Normalised CDF plot of $t_r$ for the SR-Site Hydrogeological base case (Base case) and five different borehole sealing variants (conductivity in m/s), for all Q2 discharge particles released at 2000 AD and successfully reaching the model boundary.*

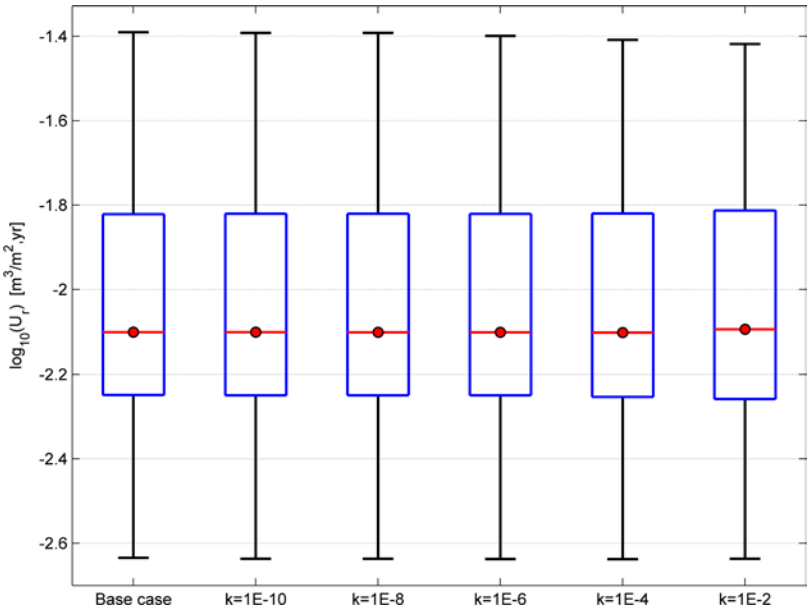


***Figure 3-42.*** *Bar and whisker plot of $U_r$ for the SR-Site Hydrogeological base case (Base case) and five different borehole sealing variants (conductivity in m/s), for all Q2 discharge particles released at 2000 AD and successfully reaching the model boundary. The statistical measures are the median (red), 25$^{th}$ and 75$^{th}$ percentile (blue bar) and the 5$^{th}$ and 95$^{th}$ percentile (black "whiskers").*

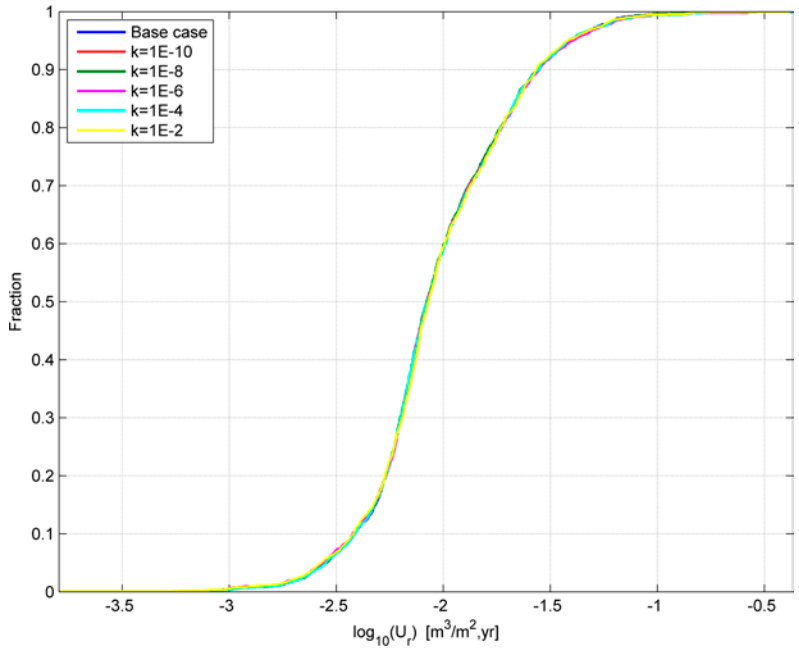


***Figure 3-43.*** *Normalised CDF plot of $U_r$ for the SR-Site Hydrogeological base case (Base case) and five different borehole sealing variants (conductivity in m/s), for all Q2 discharge particles released at 2000 AD and successfully reaching the model boundary.*

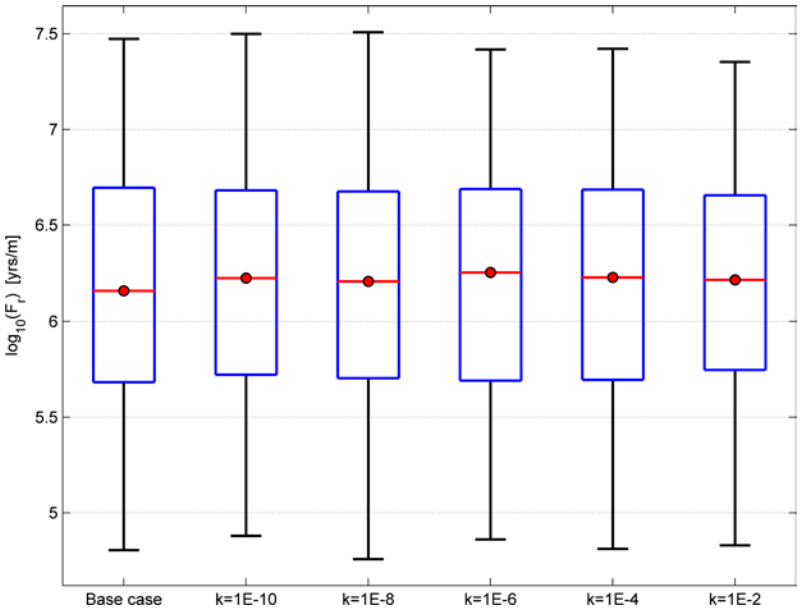


***Figure 3-44.*** *Bar and whisker plot of $F_r$ for the SR-Site Hydrogeological base case (Base case) and five different borehole sealing variants (conductivity in m/s), for all Q2 discharge particles released at 2000 AD and successfully reaching the model boundary. The statistical measures are the median (red), 25$^{th}$ and 75$^{th}$ percentile (blue bar) and the 5$^{th}$ and 95$^{th}$ percentile (black "whiskers").*

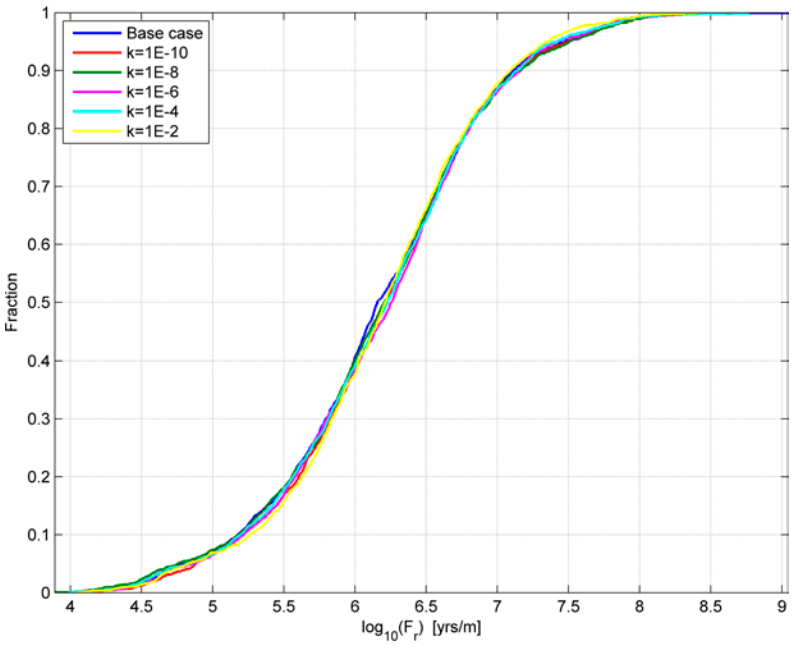


***Figure 3-45.*** *Normalised CDF plot of $F_r$ for the SR-Site Hydrogeological base case (Base case) and five different borehole sealing variants (conductivity in m/s), for all Q2 discharge particles released at 2000 AD and successfully reaching the model boundary.*

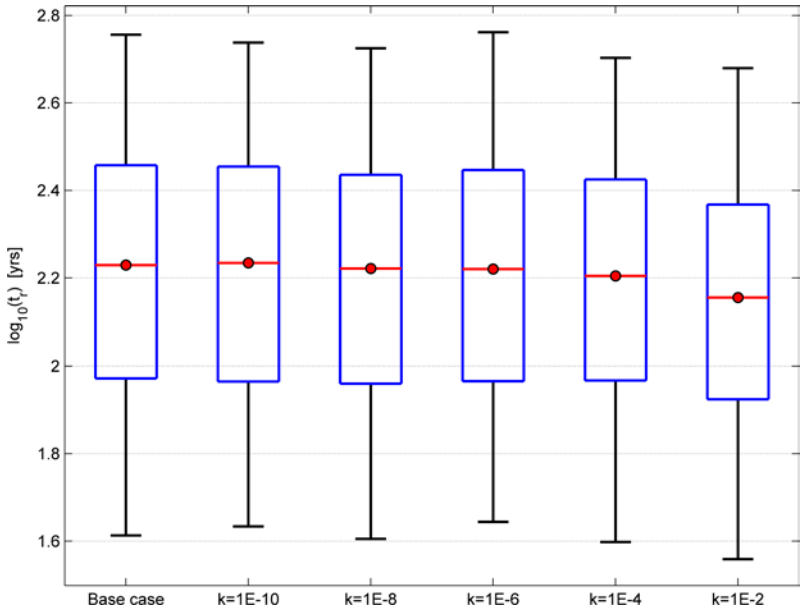


***Figure 3-46.*** *Bar and whisker plot of $t_r$ for the SR-Site Hydrogeological base case (Base case) and five different borehole sealing variants (conductivity in m/s), for all Q3 discharge particles released at 2000 AD and successfully reaching the model boundary. The statistical measures are the median (red), 25$^{th}$ and 75$^{th}$ percentile (blue bar) and the 5$^{th}$ and 95$^{th}$ percentile (black "whiskers").*

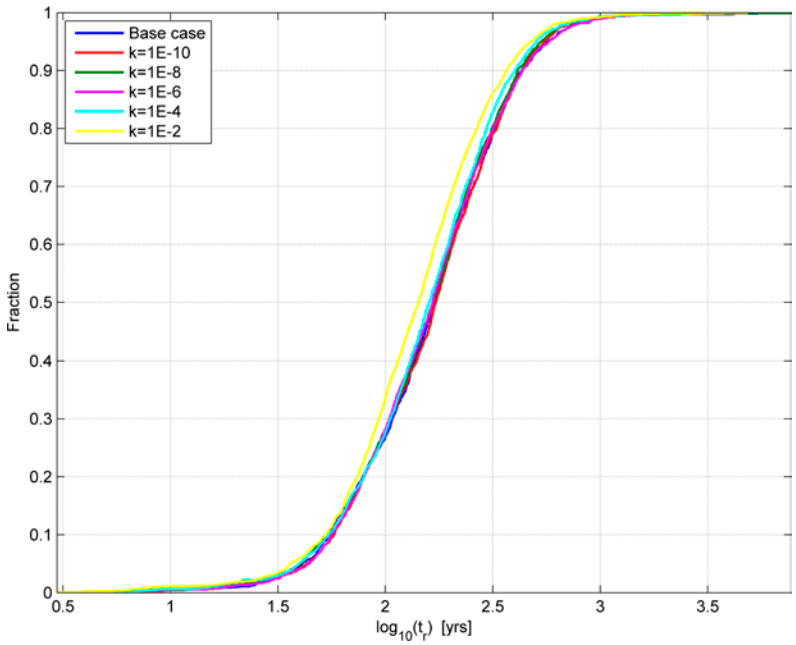


***Figure 3-47.*** *Normalised CDF plot of $t_r$ for the SR-Site Hydrogeological base case (Base case) and five different borehole sealing variants (conductivity in m/s), for all Q3 discharge particles released at 2000 AD and successfully reaching the model boundary.*

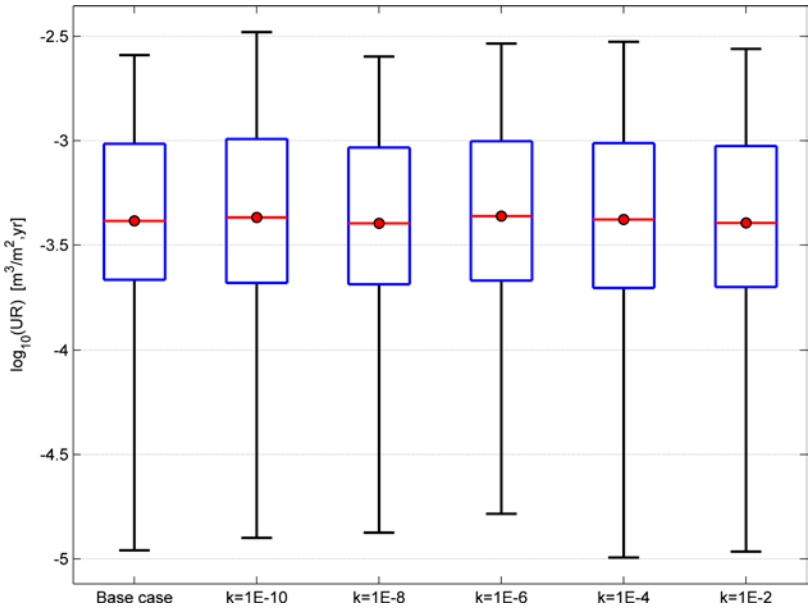


***Figure 3-48.*** *Bar and whisker plot of $U_r$ for the SR-Site Hydrogeological base case (Base case) and five different borehole sealing variants (conductivity in m/s), for all Q3 discharge particles released at 2000 AD and successfully reaching the model boundary. The statistical measures are the median (red), 25$^{th}$ and 75$^{th}$ percentile (blue bar) and the 5$^{th}$ and 95$^{th}$ percentile (black "whiskers").*

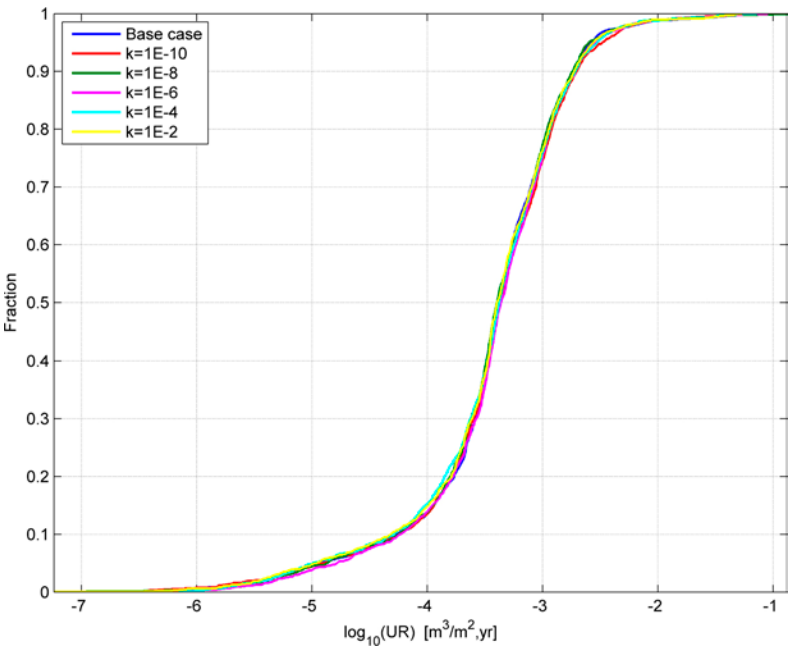


***Figure 3-49.*** *Normalised CDF plot of $U_r$ for the SR-Site Hydrogeological base case (Base case) and five different borehole sealing variants (conductivity in m/s), for all Q3 discharge particles released at 2000 AD and successfully reaching the model boundary.*

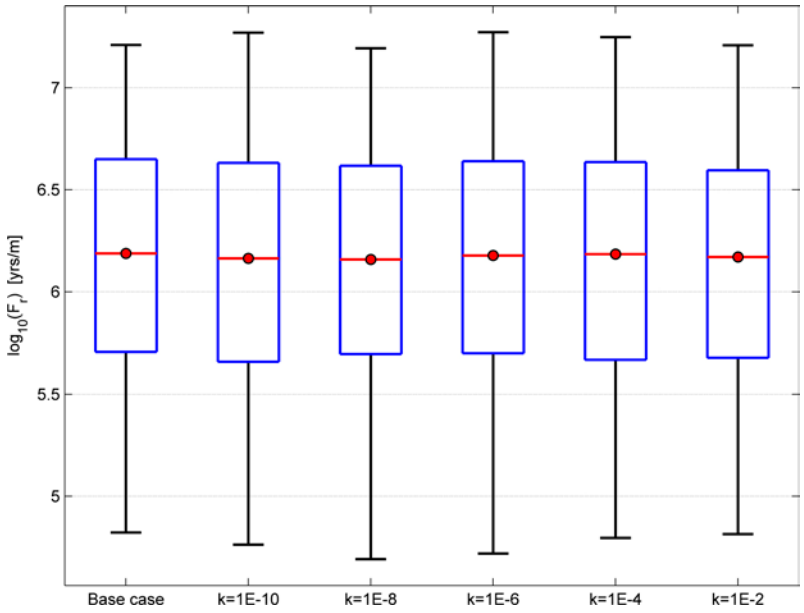


***Figure 3-50.*** *Bar and whisker plot of $F_r$ for the SR-Site Hydrogeological base case (Base case) and five different borehole sealing variants (conductivity in m/s), for all Q3 discharge particles released at 2000 AD and successfully reaching the model boundary. The statistical measures are the median (red), 25$^{th}$ and 75$^{th}$ percentile (blue bar) and the 5$^{th}$ and 95$^{th}$ percentile (black "whiskers").*

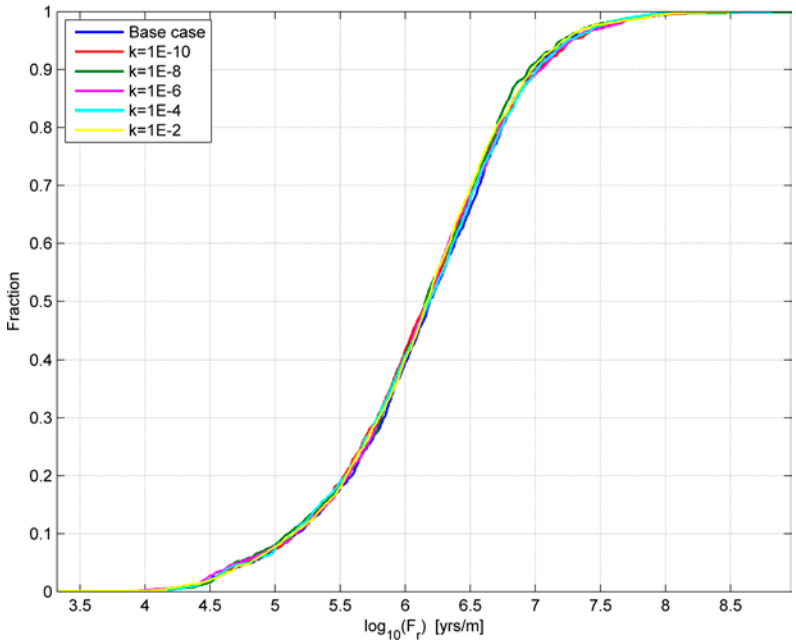


***Figure 3-51.*** *Normalised CDF plot of $F_r$ for the SR-Site Hydrogeological base case (Base case) and five different borehole sealing variants (conductivity in m/s), for all Q3 discharge particles released at 2000 AD and successfully reaching the model boundary.*

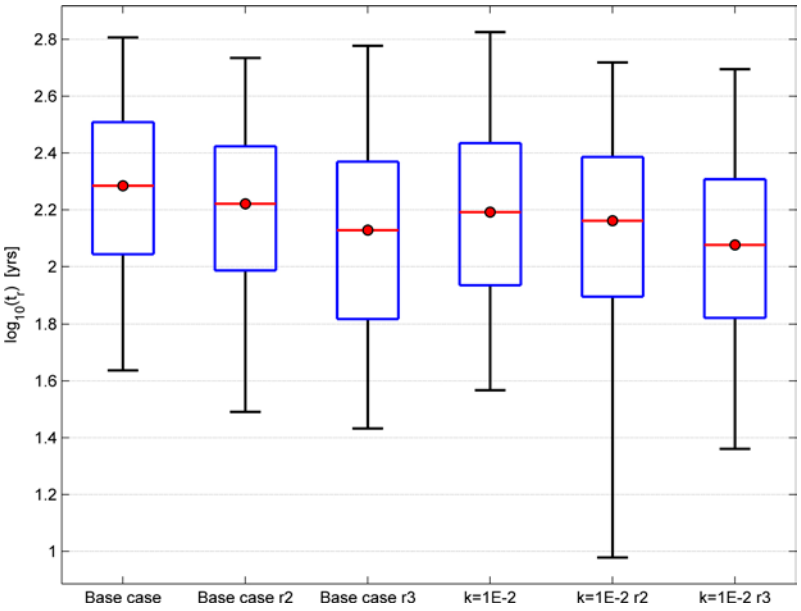


***Figure 3-52.*** *Bar and whisker plot of $t_r$ for the SR-Site Hydrogeological base case (Base case) and the borehole sealing variant, Case 8 ($k = 10^{-2}$ m/s), with two additional realisations, for all Q1 discharge particles released at 2000 AD and successfully reaching the model boundary. The statistical measures are the median (red), 25$^{th}$ and 75$^{th}$ percentile (blue bar) and the 5$^{th}$ and 95$^{th}$ percentile (black "whiskers").*

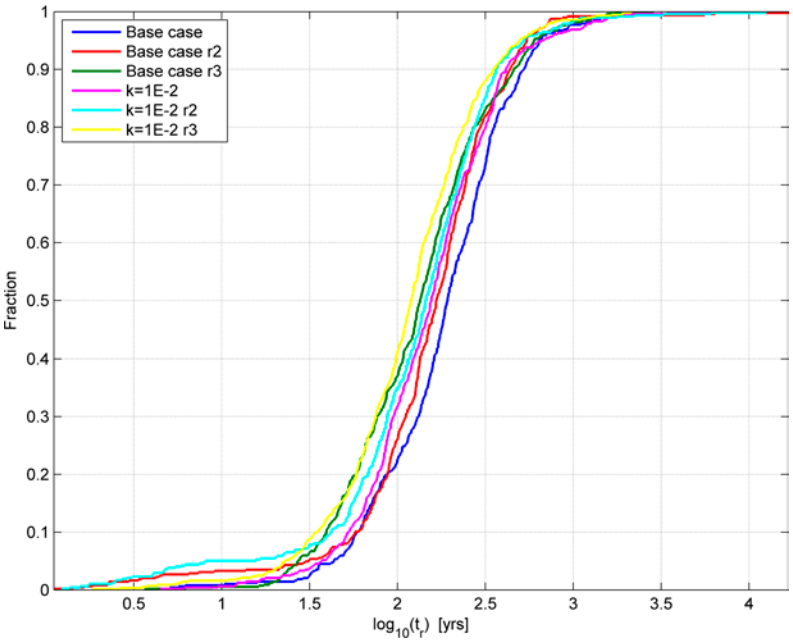


***Figure 3-53.*** *Normalised CDF plot of $t_r$ for the SR-Site Hydrogeological base case (Base case) and the borehole sealing variant, Case 8 ($k = 10^{-2}$ m/s), with two additional realisations, for all Q1 discharge particles released at 2000 AD and successfully reaching the model boundary.*

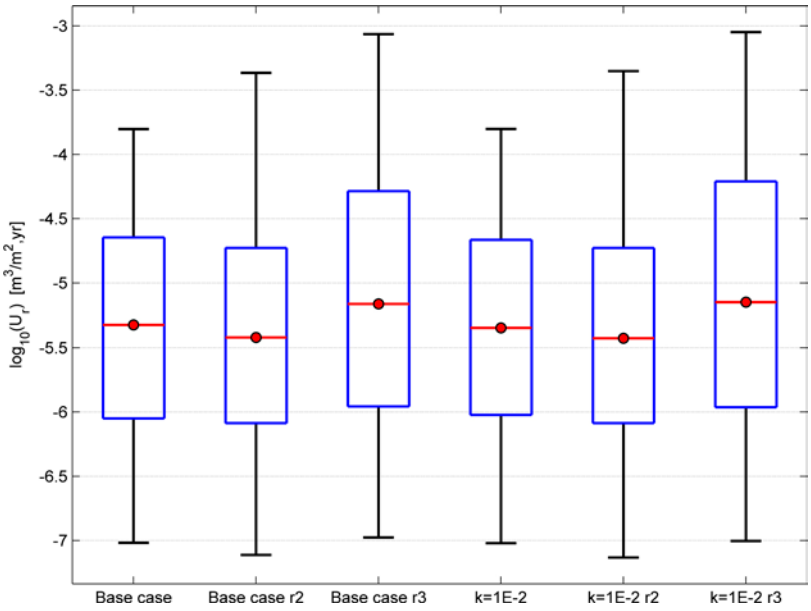


***Figure 3-54.*** *Bar and whisker plot of $U_r$ for the SR-Site Hydrogeological base case (Base case) and the borehole sealing variant, Case 8 ($k = 10^{-2}$ m/s), with two additional realisations, for all Q1 discharge particles released at 2000 AD and successfully reaching the model boundary. The statistical measures are the median (red), 25th and 75th percentile (blue bar) and the 5th and 95th percentile (black "whiskers").*

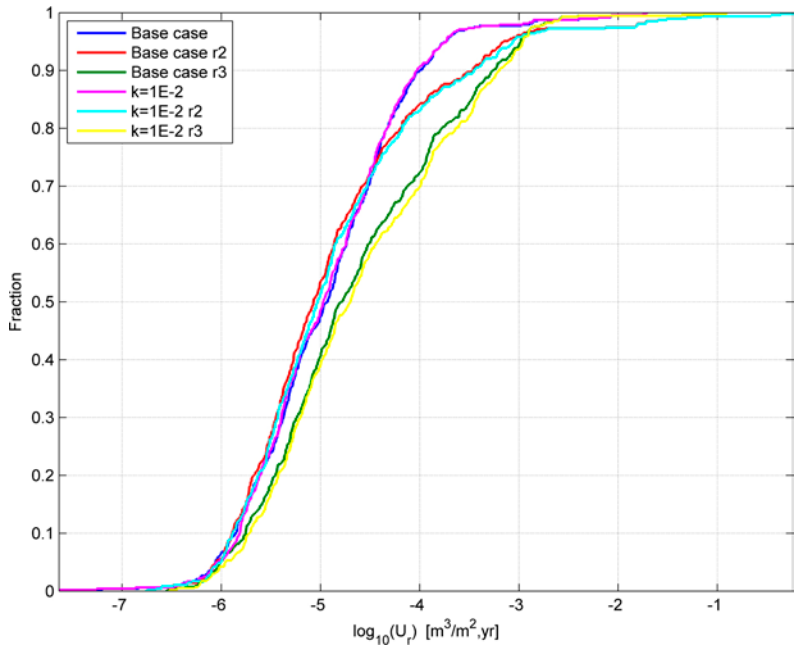


***Figure 3-55.*** *Normalised CDF plot of $U_r$ for the SR-Site Hydrogeological base case (Base case) and the borehole sealing variant, Case 8 ($k = 10^{-2}$ m/s), with two additional realisations, for all Q1 discharge particles released at 2000 AD and successfully reaching the model boundary.*

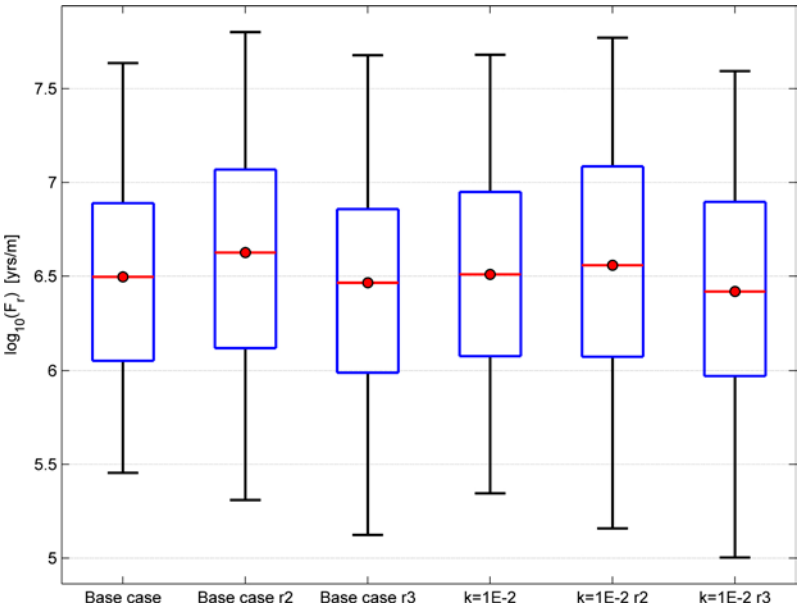


***Figure 3-56.*** *Bar and whisker plot of $F_r$ for the SR-Site Hydrogeological base case (Base case) and the borehole sealing variant, Case 8 ($k = 10^{-2}$ m/s), with two additional realisations, for all Q1 discharge particles released at 2000 AD and successfully reaching the model boundary. The statistical measures are the median (red), 25$^{th}$ and 75$^{th}$ percentile (blue bar) and the 5$^{th}$ and 95$^{th}$ percentile (black "whiskers").*

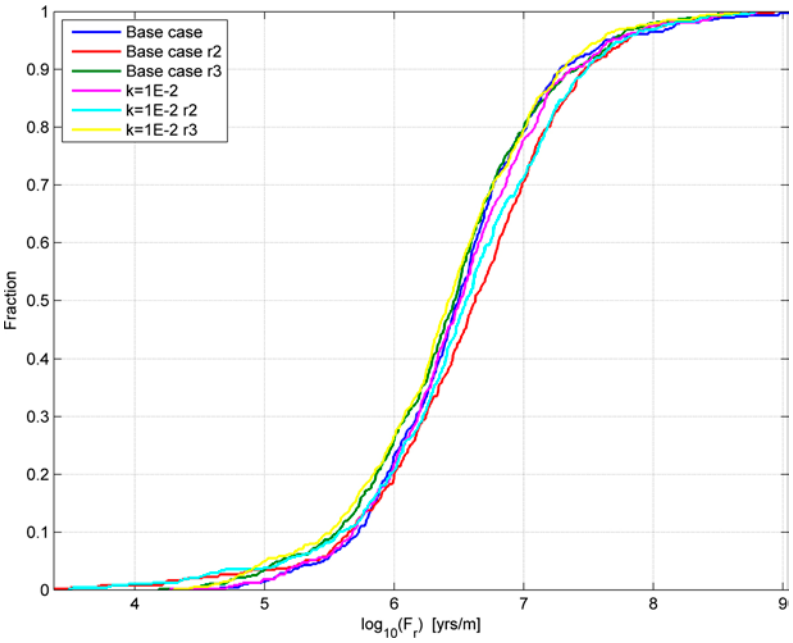


***Figure 3-57.*** *Normalised CDF plot of $F_r$ for the SR-Site Hydrogeological base case (Base case) and the borehole sealing variant, Case 8 ($k = 10^{-2}$ m/s), with two additional realisations, for all Q1 discharge particles released at 2000 AD and successfully reaching the model boundary.*

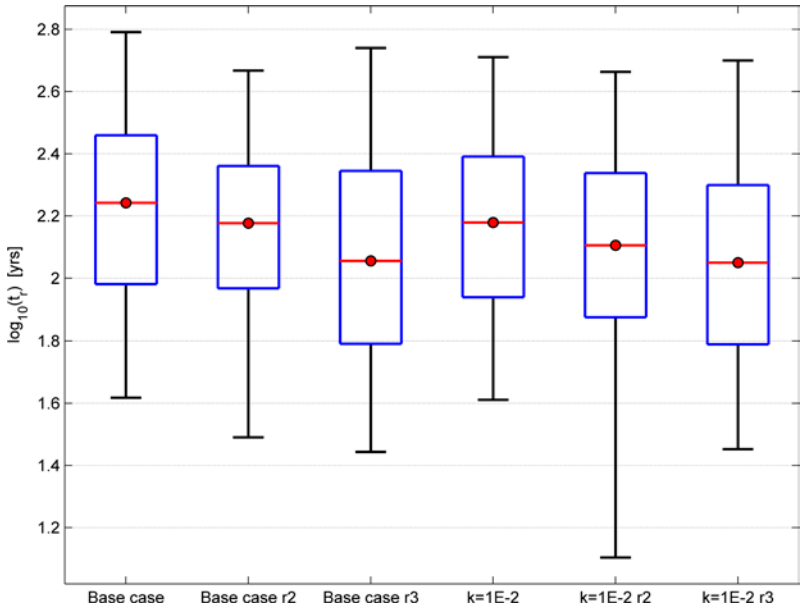


***Figure 3-58.*** *Bar and whisker plot of $t_r$ for the SR-Site Hydrogeological base case (Base case) and the borehole sealing variant, Case 8 ($k = 10^{-2}$ m/s), with two additional realisations, for all Q2 discharge particles released at 2000 AD and successfully reaching the model boundary. The statistical measures are the median (red), 25th and 75th percentile (blue bar) and the 5th and 95th percentile (black "whiskers").*

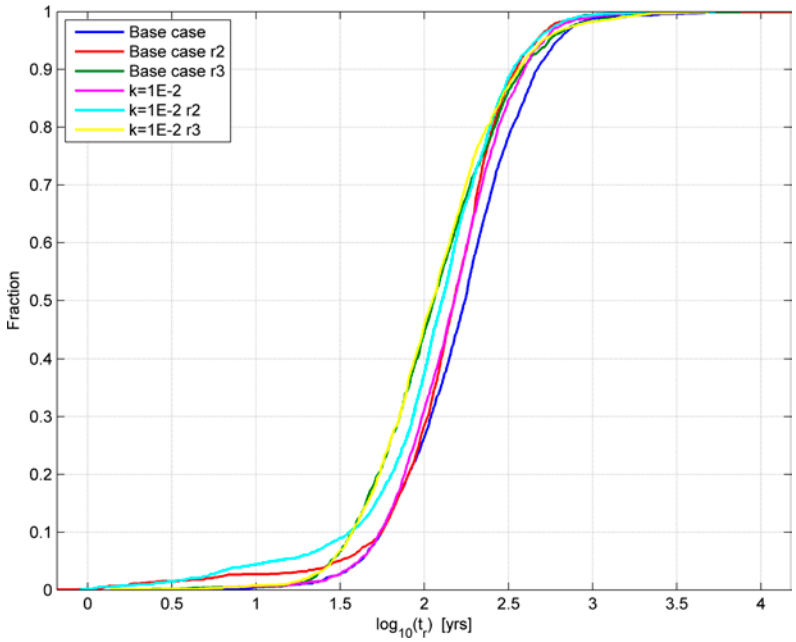


***Figure 3-59.*** *Normalised CDF plot of $t_r$ for the SR-Site Hydrogeological base case (Base case) and the borehole sealing variant, Case 8 ($k = 10^{-2}$ m/s), with two additional realisations, for all Q2 discharge particles released at 2000 AD and successfully reaching the model boundary.*

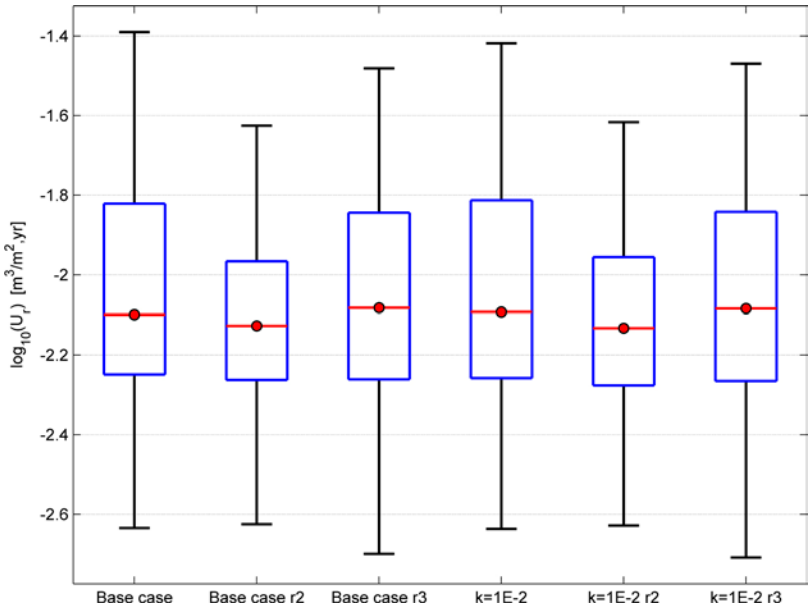


***Figure 3-60.*** *Bar and whisker plot of $U_r$ for the SR-Site Hydrogeological base case (Base case) and the borehole sealing variant, Case 8 ($k = 10^{-2}$ m/s), with two additional realisations, for all Q2 discharge particles released at 2000 AD and successfully reaching the model boundary. The statistical measures are the median (red), 25th and 75th percentile (blue bar) and the 5th and 95th percentile (black "whiskers").*

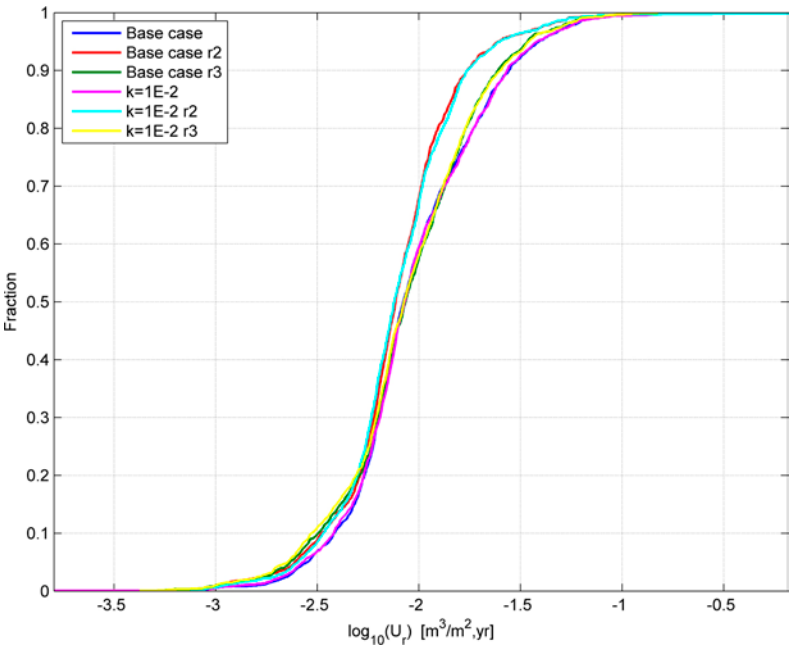


***Figure 3-61.*** *Normalised CDF plot of $U_r$ for the SR-Site Hydrogeological base case (Base case) and the borehole sealing variant, Case 8 ($k = 10^{-2}$ m/s), with two additional realisations, for all Q2 discharge particles released at 2000 AD and successfully reaching the model boundary.*

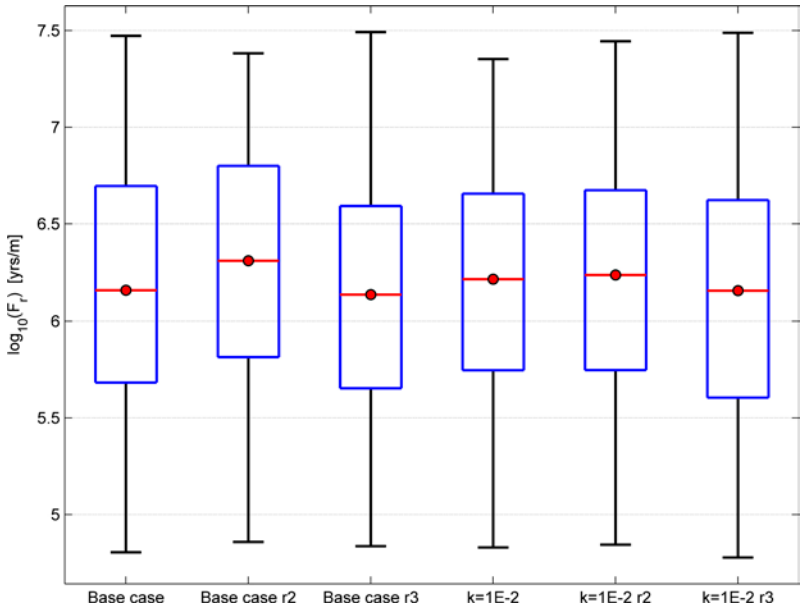


***Figure 3-62.*** *Bar and whisker plot of $F_r$ for the SR-Site Hydrogeological base case (Base case) and the borehole sealing variant, Case 8 ($k = 10^{-2}$ m/s), with two additional realisations, for all Q2 discharge particles released at 2000 AD and successfully reaching the model boundary. The statistical measures are the median (red), 25th and 75th percentile (blue bar) and the 5th and 95th percentile (black "whiskers").*

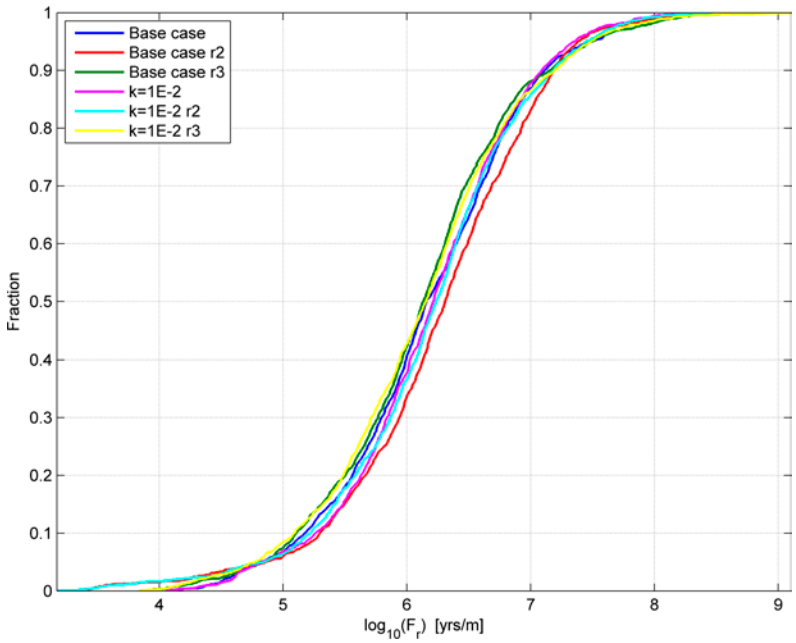


***Figure 3-63.*** *Normalised CDF plot of $F_r$ for the SR-Site Hydrogeological base case (Base case) and the borehole sealing variant, Case 8 ($k = 10^{-2}$ m/s), with two additional realisations, for all Q2 discharge particles released at 2000 AD and successfully reaching the model boundary.*

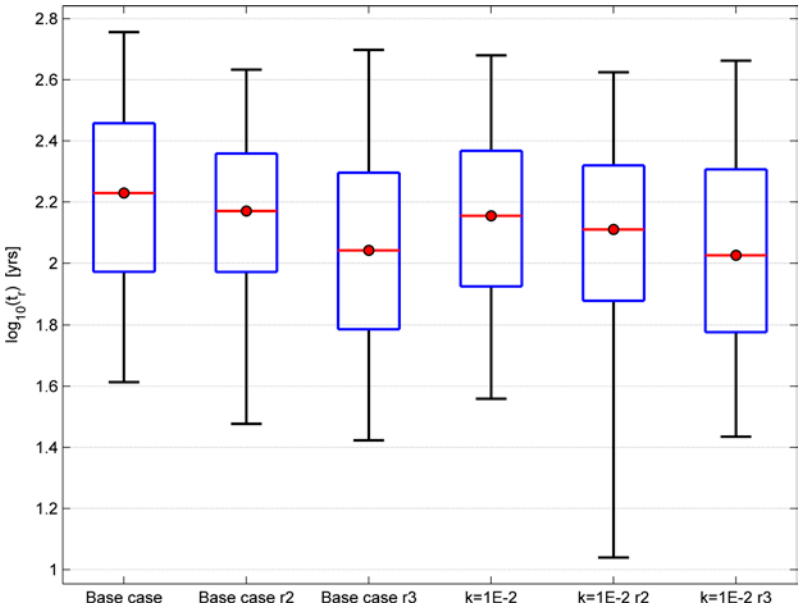


***Figure 3-64.*** *Bar and whisker plot of $t_r$ for the SR-Site Hydrogeological base case (Base case) and the borehole sealing variant, Case 8 ($k = 10^{-2}$ m/s), with two additional realisations, for all Q3 discharge particles released at 2000 AD and successfully reaching the model boundary. The statistical measures are the median (red), 25th and 75th percentile (blue bar) and the 5th and 95th percentile (black "whiskers").*

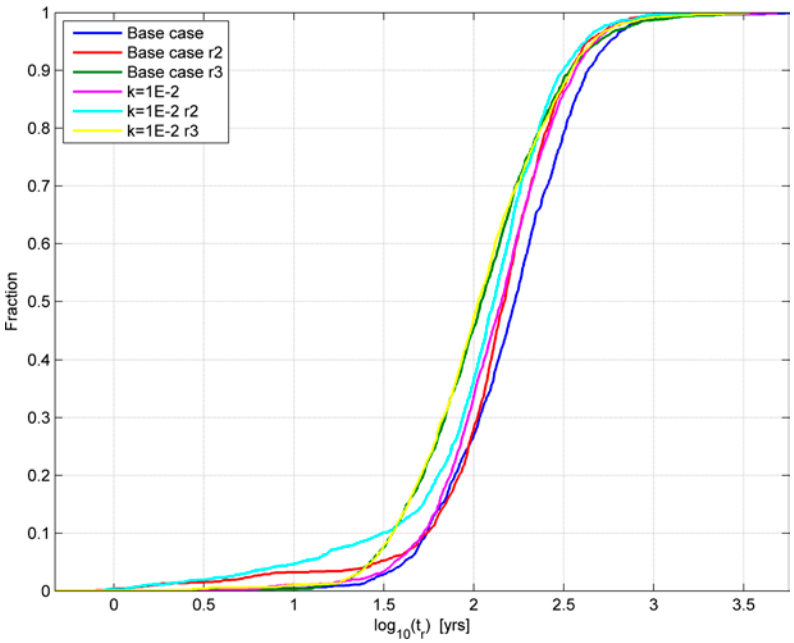


***Figure 3-65.*** *Normalised CDF plot of $t_r$ for the SR-Site Hydrogeological base case (Base case) and the borehole sealing variant, Case 8 ($k = 10^{-2}$ m/s), with two additional realisations, for all Q3 discharge particles released at 2000 AD and successfully reaching the model boundary.*

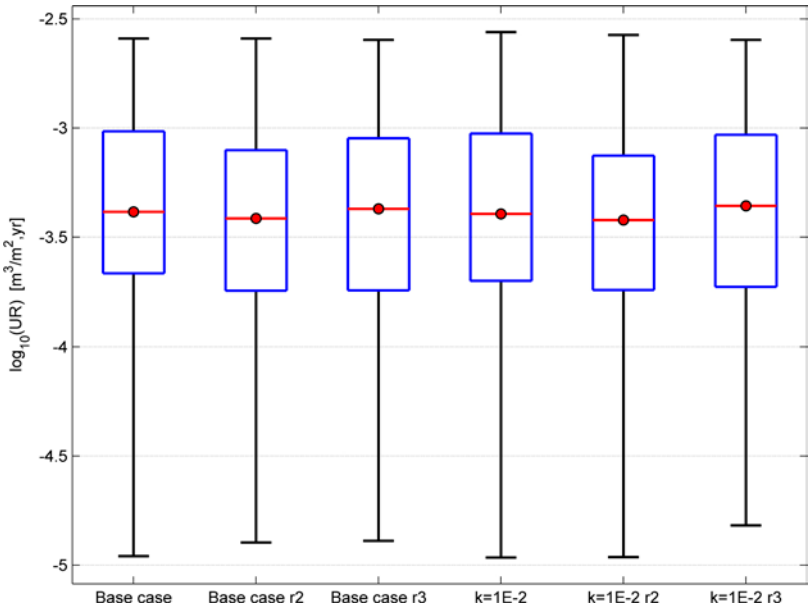


***Figure 3-66.*** *Bar and whisker plot of $U_r$ for the SR-Site Hydrogeological base case (Base case) and the borehole sealing variant, Case 8 ($k = 10^{-2}$ m/s), with two additional realisations, for all Q3 discharge particles released at 2000 AD and successfully reaching the model boundary. The statistical measures are the median (red), 25th and 75th percentile (blue bar) and the 5th and 95th percentile (black "whiskers").*

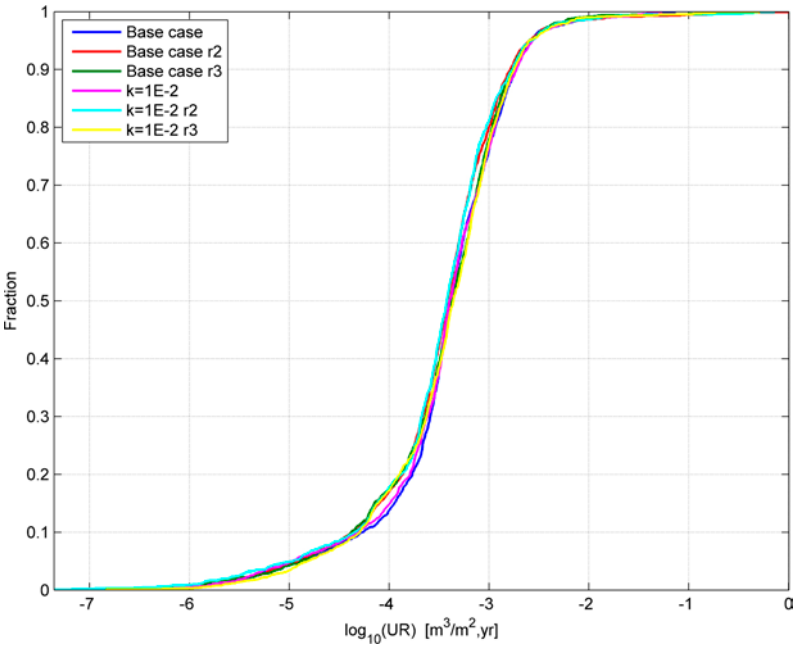


***Figure 3-67.*** *Normalised CDF plot of $U_r$ for the SR-Site Hydrogeological base case (Base case) and the borehole sealing variant, Case 8 ($k = 10^{-2}$ m/s), with two additional realisations, for all Q3 discharge particles released at 2000 AD and successfully reaching the model boundary.*

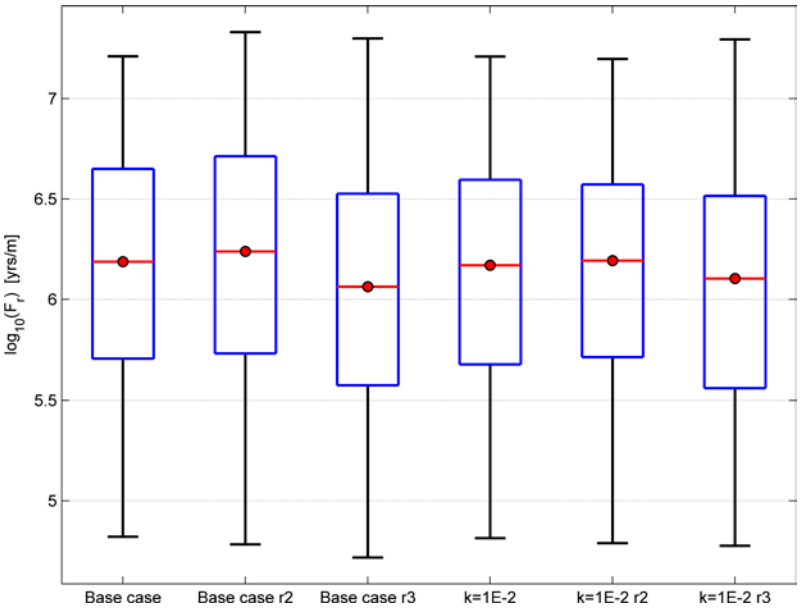


***Figure 3-68.*** *Bar and whisker plot of $F_r$ for the SR-Site Hydrogeological base case (Base case) and the borehole sealing variant, Case 8 ($k = 10^{-2}$ m/s), with two additional realisations, for all Q3 discharge particles released at 2000 AD and successfully reaching the model boundary. The statistical measures are the median (red), 25$^{th}$ and 75$^{th}$ percentile (blue bar) and the 5$^{th}$ and 95$^{th}$ percentile (black "whiskers").*

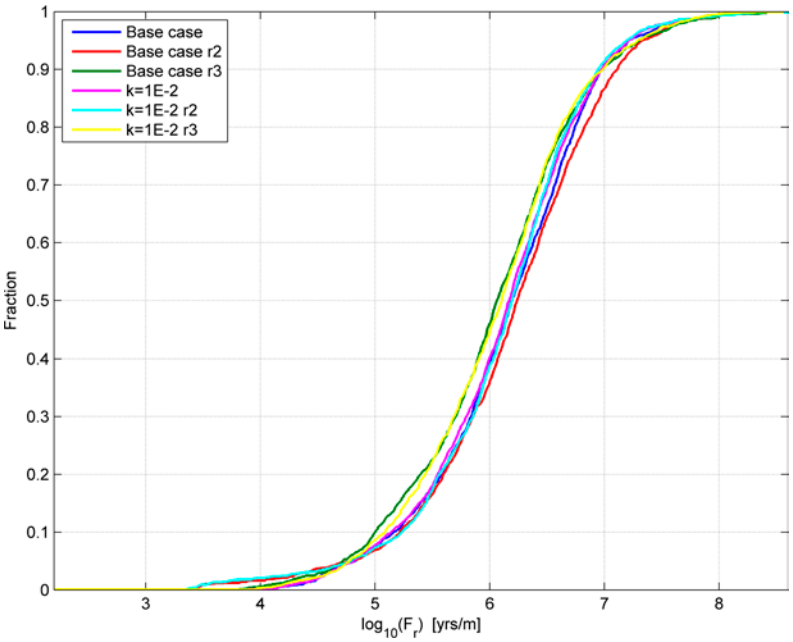


***Figure 3-69.*** *Normalised CDF plot of $F_r$ for the SR-Site Hydrogeological base case (Base case) and the borehole sealing variant, Case 8 ($k = 10^{-2}$ m/s), with two additional realisations, for all Q3 discharge particles released at 2000 AD and successfully reaching the model boundary.*

### *Recharge temperate conditions*

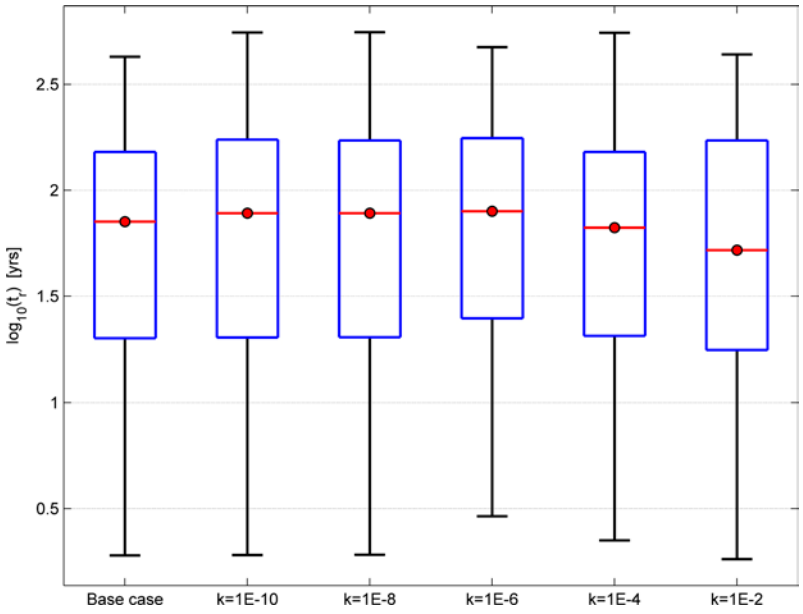


***Figure 3-70.*** *Bar and whisker plot of $t_r$ for the SR-Site Hydrogeological base case (Base case) and five different borehole sealing variants (conductivity in m/s), for all Q1 recharge particles released at 2000 AD and successfully tracked back to the model boundary. The statistical measures are the median (red), 25$^{th}$ and 75$^{th}$ percentile (blue bar) and the 5$^{th}$ and 95$^{th}$ percentile (black "whiskers").*

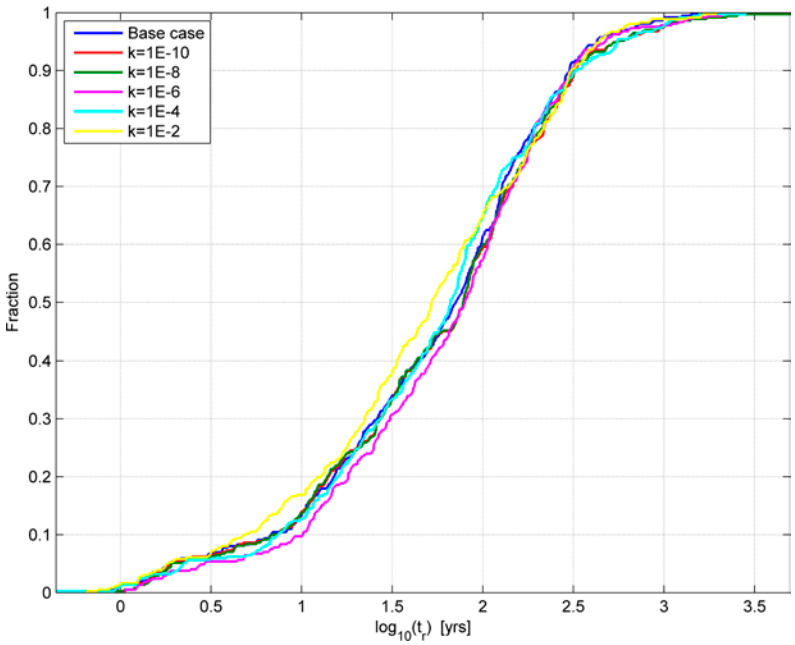


***Figure 3-71.*** *Normalised CDF plot of $t_r$ for the SR-Site Hydrogeological base case (Base case) and five different borehole sealing variants (conductivity in m/s), for all Q1 recharge particles released at 2000 AD and successfully tracked back to the model boundary.*

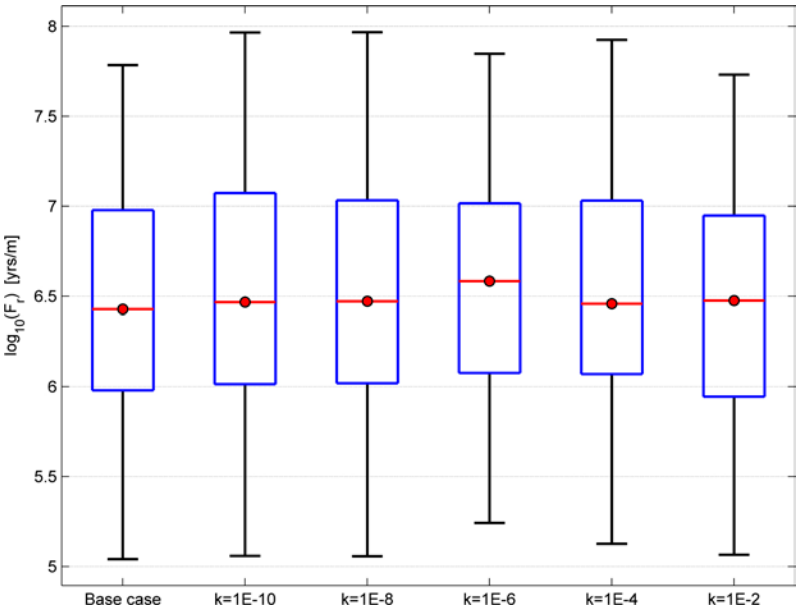


***Figure 3-72.*** *Bar and whisker plot of $F_r$ for the SR-Site Hydrogeological base case (Base case) and five different borehole sealing variants (conductivity in m/s), for all Q1 recharge particles released at 2000 AD and successfully tracked back to the model boundary. The statistical measures are the median (red), 25$^{th}$ and 75$^{th}$ percentile (blue bar) and the 5$^{th}$ and 95$^{th}$ percentile (black "whiskers").*

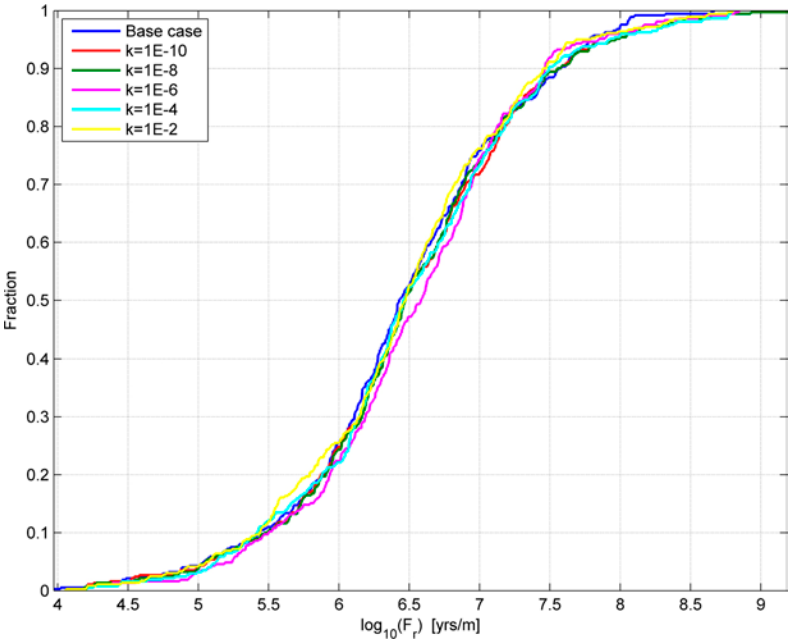


***Figure 3-73.*** *Normalised CDF plot of $F_r$ for the SR-Site Hydrogeological base case (Base case) and five different borehole sealing variants (conductivity in m/s), for all Q1 recharge particles released at 2000 AD and successfully tracked back to the model boundary.*

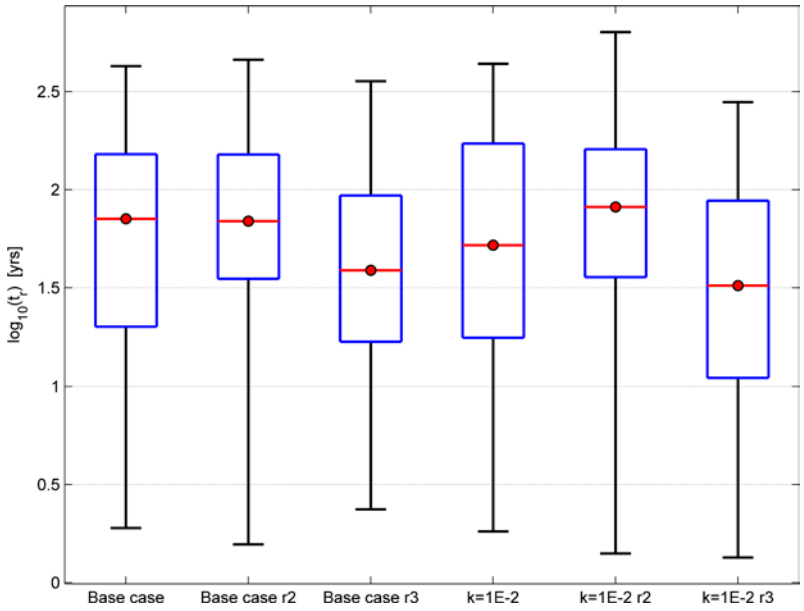


***Figure 3-74.*** *Bar and whisker plot of $t_r$ for the SR-Site Hydrogeological base case (Base case) and the borehole sealing variant, Case 8 ($k = 10^{-2}$ m/s), with two additional realisations, for all Q1 recharge particles released at 2000 AD and successfully tracked back to the model boundary. The statistical measures are the median (red), 25th and 75th percentile (blue bar) and the 5th and 95th percentile (black "whiskers").*

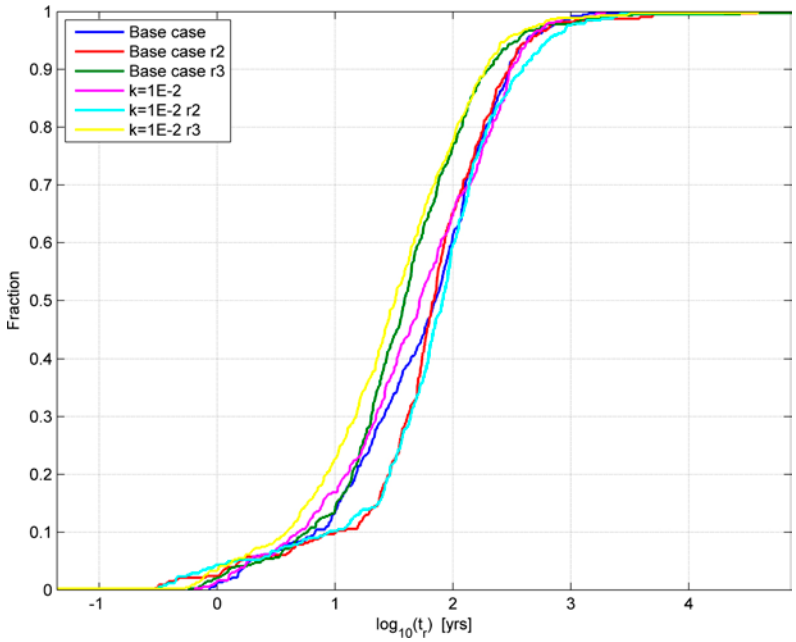


***Figure 3-75.*** *Normalised CDF plot of $t_r$ for the SR-Site Hydrogeological base case (Base case) and the borehole sealing variant, Case 8 ($k = 10^{-2}$ m/s), with two additional realisations, for all Q1 recharge particles released at 2000 AD and successfully tracked back to the model boundary.*

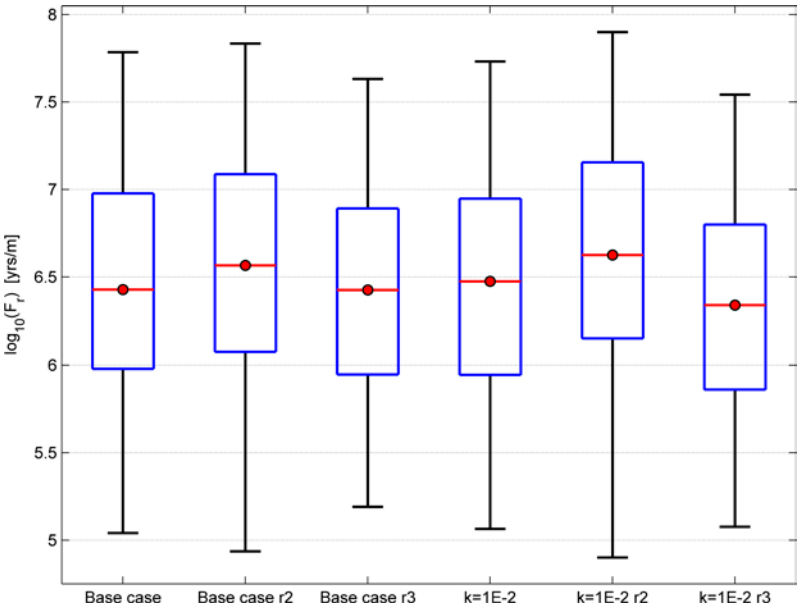


***Figure 3-76.*** *Bar and whisker plot of $F_r$ for the SR-Site Hydrogeological base case (Base case) and the borehole sealing variant, Case 8 ($k = 10^{-2}$ m/s), with two additional realisations, for all Q1 recharge particles released at 2000 AD and successfully tracked back to the model boundary. The statistical measures are the median (red), 25$^{th}$ and 75$^{th}$ percentile (blue bar) and the 5$^{th}$ and 95$^{th}$ percentile (black "whiskers").*

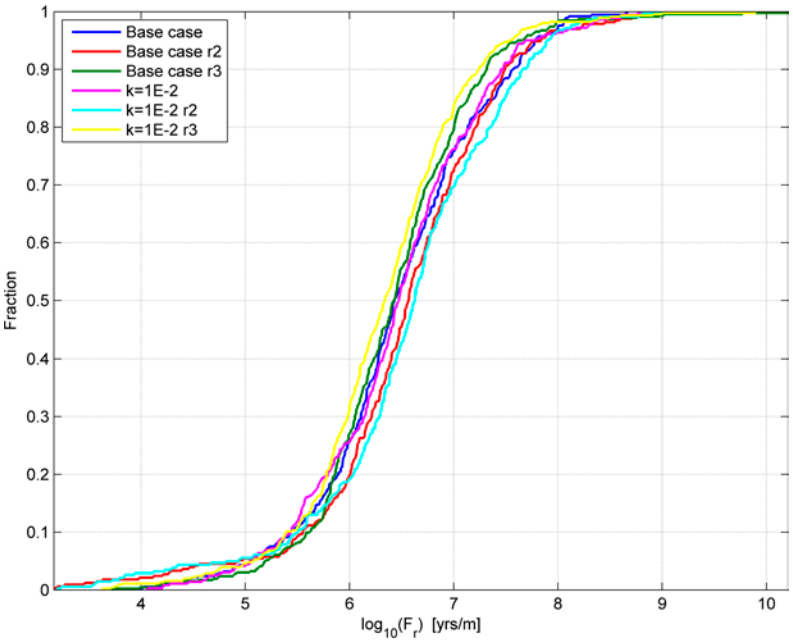


***Figure 3-77.*** *Normalised CDF plot of $F_r$ for the SR-Site Hydrogeological base case (Base case) and the borehole sealing variant, Case 8 ($k = 10^{-2}$ m/s), with two additional realisations, for all Q1 recharge particles released at 2000 AD and successfully tracked back to the model boundary.*

### *Discharge glacial conditions*

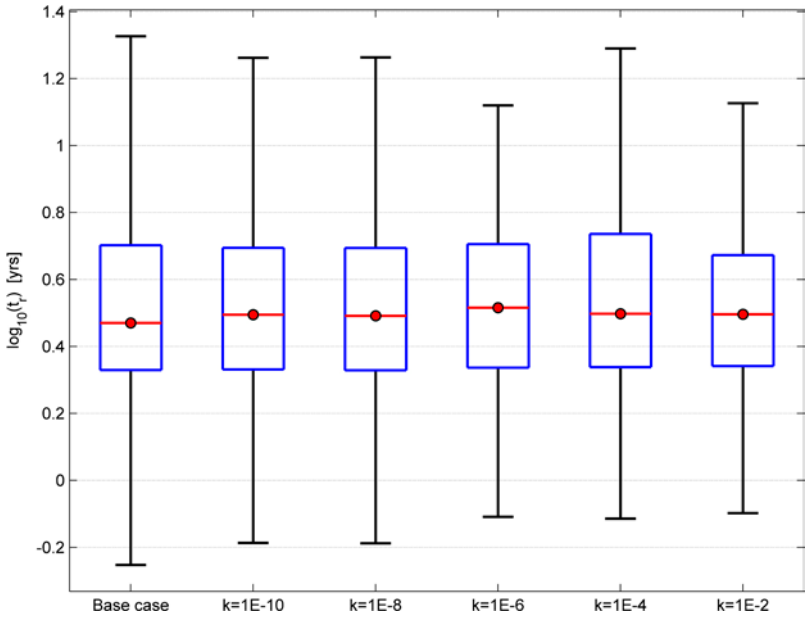


***Figure 3-78.*** *Bar and whisker plot of $t_r$ for the SR-Site Hydrogeological base case (Base case) and five different borehole sealing variants (conductivity in m/s), for all Q1 discharge particles released for glacial ice front location II and successfully reaching the model boundary. The statistical measures are the median (red), 25$^{th}$ and 75$^{th}$ percentile (blue bar) and the 5$^{th}$ and 95$^{th}$ percentile (black "whiskers").*

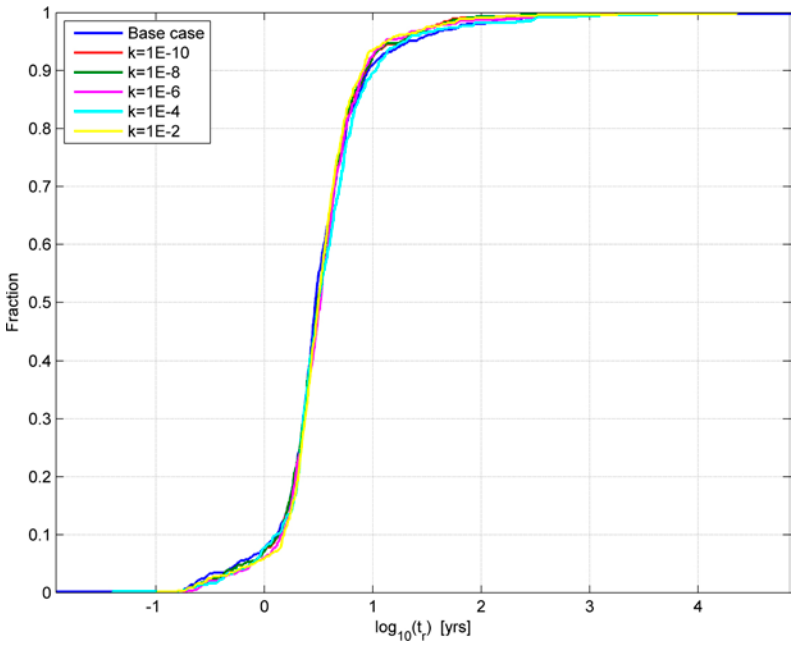


***Figure 3-79.*** *Normalised CDF plot of $t_r$ for the SR-Site Hydrogeological base case (Base case) and five different borehole sealing variants (conductivity in m/s), for all Q1 discharge particles released for glacial ice front location II and successfully reaching the model boundary.*

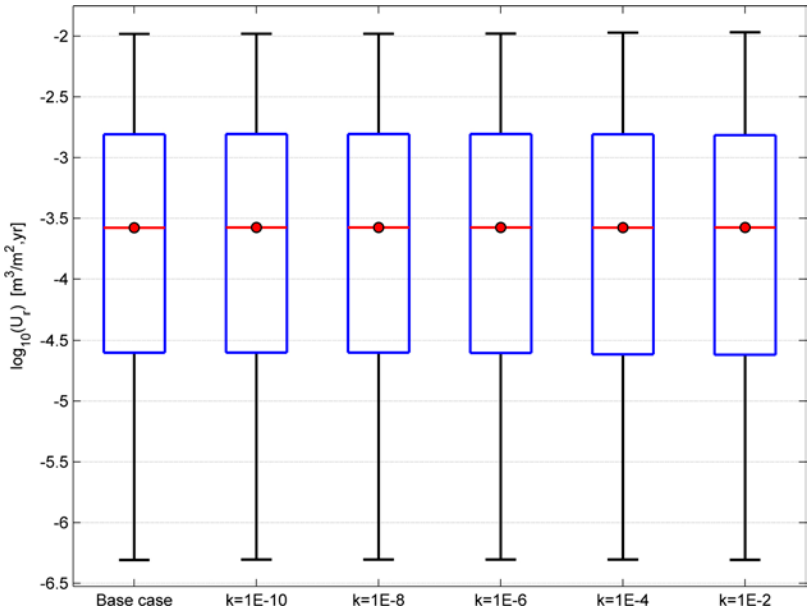


***Figure 3-80.*** *Bar and whisker plot of $U_r$ for the SR-Site Hydrogeological base case (Base case) and five different borehole sealing variants (conductivity in m/s), for all Q1 discharge particles released for glacial ice front location II and successfully reaching the model boundary. The statistical measures are the median (red), 25$^{th}$ and 75$^{th}$ percentile (blue bar) and the 5$^{th}$ and 95$^{th}$ percentile (black "whiskers").*

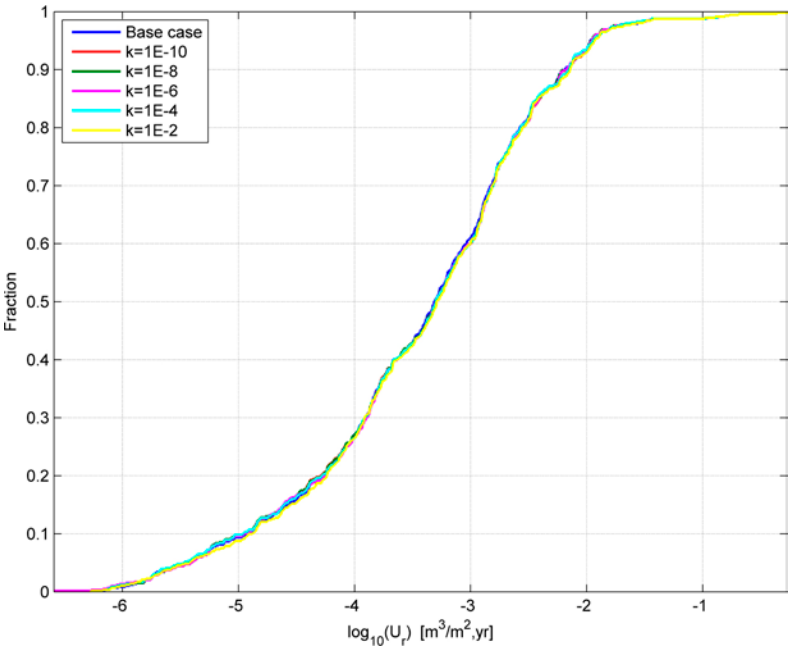


***Figure 3-81.*** *Normalised CDF plot of $U_r$ for the SR-Site Hydrogeological base case (Base case) and five different borehole sealing variants (conductivity in m/s), for all Q1 discharge particles released for glacial ice front location II and successfully reaching the model boundary.*

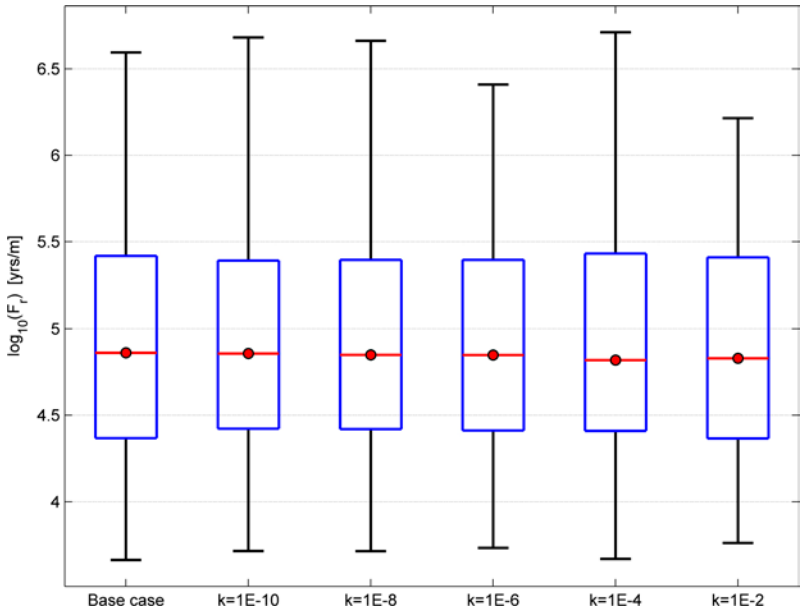


***Figure 3-82.*** *Bar and whisker plot of $F_r$ for the SR-Site Hydrogeological base case (Base case) and five different borehole sealing variants (conductivity in m/s), for all Q1 discharge particles released for glacial ice front location II and successfully reaching the model boundary. The statistical measures are the median (red), 25$^{th}$ and 75$^{th}$ percentile (blue bar) and the 5$^{th}$ and 95$^{th}$ percentile (black "whiskers").*

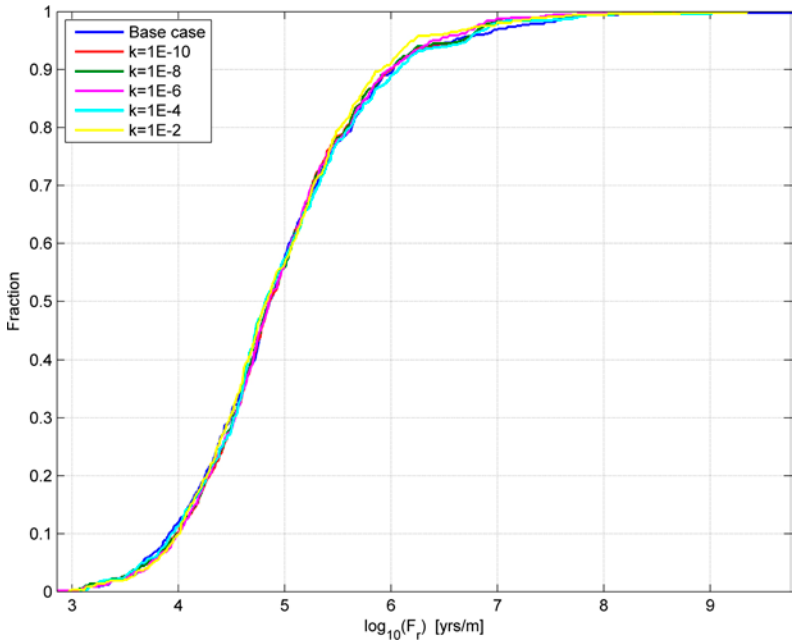


***Figure 3-83.*** *Normalised CDF plot of $F_r$ for the SR-Site Hydrogeological base case (Base case) and five different borehole sealing variants (conductivity in m/s), for all Q1 discharge particles released for glacial ice front location II and successfully reaching the model boundary.*

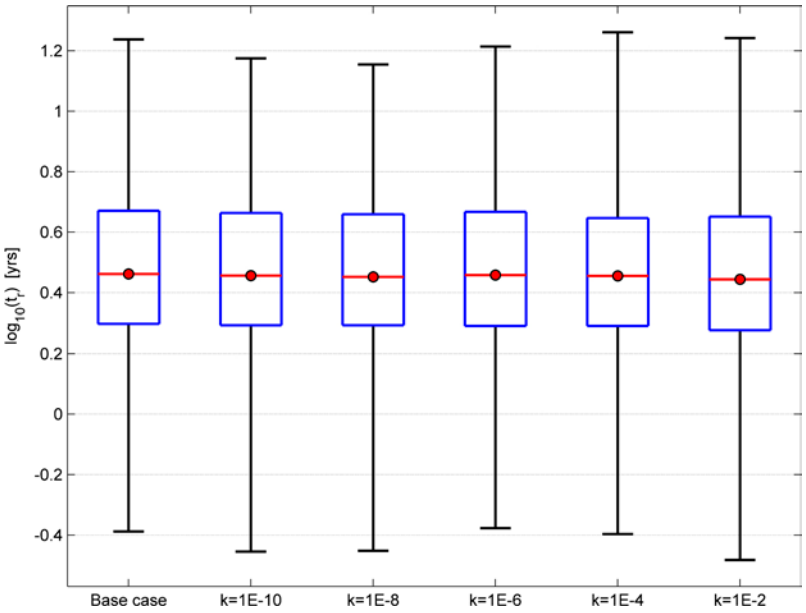


***Figure 3-84.*** *Bar and whisker plot of $t_r$ for the SR-Site Hydrogeological base case (Base case) and five different borehole sealing variants (conductivity in m/s), for all Q2 discharge particles released for glacial ice front location II and successfully reaching the model boundary. The statistical measures are the median (red), 25$^{th}$ and 75$^{th}$ percentile (blue bar) and the 5$^{th}$ and 95$^{th}$ percentile (black "whiskers").*

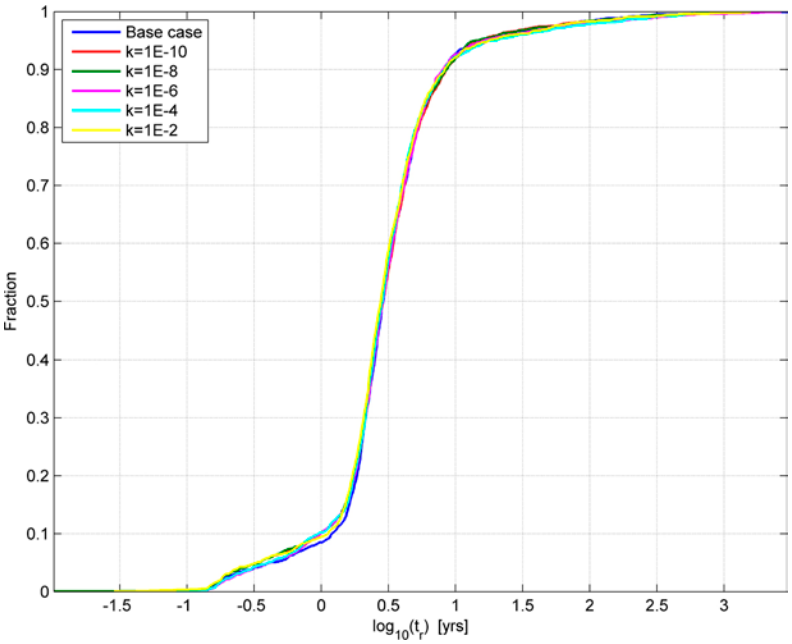


***Figure 3-85.*** *Normalised CDF plot of $t_r$ for the SR-Site Hydrogeological base case (Base case) and five different borehole sealing variants (conductivity in m/s), for all Q2 discharge particles released for glacial ice front location II and successfully reaching the model boundary.*

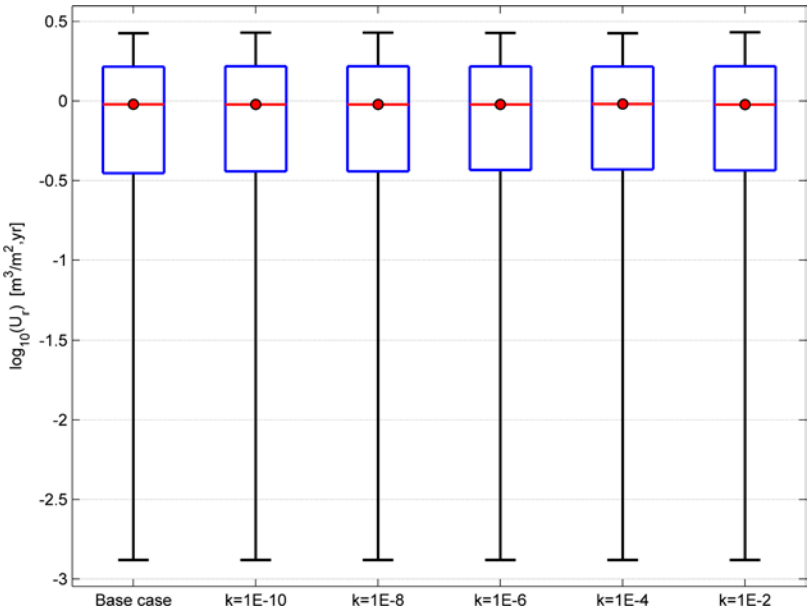


***Figure 3-86.*** *Bar and whisker plot of $U_r$ for the SR-Site Hydrogeological base case (Base case) and five different borehole sealing variants (conductivity in m/s), for all Q2 discharge particles released for glacial ice front location II and successfully reaching the model boundary. The statistical measures are the median (red), 25$^{th}$ and 75$^{th}$ percentile (blue bar) and the 5$^{th}$ and 95$^{th}$ percentile (black "whiskers").*

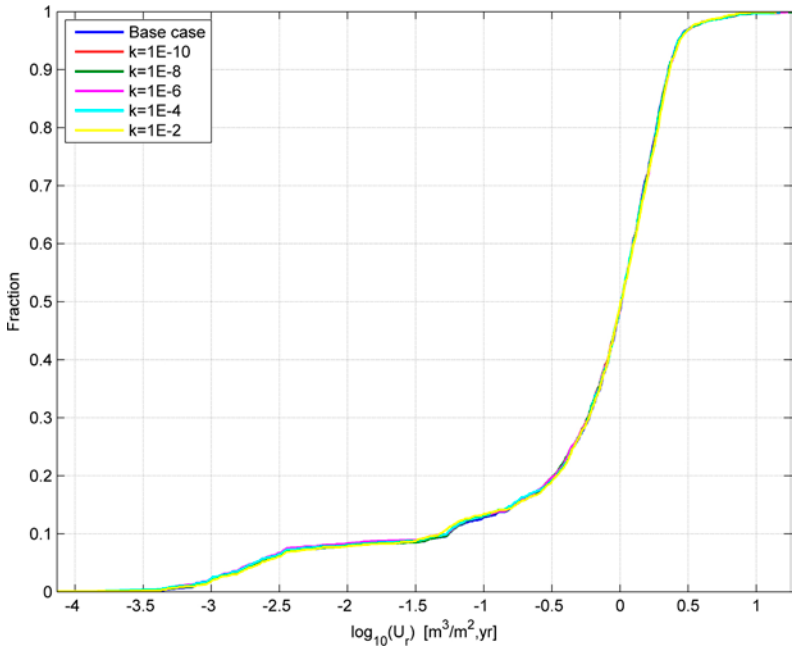


***Figure 3-87.*** *Normalised CDF plot of $U_r$ for the SR-Site Hydrogeological base case (Base case) and five different borehole sealing variants (conductivity in m/s), for all Q2 discharge particles released for glacial ice front location II and successfully reaching the model boundary.*

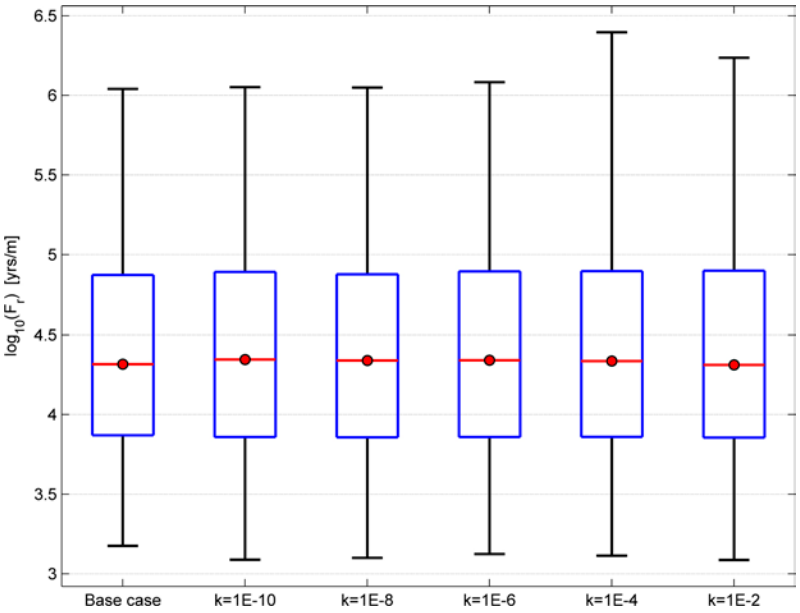


***Figure 3-88.*** *Bar and whisker plot of $F_r$ for the SR-Site Hydrogeological base case (Base case) and five different borehole sealing variants (conductivity in m/s), for all Q2 discharge particles released for glacial ice front location II and successfully reaching the model boundary. The statistical measures are the median (red), 25$^{th}$ and 75$^{th}$ percentile (blue bar) and the 5$^{th}$ and 95$^{th}$ percentile (black "whiskers").*

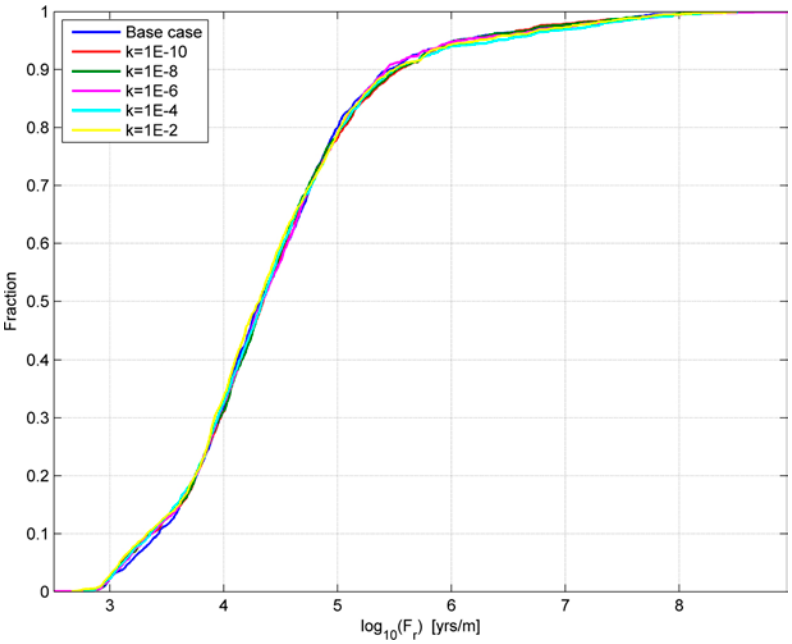


***Figure 3-89.*** *Normalised CDF plot of $F_r$ for the SR-Site Hydrogeological base case (Base case) and five different borehole sealing variants (conductivity in m/s), for all Q2 discharge particles released for glacial ice front location II and successfully reaching the model boundary.*

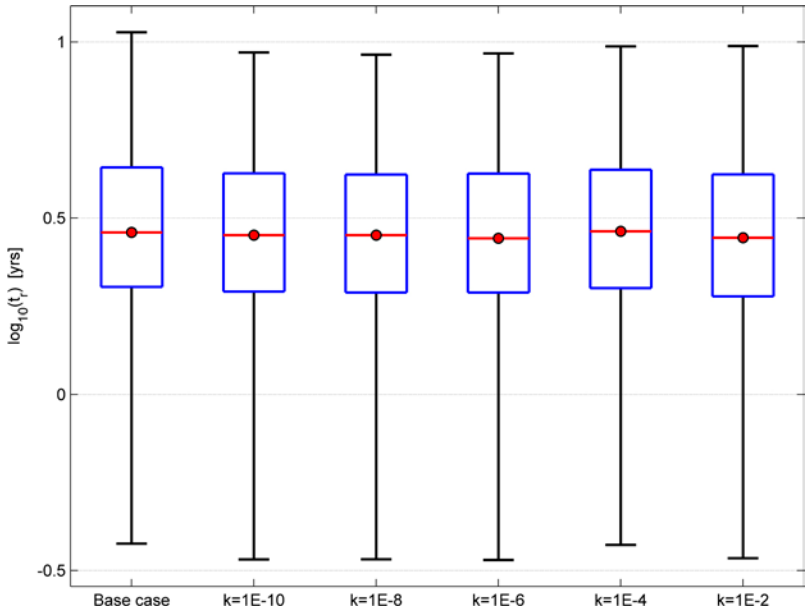


***Figure 3-90.*** *Bar and whisker plot of $t_r$ for the SR-Site Hydrogeological base case (Base case) and five different borehole sealing variants (conductivity in m/s), for all Q3 discharge particles released for glacial ice front location II and successfully reaching the model boundary. The statistical measures are the median (red), 25th and 75th percentile (blue bar) and the 5th and 95th percentile (black "whiskers").*

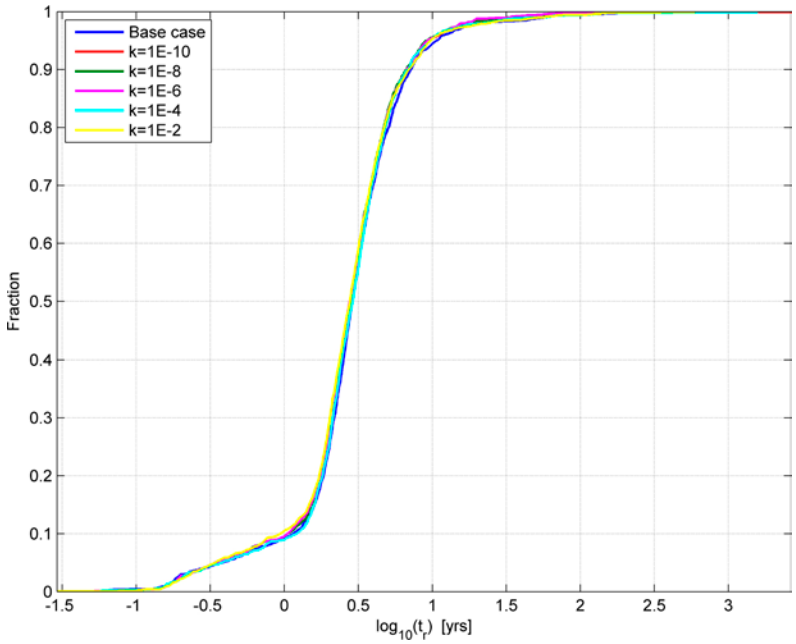


***Figure 3-91.*** *Normalised CDF plot of $t_r$ for the SR-Site Hydrogeological base case (Base case) and five different borehole sealing variants (conductivity in m/s), for all Q3 discharge particles released for glacial ice front location II and successfully reaching the model boundary.*

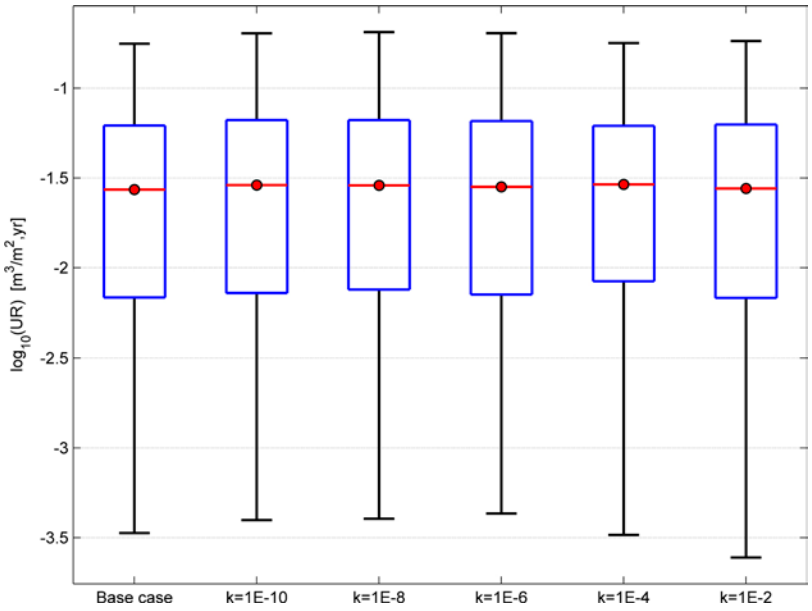


***Figure 3-92.*** *Bar and whisker plot of $U_r$ for the SR-Site Hydrogeological base case (Base case) and five different borehole sealing variants (conductivity in m/s), for all Q3 discharge particles released for glacial ice front location II and successfully reaching the model boundary. The statistical measures are the median (red), 25$^{th}$ and 75$^{th}$ percentile (blue bar) and the 5$^{th}$ and 95$^{th}$ percentile (black "whiskers").*

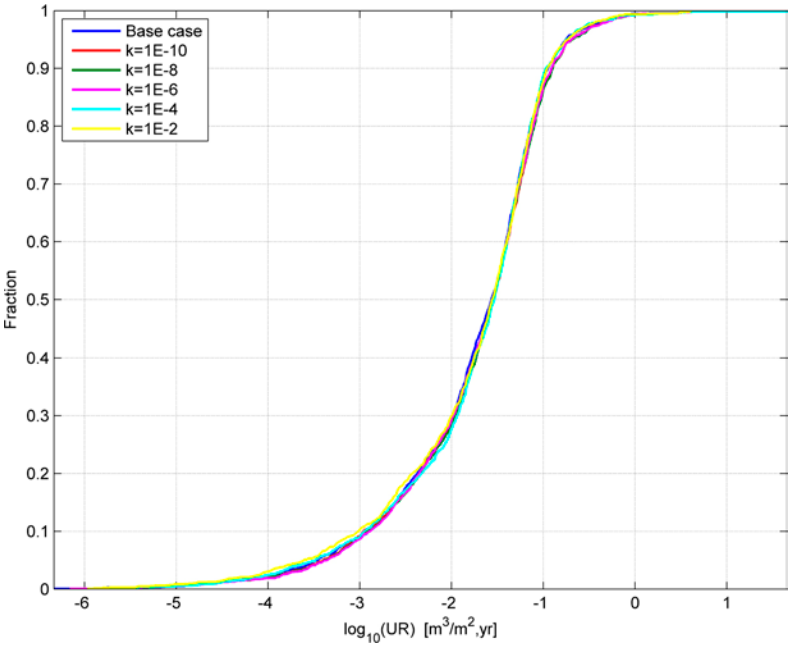


***Figure 3-93.*** *Normalised CDF plot of $U_r$ for the SR-Site Hydrogeological base case (Base case) and five different borehole sealing variants (conductivity in m/s), for all Q3 discharge particles released for glacial ice front location II and successfully reaching the model boundary.*

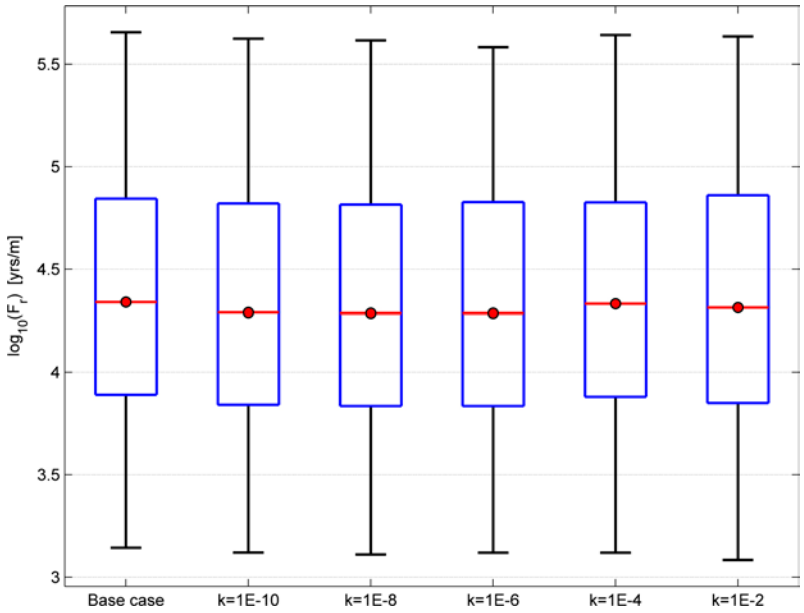


***Figure 3-94.*** *Bar and whisker plot of $F_r$ for the SR-Site Hydrogeological base case (Base case) and five different borehole sealing variants (conductivity in m/s), for all Q3 discharge particles released for glacial ice front location II and successfully reaching the model boundary. The statistical measures are the median (red), 25$^{th}$ and 75$^{th}$ percentile (blue bar) and the 5$^{th}$ and 95$^{th}$ percentile (black "whiskers").*

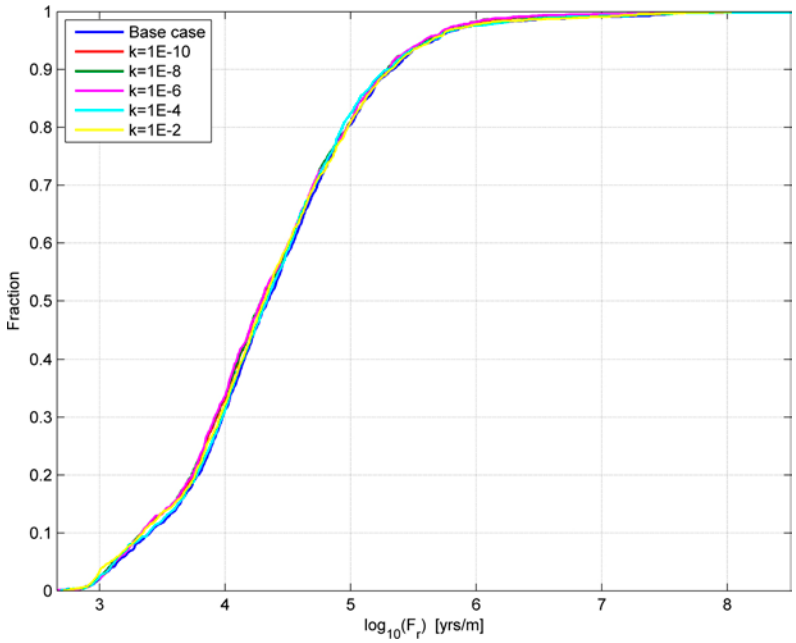


***Figure 3-95.*** *Normalised CDF plot of $F_r$ for the SR-Site Hydrogeological base case (Base case) and five different borehole sealing variants (conductivity in m/s), for all Q3 discharge particles released for glacial ice front location II and successfully reaching the model boundary.*

### *Recharge glacial conditions*

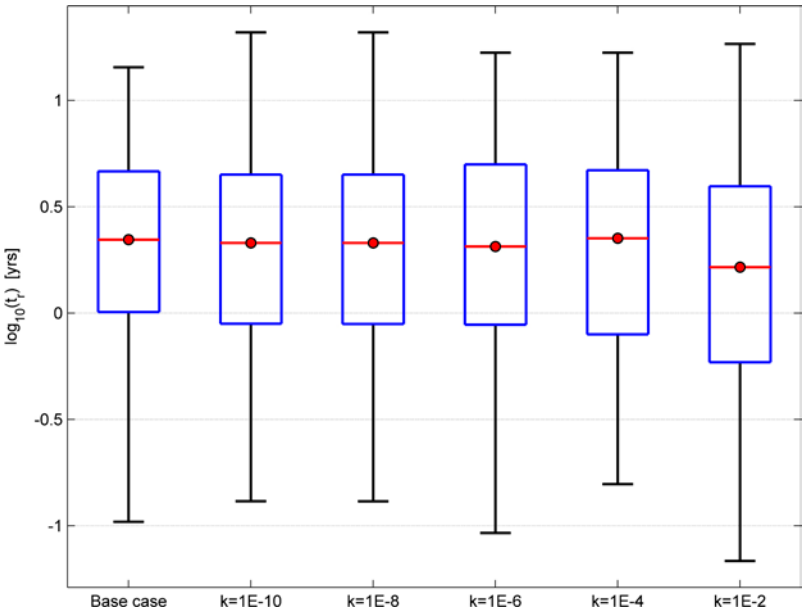


***Figure 3-96.*** *Bar and whisker plot of $t_r$ for the SR-Site Hydrogeological base case (Base case) and five different borehole sealing variants (conductivity in m/s), for all Q1 recharge particles released for glacial ice front location II and successfully reaching the model boundary. The statistical measures are the median (red), 25$^{th}$ and 75$^{th}$ percentile (blue bar) and the 5$^{th}$ and 95$^{th}$ percentile (black "whiskers").*

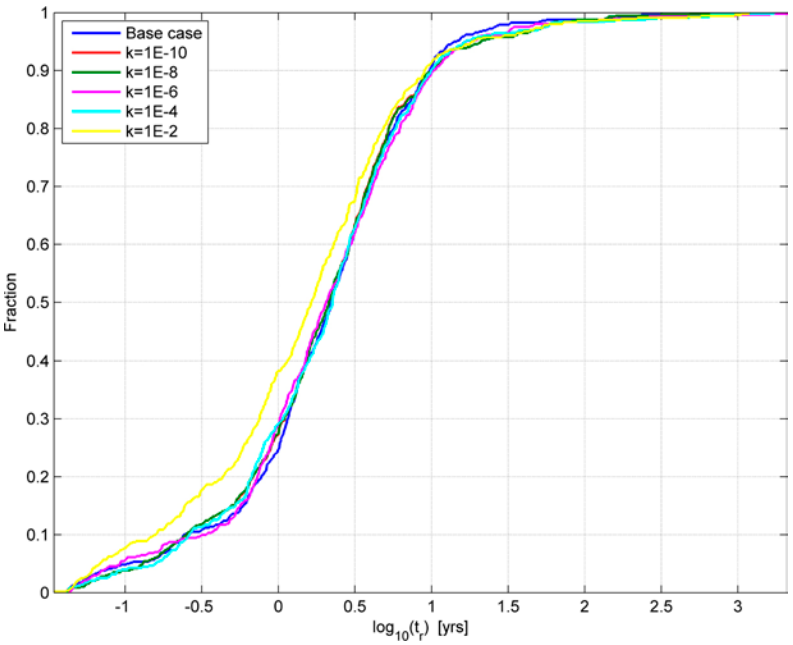


***Figure 3-97.*** *Normalised CDF plot of $t_r$ for the SR-Site Hydrogeological base case (Base case) and five different borehole sealing variants (conductivity in m/s), for all Q1 recharge particles released for glacial ice front location II and successfully reaching the model boundary.*

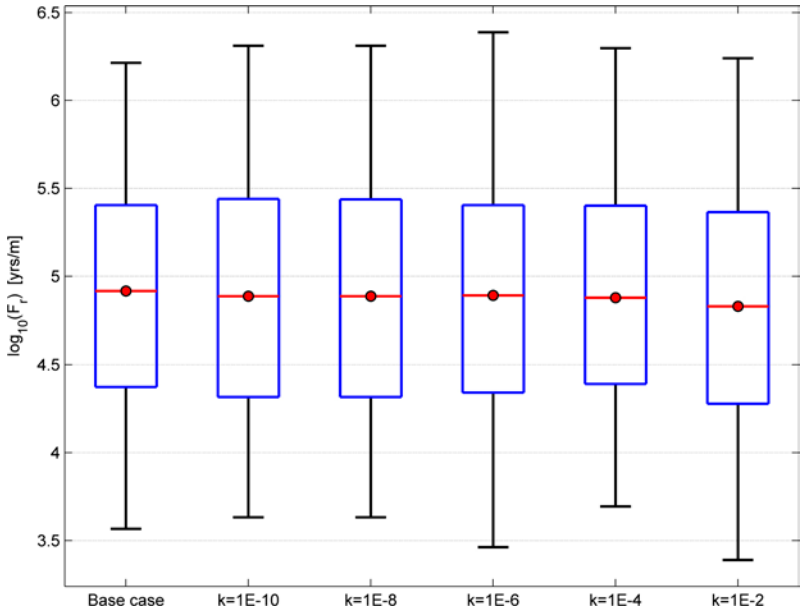


***Figure 3-98.*** *Bar and whisker plot of $F_r$ for the SR-Site Hydrogeological base case (Base case) and five different borehole sealing variants (conductivity in m/s), for all Q1 recharge particles released for glacial ice front location II and successfully tracked back to the model boundary. The statistical measures are the median (red), 25$^{th}$ and 75$^{th}$ percentile (blue bar) and the 5$^{th}$ and 95$^{th}$ percentile (black "whiskers").*

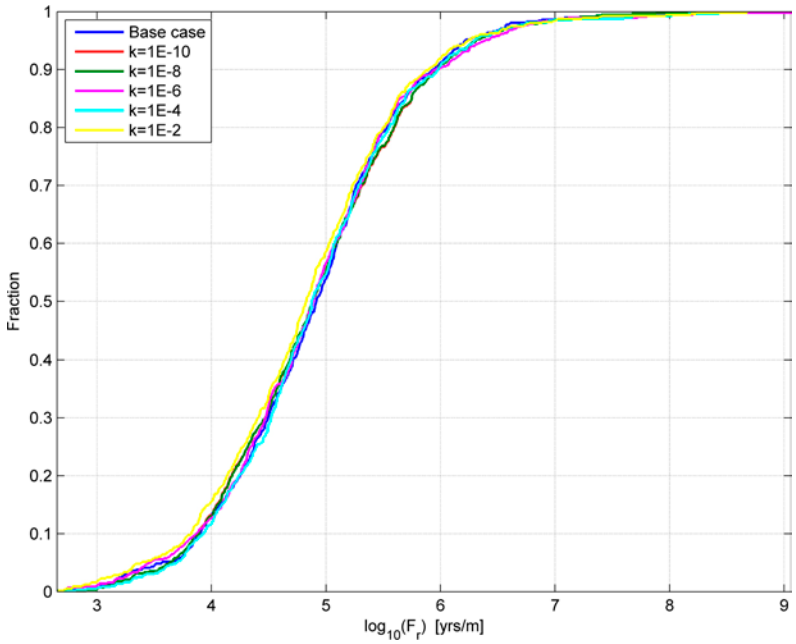


***Figure 3-99.*** *Normalised CDF plot of $F_r$ for the SR-Site Hydrogeological base case (Base case) and five different borehole sealing variants (conductivity in m/s), for all Q1 recharge particles released for glacial ice front location II and successfully tracked back to the model boundary.*

### *Selection of particles entering the sealed boreholes*

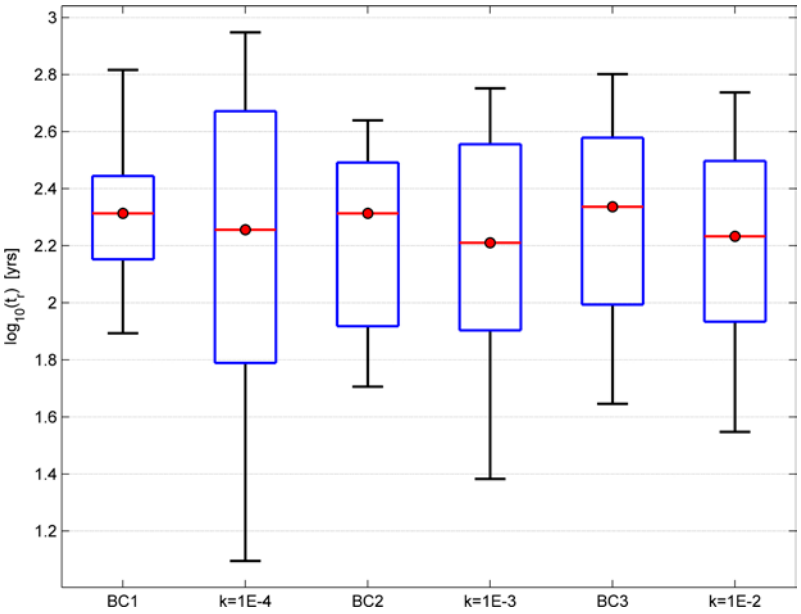


***Figure 3-100.*** *Bar and whisker plot of $t_r$ for three different borehole sealing variants (conductivity in m/s) and the corresponding set of particles in the SR-Site Hydrogeological base case (BC1−BC3), for only the Q3 discharge particles released at 2000 AD that enter the boreholes and successfully reaching the model boundary. The statistical measures are the median (red), 25$^{th}$ and 75$^{th}$ percentile (blue bar) and the 5$^{th}$ and 95$^{th}$ percentile (black "whiskers").*

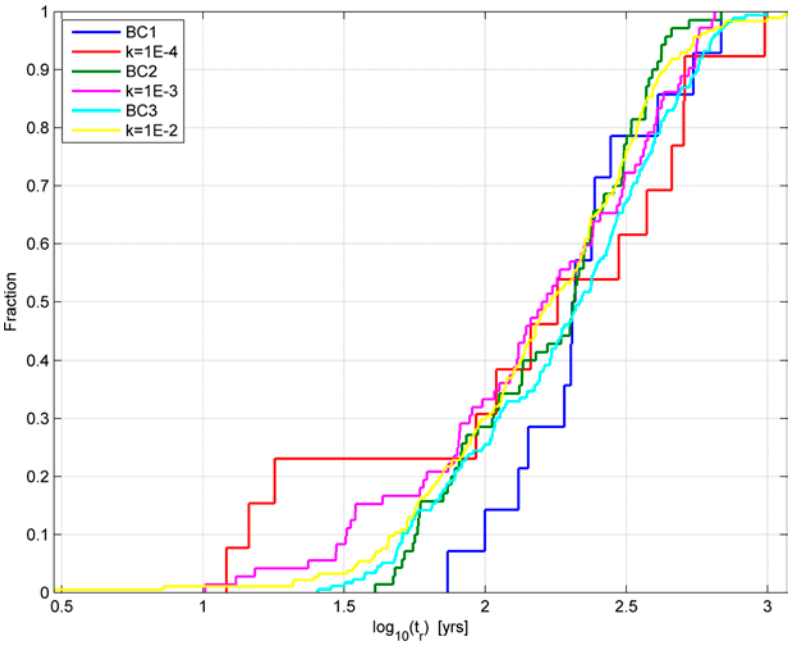


***Figure 3-101.*** *Normalised CDF plot of $t_r$ for three different borehole sealing variants (conductivity in m/s) and the corresponding set of particles in the SR-Site Hydrogeological base case (BC1−BC3), for only the Q3 discharge particles released at 2000 AD that enter the boreholes and successfully reaching the model boundary.*

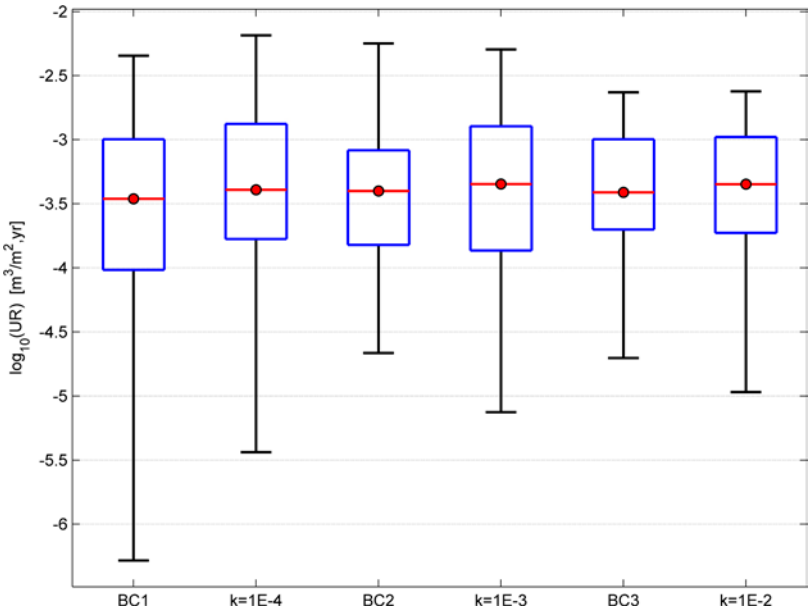


***Figure 3-102.*** *Bar and whisker plot of $U_r$ for three different borehole sealing variants (conductivity in m/s) and the corresponding set of particles in the SR-Site Hydrogeological base case (BC1−BC3), for only the Q3 discharge particles released at 2000 AD that enter the boreholes and successfully reaching the model boundary. The statistical measures are the median (red), 25th and 75th percentile (blue bar) and the 5th and 95th percentile (black "whiskers").*

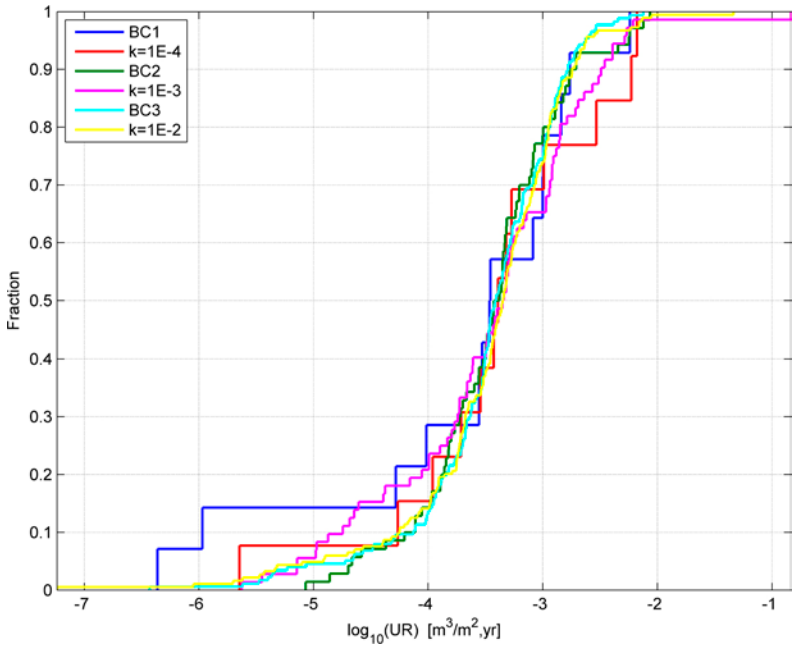


***Figure 3-103.*** *Normalised CDF plot of $U_r$ for three different borehole sealing variants (conductivity in m/s) and the corresponding set of particles in the SR-Site Hydrogeological base case (BC1−BC3), for only the Q3 discharge particles released at 2000 AD that enter the boreholes and successfully reaching the model boundary.*

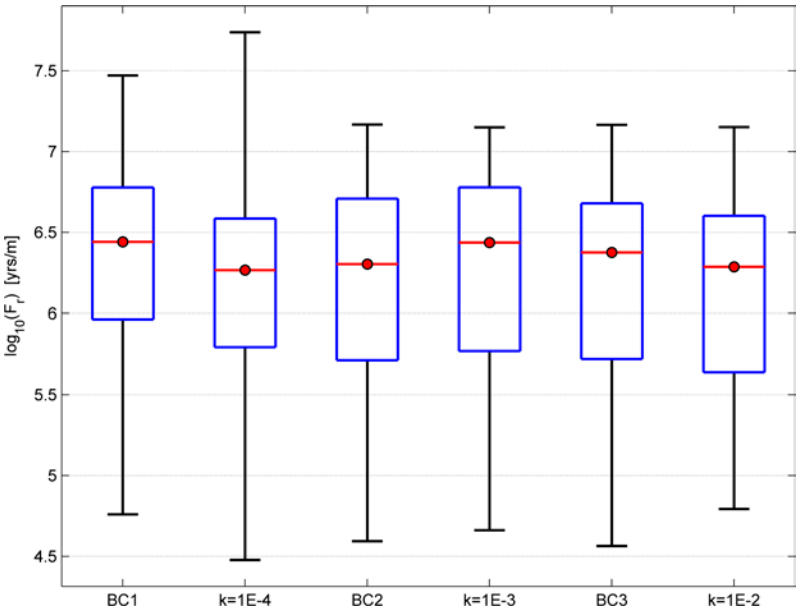


***Figure 3-104.*** *Bar and whisker plot of $F_r$ for three different borehole sealing variants (conductivity in m/s) and the corresponding set of particles in the SR-Site Hydrogeological base case (BC1−BC3), for only the Q3 discharge particles released at 2000 AD that enter the boreholes and successfully reaching the model boundary. The statistical measures are the median (red), 25$^{th}$ and 75$^{th}$ percentile (blue bar) and the 5$^{th}$ and 95$^{th}$ percentile (black "whiskers").*

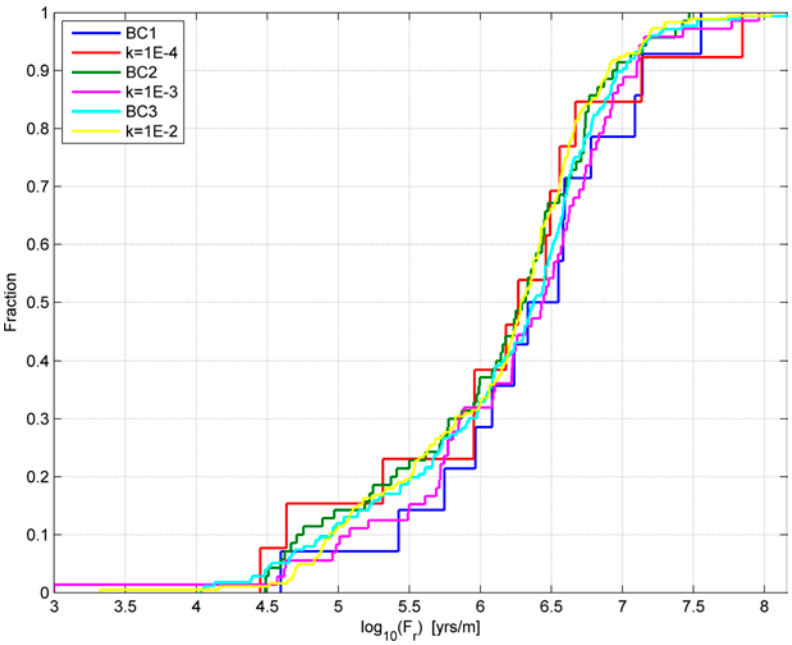


***Figure 3-105.*** *Normalised CDF plot of $F_r$ for three different borehole sealing variants (conductivity in m/s) and the corresponding set of particles in the SR-Site Hydrogeological base case (BC1−BC3), for only the Q3 discharge particles released at 2000 AD that enter the boreholes and successfully reaching the model boundary.*

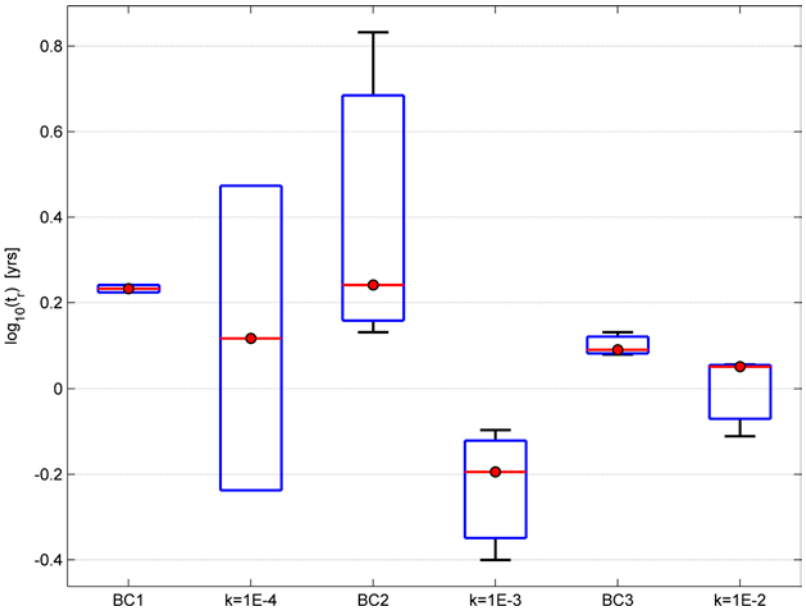


***Figure 3-106.*** *Bar and whisker plot of $t_r$ for three different borehole sealing variants (conductivity in m/s) and the corresponding set of particles in the SR-Site Hydrogeological base case (BC1−BC3), for only the Q3 discharge particles released for glacial ice front location II that enter the boreholes and successfully reaching the model boundary. The statistical measures are the median (red), 25th and 75th percentile (blue bar) and the 5th and 95th percentile (black "whiskers").*

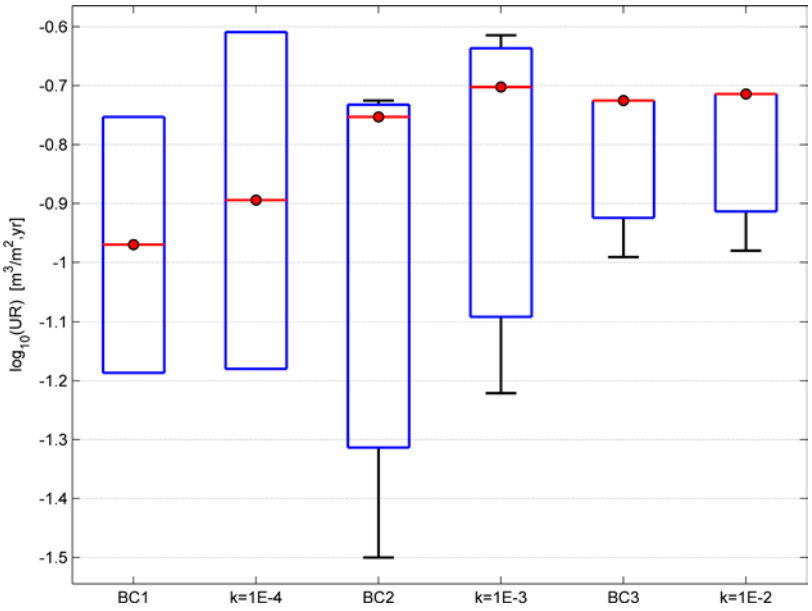


***Figure 3-107.*** *Bar and whisker plot of $U_r$ for three different borehole sealing variants (conductivity in m/s) and the corresponding set of particles in the SR-Site Hydrogeological base case (BC1−BC3), for only the Q3 discharge particles released for glacial ice front location II that enter the boreholes and successfully reaching the model boundary. The statistical measures are the median (red), 25th and 75th percentile (blue bar) and the 5th and 95th percentile (black "whiskers").*

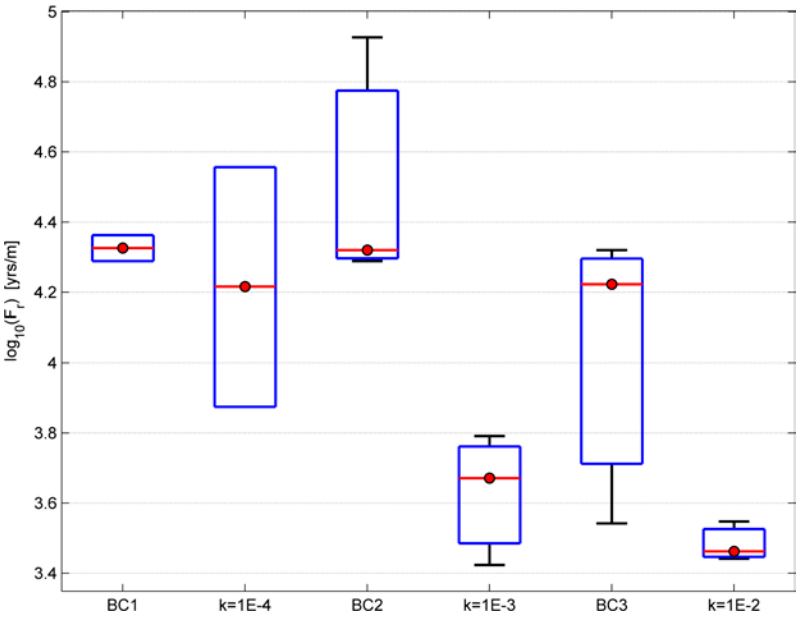


***Figure 3-108.*** *Bar and whisker plot of $F_r$ for three different borehole sealing variants (conductivity in m/s) and the corresponding set of particles in the SR-Site Hydrogeological base case (BC1−BC3), for only the Q3 discharge particles released for glacial ice front location II that enter the boreholes and successfully reaching the model boundary. The statistical measures are the median (red), 25$^{th}$ and 75$^{th}$ percentile (blue bar) and the 5$^{th}$ and 95$^{th}$ percentile (black "whiskers").*

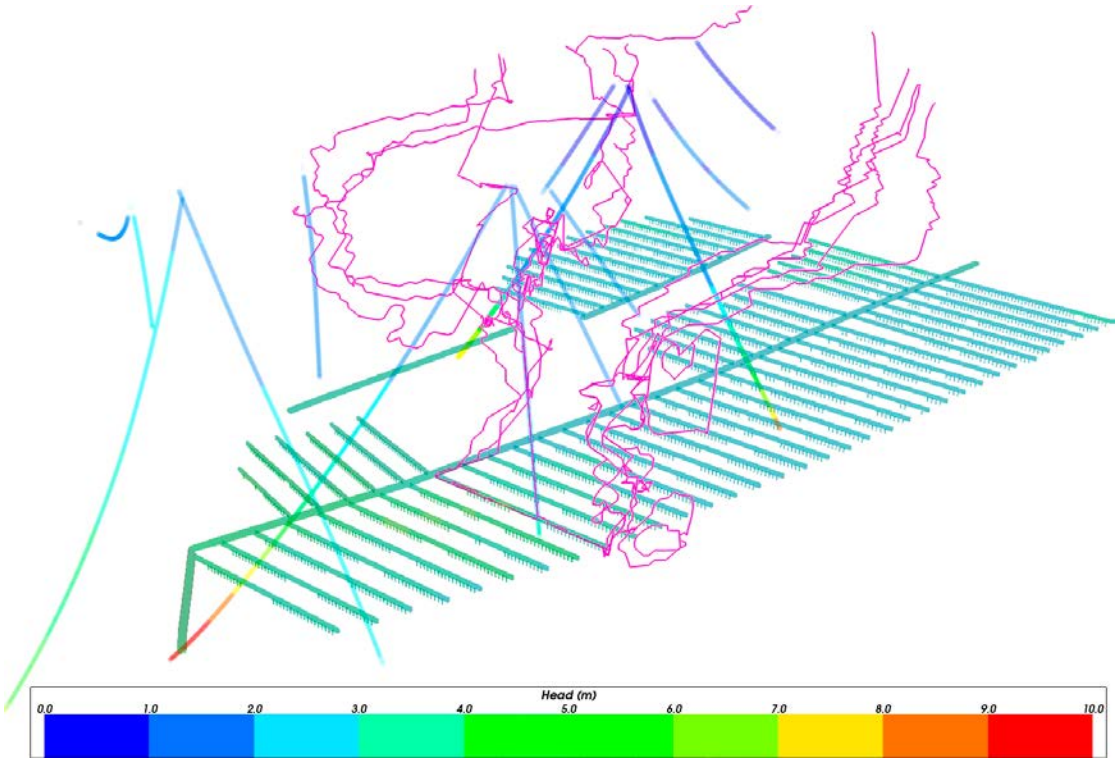


***Figure 3-109.*** *Discharge pathways for a selection of 21 particles released from starting positions 950−970 in Case 6 (shown in purple). All structures are coloured by head (blue is low, red is high).*

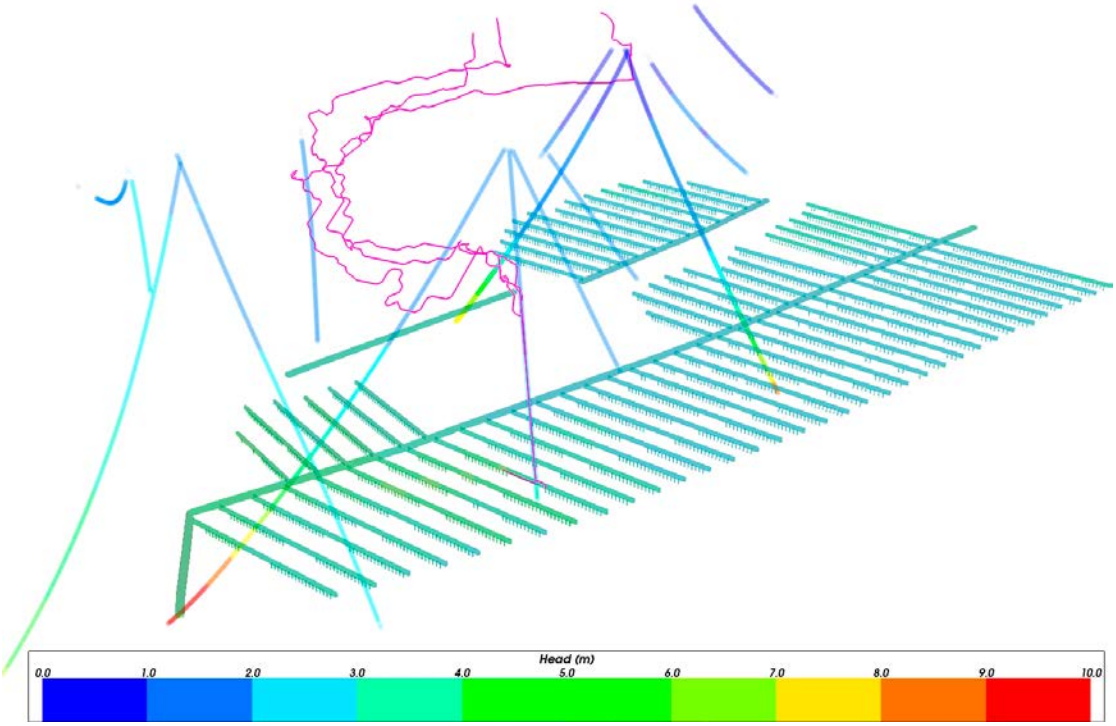


***Figure 3-110.*** *Discharge pathways for three particles released from starting positions 958−960 in Case 6 (shown in purple) entering borehole KFM07C. All structures are coloured by head (blue is low, red is high).*

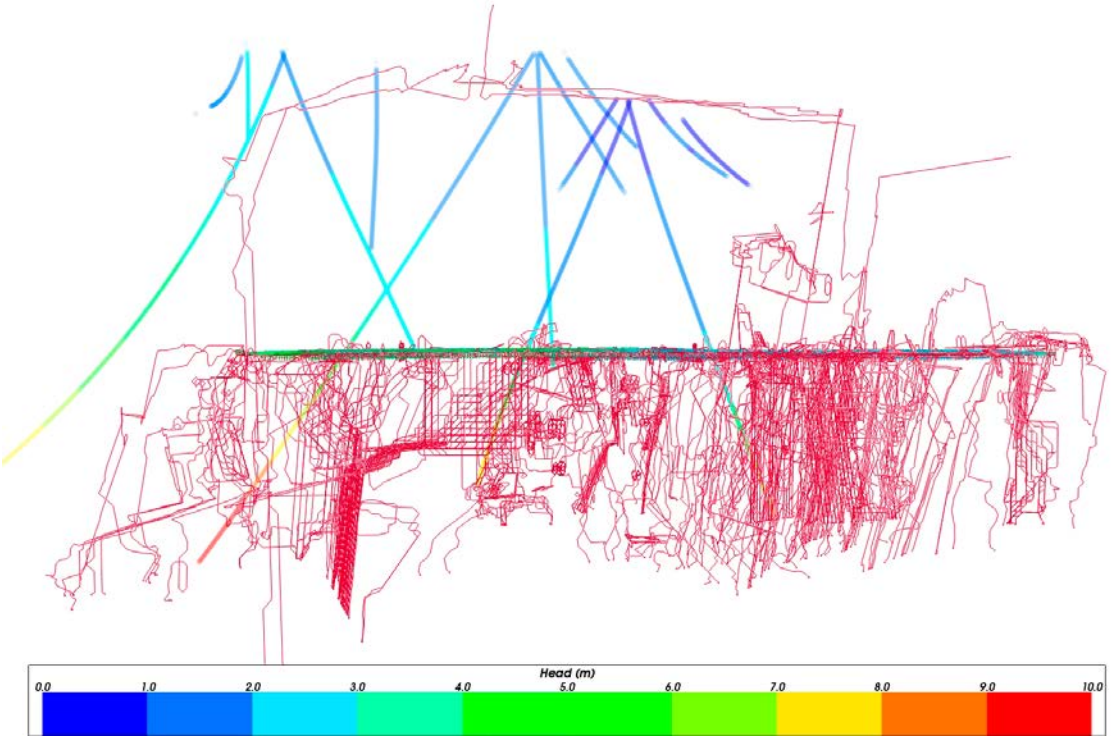


***Figure 3-111.*** *Vertical section through the Case 6 model showing the recharge pathways of the particles released from the repository block 1 (paths shown in red). All structures are coloured by head (blue is low, red is high).*

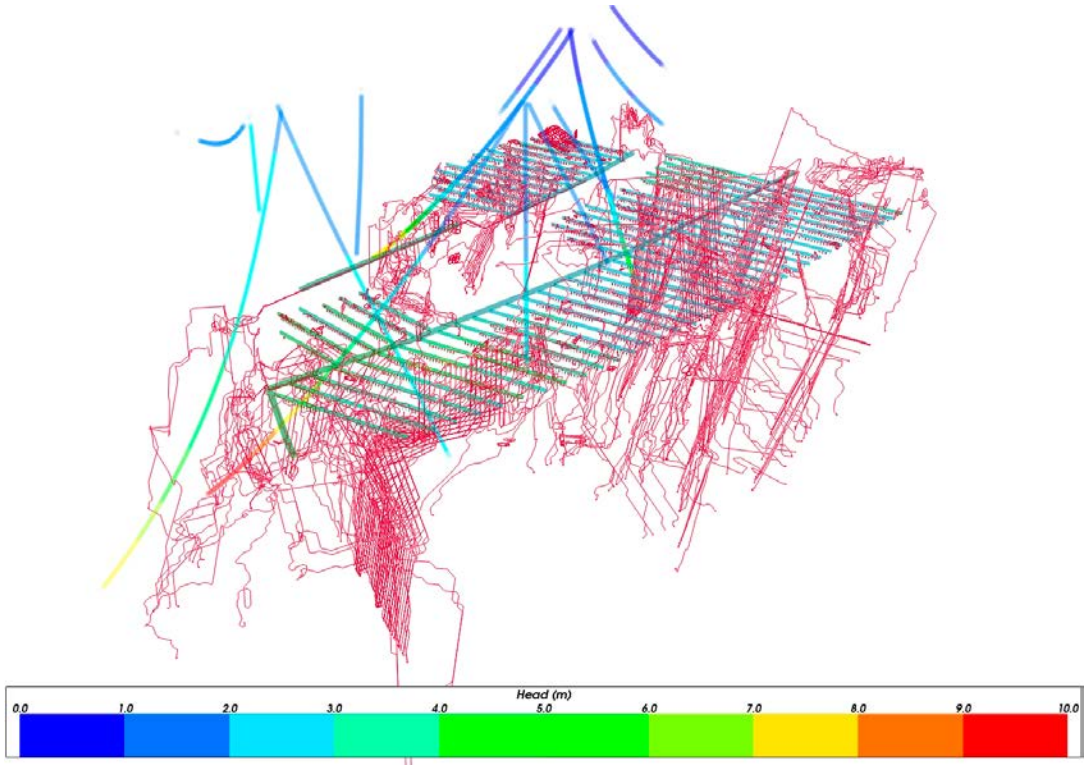


***Figure 3-112.*** *Oblique view of the Case 6 model showing the recharge pathways of the particles released from the repository block 1 (paths shown in red). All structures are coloured by head (blue is low, red is high).*

# 4 Conclusions

## 4.1 Ramp and shaft variants

It can be concluded that within the context of the modelling reported here, the properties of the ramp and shafts and the properties of the EDZ for the ramp and shafts have little effect on the performance measure statistics or their distribution. The maximum difference in median values between cases is around 25 % and most of the differences are much less for both the temperate and glacial climate situations. These differences are much less than those between several variants examined for SR-Site (Joyce et al. 2010), such as changing EDZ properties for the tunnels, or even between different realisations of the HRD. The reason for the small effects seen for this study is probably because the flows in the Forsmark models, and hence the particle pathways, are dominated by the deformation zones. The deformation zones tend to carry particles to the surface without involving the ramp or shafts for those backfill properties considered here.

However, there are effects seen for individual particle pathways when the ramp and shaft properties are changed. In some cases, exit locations are changed or particles use the ramp or shafts for part of their pathway.

Although there are differences in performance measures between the different realisations considered for alternative 2, there is little difference in performance measures between variants for a given realisation. This indicates that the effect of the ramp and shaft properties on performance measures is not sensitive to the realisation considered. It is of course possible that for other realisations, the performance measures may be more sensitive to the ramp and shaft properties. Only a few realisations were considered here, which is insufficient to give a full statistical analysis of the uncertainties involved, but gives some indication of the sensitivities.

The overall conclusion is that changing the ramp or shaft properties or the associated EDZ, within the scope reported here, has little effect on the overall recharge of potentially oxygenated or dilute water to the repository or on the discharge of radionuclides to the ground surface. It is possible that different properties for the repository structures, or different combinations of properties, could lead to greater effects. However, the properties were chosen to represent a number of engineering scenarios that partially explore the range of alternative designs and to be consistent with the existing framework for SR-Site.

## 4.2 Sealing of investigation boreholes

The modelling of sealed boreholes conducted in the present report shows that the sealing properties of the boreholes have little effect on the performance measure statistics or their distribution. It has been shown that there is little or no effect from the boreholes on the particle pathways, recharge or discharge, when the borehole conductivity is less than $10^{-6}$ m/s. In order to have a significant impact on the pathways, at least in the sense of particles entering boreholes, the borehole hydraulic conductivity needs to be greater than $10^{-4}$ m/s. The conclusion is the same for both of the modelled climate situations, the temperate and the glacial period. The differences between the variants in median and $10^{th}$ percentile values stay within 28 % and usually much less when comparing the ensemble results. Even if the overall effect on the released particles is small, there are individual particles that show larger effects on the performance measure statistics. These are typically particles that enter the sealed boreholes. When analysing only the subset of particles that enter the boreholes, an increased difference in performance measures can be seen comparing a given variant for different realisations but also for different variants within a given realisation. Hence, some sensitivity to the choice of realisation can be seen in the results but the number of realisations analysed is too small to make any general conclusion.

The small effect from the boreholes on the recharge and discharge pathways is likely due to assigned low conductivities making the boreholes effectively invisible to flow in the bedrock. The recharge pathways indicate that no significant amount of potentially oxygenated water is drawn from the surface down to repository depths.

Due to time constraints there had to be some simplifications made to the model. Here is a summary of the main ones related to the representation of boreholes:

- In the reference design, sections intersected by transmissive fracture zones are filled with silica concrete, which is permeable and erosion resistant. In the model however, no such modification to the properties of the boreholes and surrounding fracture zones was done.
- In reality the boreholes have varying diameters with depth, but in the model, a uniform diameter was used. Also, all boreholes were assigned the same diameter even if the diameter varies between boreholes.
- In the model, the boreholes were assigned homogeneous properties (hydraulic conductivity and porosity) which is not necessarily the case in reality.
- A freshwater density was assigned to the boreholes, which should be a conservative assumption in terms of hydraulic driving forces. However, it is uncertain what the initial conditions in the boreholes would be after sealing.

# References

SKB's (Svensk Kärnbränslehantering AB) publications can be found at www.skb.com/publications.

**Bockgård N, 2010.** Groundwater flow modelling of an abandoned partially open repository. SKB R-10-41, Svensk Kärnbränslehantering AB.

**Joyce S, Simpson T, Hartley L, Applegate D, Hoek J, Jackson P, Swan D, Marsic N, Follin S, 2010.** Groundwater flow modelling of periods with temperate climate conditions − Forsmark. SKB R-09-20, Svensk Kärnbränslehantering AB.

**Serco, 2011a.** CONNECTFLOW Release 10.1.1 Technical Summary Document. Serco Report SA/ENV/CONNECTFLOW/15, Serco Assurance, UK.

**Serco, 2011b.** NAMMU Release 10.1.1 Technical Summary Document. Serco Report SA/ENV/CONNECTFLOW/8, Serco Assurance, UK.

**Serco, 2011c.** NAPSAC Release 10.1.1 Technical Summary Document. Serco Report SA/ENV/CONNECTFLOW/12, Serco Assurance, UK.